



**Whistler, BC**  
September 29<sup>th</sup> – October 1<sup>st</sup>, 2016

# Conference Proceedings

5<sup>th</sup> Canadian Young Geotechnical Engineers and  
Geoscientists Conference

---

5e Conférence canadienne des jeunes géotechniciens  
et géoscientifiques

## Message from the Chairs

On behalf of the 5<sup>th</sup> Canadian Young Geotechnical Engineers and Geoscientists Conference (cYGEgc) Organizing Committee, we'd like to welcome you to Whistler, British Columbia. The 5<sup>th</sup> cYGEgc provides a unique experience among conferences. Instead of the participants being brought together around a common technical topic, we are gathered together both by our broad professional interests and by our common age and level of experience. We hope all participating members will enjoy the networking and learning opportunities that this conference provides.

In the following pages you will find the conference proceedings, including the conference schedule, a list of delegates and keynote speakers, and our sponsor's logos.

The cYGEgc is a triennial Canadian Geotechnical Society (CGS) conference. The Canadian Young Geotechnical Engineers and Geoscientists conference was first held in 2004. The goal of the conference was to provide a venue for young professionals in the geoscience and geotechnical engineering fields to meet, network, improve their professional skills, and learn from keynote addresses by senior professionals. The conference runs every three years along with the CGS national conference. Since its inception the cYGEgc has been held as an inclusive retreat style conference to promote an environment of networking and engagement among the conference attendees.

This is the fifth cYGEgc in 12 years. Over the years, this conference series has provided a venue for 170 young engineers and geoscientists to present their work to their peers. This year we feel exceptionally lucky to have 53 conference delegates, along with five keynote speakers here to share their experiences with us.

The five keynotes have a broad range of experiences in the geotechnical and geosciences fields. We are privileged to have the opportunity to hear from Mr. Doug VanDine, Dr. Norbert Morgenstern, Mr. Al Hoffman, Dr. Suzanne Lacasse, and Dr. Evert Hoek.

Among our 53 delegates we have 17 representatives from industry and 36 university students. Our delegates come from across Canada, from British Columbia to New Brunswick, and internationally from the United States, Hong Kong, and the United Kingdom. Delegates will present on a range of topics, from laboratory testing to geohazards and slope stability, planning and guidelines to foundation engineering, and numerical modelling to site characterization. The breadth of topics presented provides an understanding of the broad scope in which one can operate as a young geotechnical and geoscience professional in Canada.

We want to encourage delegates to approach the conference with a curious mind. Ask the questions that jump out to you. Talk to the person who works on things you have never heard of. Corner the keynote speakers and ask them about their careers, or about their paper that you have read 15 times. If we all approach the conference with curious minds, we will leave enriched.

Finally, we would like to thank everyone who made this conference possible. Thank you to our Gold, Silver, and Bronze sponsors for financially supporting the conference. Thank you to the CGS for their continuous support during the conference organization. In particular, we would like to thank Mr. Doug VanDine, Dr. Ariane Locat, Dr. Michel Aubertin, Dr. Jinyuan Liu, Mr. Wayne Gibson, and the CGS board for their frequent and insightful guidance.

Lastly we want to thank our organizing committee. The conference is a result of the hard work and combined vision of the 16 individuals from both industry and academia. They made the hard work seem easy. Thank you.

We look forward to meeting all the delegates over the coming days. Thanks for contributing to the 5<sup>th</sup> cYGEGC.

Julian McGreevy and Maraika De Groot  
5<sup>th</sup> cYGEGC Co-Chairs

## Message des présidents

Au nom du comité organisateur de la 5<sup>e</sup> Conférence canadienne des jeunes géotechniciens et géoscientifiques (CCJGG), nous sommes heureux de vous accueillir à Whistler (Colombie-Britannique). La 5<sup>e</sup> CCJGG offre une expérience unique parmi les autres conférences techniques du domaine. Au lieu de réunir ses participants autour d'un sujet commun à tous, nous y sommes plutôt rassemblés par des intérêts professionnels communs, par notre âge commun et notre niveau d'expérience. Nous espérons que tous les participants apprécieront les opportunités de réseautage et d'apprentissage offertes par cette conférence.

Vous trouverez dans les pages qui suivent les comptes rendus de la conférence, incluant l'horaire de la conférence, la liste des délégués et des conférenciers invités ainsi que les logos de nos commanditaires.

La CCJGG est un événement triennal de la Société canadienne de géotechnique (SCG). La première Conférence canadienne de jeunes géotechniciens et géoscientifiques a eu lieu en 2004. Le but de cette conférence était de fournir aux jeunes professionnels de la géotechnique et des géosciences une opportunité de se rencontrer, de tisser des liens, de perfectionner ses connaissances techniques et d'apprendre de l'expérience des conférenciers invités. La conférence a lieu tous les trois ans, en marge de la Conférence canadienne de géotechnique annuelle. Depuis ses débuts, la CCJGG a été tenue à la manière d'une conférence inclusive en retraite fermée pour promouvoir un environnement favorable au réseautage et à l'engagement des délégués.

L'édition 2016 de la CCJGG 2016 est la 5<sup>e</sup> à être tenue en 12 ans. Au fil des ans, cette conférence a permis à quelque 170 jeunes ingénieurs et géoscientifiques de présenter leur travail devant leurs pairs. Nous nous sentons extrêmement choyés cette année d'accueillir à la conférence 53 délégués et cinq conférenciers invités pour partager leur expérience avec nous.

Les cinq conférenciers invités partagent une vaste expérience dans les domaines de la géotechnique et des géosciences. Nous sommes privilégiés d'avoir l'opportunité de recevoir M. Doug VanDine, Dr Norbert Morgenstern, M. Al Hoffman, Dre Suzanne Lacasse et Dr Evert Hoek.

Parmi les 53 délégués de la conférence se retrouvent 17 représentants de l'industrie et 36 étudiants universitaires. Ces délégués proviennent du Canada, de la Colombie-Britannique au Nouveau-Brunswick, et de l'international (États-Unis, Hong Kong et Royaume-Uni). Les présentations des délégués incluront un éventail de sujets allant des expérimentations en laboratoire aux géorisques et stabilités de pentes, de la planification et guides à l'ingénierie des fondations, de la modélisation numérique à la caractérisation de site. L'étendue des sujets abordés montre bien l'ampleur des domaines de travail possible pour un jeune professionnel de la géotechnique et des géosciences au Canada.

Nous désirons encourager les délégués à aborder cette conférence l'esprit ouvert. Posez les questions qui vous tracassent, parlez aux gens qui travaillent sur des choses dont vous n'avez jamais entendu parler. Abordez les conférenciers invités pour en savoir plus sur leur carrière, ou sur leur article que vous avez lu 15 fois. Si nous abordons tous cette conférence l'esprit curieux, nous en sortirons tous enrichis.

Enfin, nous voulons remercier notre comité d'organisation. Cette conférence est le résultat du travail acharné et de la vision commune de 16 jeunes professionnels provenant de l'industrie et du milieu académique. Ils ont fait en sorte que le travail exigeant semblait facile. Merci.

Nous avons bien hâte de rencontrer tous les délégués au cours des prochains jours. Merci d'avoir contribué à la 5<sup>e</sup> CCJGG.

Julian McGreevy et Maraika De Groot  
Présidents de la 5<sup>e</sup> CCJGG

Julian McGreevy et Maraika De Groot  
Présidents de la 5<sup>e</sup> CCJGG

## Conference Schedule

Start	End	Description
<b>Thursday, September 29, 2016</b>		
7:00	8:00	Breakfast and Registration at 980 Howe St. Vancouver
8:00		Departure from Vancouver
8:00	17:00	Technical Tour
17:00		Arrival to Whistler
19:00		Dinner at Garibaldi Lift Company
<b>Friday, September 30, 2016</b>		
7:00	8:00	Breakfast
8:00	8:30	Opening Ceremony
8:30	9:15	<b>Keynote Address: Doug VanDine</b>
9:15	10:00	<b>Keynote Address: Norbert Morgenstern</b>
10:00	10:30	Coffee Break
10:30	12:00	Technical Session 1: Laboratory Testing
12:00	13:00	Lunch
13:00	13:45	<b>Keynote Address: Al Hoffman</b>
13:45	15:00	Technical Session 2: Geohazards and Slope Stability
15:00	15:15	Coffee Break
15:15	17:00	Poster Session 1
17:00	18:00	Technical Session 3: Planning and Guidelines
19:00		Dinner at Teppan Village
<b>Saturday, October 1, 2016</b>		
7:00	8:00	Breakfast
8:00	8:45	<b>Keynote Address: Suzanne Lacasse</b>
8:45	10:00	Technical Session 4: Foundation Engineering
10:00	10:30	Coffee Break
10:30	12:00	Technical Session 5: Numerical Modelling
12:00	13:00	Lunch
13:00	13:45	<b>Keynote Address: Evert Hoek</b>
13:45	15:15	Technical Session 6: Site Characterization
15:15	15:30	Coffee Break
15:30	17:15	Poster Session 2
17:15	17:30	Closing Ceremony
19:00		Semi-Formal Banquet at Delta Whistler Village Suites
<b>Sunday, October 2, 2016</b>		
-		Free time for breakfast and exploring
10:30	12:15	Return to Vancouver

## 5<sup>th</sup> cYGEGC Organizing Committee Members

<b>Name</b>	<b>Position</b>	<b>Affiliation</b>
Maraika De Groot	Co-Chair	BGC Engineering Inc.
Julian McGreevy	Co-Chair	BGC Engineering Inc.
Kristen Van Esch	Secretary	BGC Engineering Inc.
Jenna Bowling	Treasurer	Golder Associates Ltd.
Rebecca Turley	Registration	BGC Engineering Inc.
Jane Peter	Registration	Queen's University
Carie-Ann Lau	Logistics	BGC Engineering Inc.
Bill Shuihan Li	Logistics	Ryerson University
Natalie Blacklock	Technical Committee	Queen's University
Vincent Castonguay	Technical Committee	Université Laval
Erik Stevenson	Technical Committee	Thurber Engineering Ltd.
Meredith Kealty	Sponsorship	Klohn Crippen Berger Ltd.
Douglas Haney	Webmaster	WorleyParsons: Advisian
Andries Kirstein	Promotions	Ryerson University
Ioannis Vazaios	Member at Large	Queen's University
Nick Beier	Member at Large	University of Alberta

Thank you to our Sponsors!

## Gold Sponsors





**Klohn Crippen Berger**

65 years of service



**Clifton Associates**

**B|G|C**





Silver Sponsors

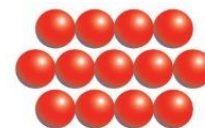


**THURBER** ENGINEERING LTD.



**Geotech**  
DRILLING

***Knight Piésold***  
**CONSULTING**



**REINFORCED eARTH®**



**Bronze Sponsor**



**Delegate Sponsors**

Thank you to the Cold Regions Geotechnology Division of the CGS for sponsoring Simon Dumais to attend the conference.

Thank you to the Vancouver Geotechnical Society for sponsoring Christian Sampaleanu to attend the conference.

## List of Abstracts

<b>Technical Session 1: Laboratory Testing</b>	
Chair: Erika Schmidt	
Erika Schmidt	Hydraulic stimulation as a means of controlling fault slip-induced rockbursts in deep mines
Manuel Malenfant	Influence of macroporosity in northern Quebec tills
Jiechun Wu	Impact of tetrahydrofuran hydrate veins on the shear strength of hydrate-bearing fine-grained soil specimens
Hubert Michaud	Cisaillement annulaire à volume constant des argiles sensibles
Dongri Song	Dynamic response of rigid barrier under boulder-entrained debris flow impact
Haley Schafer	Freezing characteristics of fluid fine tailings and their relation to unsaturated soil properties
<b>Technical Session 2: Geohazards and Slope Stability</b>	
Chair: Ariane Locat	
Ariane Locat	Preliminary synthesis of spreads in Canadian sensitive clays
Michael Van Helden	Emergency riverbank stabilization of Lyndale Drive in Winnipeg, MB
Megan van Veen	Building a rockfall database using remote sensing data: Applications for hazard management in Canadian rail corridors
Emily Rowe	A forensics study of the deformation and structural controls on rockfalls in White Canyon using terrestrial LiDAR
Carie-Ann Lau	The August 6, 2010 Mount Meager landslide
<b>Technical Session 3: Planning and Guidelines</b>	
Chair: Scott McKean	
Scott McKean	A call to arms: Sustainability in geotechnical engineering
Hugh Gillen	Development of gravel shear-key design guidelines for railway slope stabilization
James Bartz	Development of design guidelines for sheet pile walls for railway slope stabilization
Julian McGreevy	Integrated planning for closure supported by the use of digital elevation model surfaces
<b>Technical Session 4: Foundation Engineering</b>	
Chair: Kanika Lamba	
Kanika Lamba	Estimation of lateral pile capacity for design of soil-structure interaction experiments
Earl Marvin De Guzman	Performance of a reinforced highway embankment to Canada's North
Stephen Lanyi	Behaviour of helical pile groups under axial compressive loading
Leanne McLaren	Use of moisture wicking geotextile for subgrade improvement in pavement design
Mark Redden	Design & construction of micropiles for Vale's Copper Cliff smelter

<b>Technical Session 5: Numerical Modelling</b>	
Chair: Simon Dumais	
Simon Dumais	Large-strain consolidation of thawing soils
Pedram Abootalebi	Thermal-hydraulic modelling a Canadian deep geological repository
Étienne Hébert	Geostatistical modeling of hydraulic conductivity within a compacted dam core
Joshua Winfield	Modelling of supercritical carbon dioxide sorption on various geological media
John Kingswood	Verification of geotechnical centrifuge physical modelling using slope stability and bearing capacity models
Vincent Castonguay	Direct numerical integrations of geotechnical laboratory tests: Useful tools to better understand soil behaviour
<b>Technical Session 6: Site Characterization</b>	
Chair: Lauren Hockin	
Lauren Hockin	Characterization of hazards affecting hillslopes damaged by the 2015 earthquakes in Nepal
Hazel Wong	Applications of terrain analysis in geotechnical engineering
John Danielson	The use of specific energy for open pit rock mass characterization
David Barsi	Spatial variability of particle size distribution in waste rock
Melissa Dinsdale	Resource development on karst terrain, Vancouver Island B.C.
Kathryn Dompierre	Evaluating water and chemical release from oil sands fluid fine tailings using multiple tracers
<b>Poster Session 1</b>	
Ben Olsen	Liner system design: An outside look at the state of the practice
Aditi Khurana	Measurement of dissolved gas pressures during loading and unloading of loose gassy sands
Maraika De Groot	Design of an instrumentation system for a tailings dam
Navpreet Singh	Estimation of hydraulic conductivity of coarse soil using pedotransfer functions
Shawn Beaudry	Static axial compression testing of HDTM helical piles – Case study of an active project in northern Manitoba
Allison Westin	Characterization of large rock slides using an integrated remote sensing approach
Loriane Périer	Thermal design method for culverts built on permafrost
Rebecca Turley	Estimation of optimum moisture content from Atterberg limits for borrow pit assessment at Flin Flon, MB
Damian McClarty	Cheekeye River Fan debris flow hazard
Megan Dewit	Up close with virtual rock outcrops: Geovisualization of a remotely sensed field site

Poster Session 2	
Erik Stevenson	From consulting to academia and back: A different approach to data gaps
Adam Silvester	Proposed method of shear wave velocity measurement in a flexible wall permeameter
Katie Burkell	Design of the rehabilitation for industrial process water pond project
David Muddle	Measuring macropore characteristics and hydraulic conductivity of intact clay cores using computed tomography
Ryan Kremsater	Geomorphological mapping of the Cascade Bay Landslide using a combined airborne LiDAR and terrestrial remote sensing approach
Courtney Mulhall	Large-scale testing of tie lateral resistance in two ballast materials
Dylan Kennedy	Studying embankment soil stability on the new Inuvik-Tuktoyaktuk Mackenzie Valley highway
Harmen Van Hove	Debris flow effects on steelhead trout habitat in Shovelhead Creek
Christian Sampaleanu	Evaluating rockfall hazard on the north wall of Stawamus Chief
Adam Woods	BC Hydro Transmission Engineering – annual geohazard review program & case studies

# Technical Session 1

## Laboratory Testing

# Hydraulic stimulation as a means of mitigating fault slip-induced rockbursts in deep mines



E. S. Schmidt  
 University of British Columbia, Vancouver, BC  
[eschmidt@eos.ubc.ca](mailto:eschmidt@eos.ubc.ca)

E. Eberhardt  
 University of British Columbia, Vancouver, BC  
[eeberhar@eos.ubc.ca](mailto:eeberhar@eos.ubc.ca)

## Introduction

As underground mines extend to ever-increasing depths, stress-driven rockmass failure poses a growing risk to the safety of mine personnel. One form of high stress failure, termed fault slip, occurs when ground disturbance associated with mining alters the stress regime present at depth, triggering sudden movement on pre-existing discontinuities. The resulting energy release resembles a natural earthquake, and has been shown to generate seismic magnitudes exceeding  $M_n = 5.0$  in several instances (McGarr et al. 1989). Fault-slip and associated rockbursts can be catastrophic in nature, resulting in damage to mine infrastructure, harm to equipment, and loss of life, as was the case in

the June 20, 1984 event at Falconbridge Mine (Blake & Hedley 2003).

The current research aims to investigate whether hydraulic stimulation, defined here as the injection of pressurized fluid into a rockmass, offers a means of mitigating fault-slip rockburst hazards ahead of mining. Distinction is made here between hydraulic fracturing and hydraulic shearing (Preisig et al. 2015). Hydraulic fracturing (HF) involves the injection of fluid to generate new tensile fractures. For HF to occur, the injected fluid pressure,  $p_f$ , must exceed the stresses acting around the borehole combined with the tensile strength of the intact rock,  $T_o$ :

$$p_f > 3\sigma_3 - \sigma_1 + T_o \quad [1]$$

where  $\sigma_1$  and  $\sigma_3$  are the major and minor principal stresses, respectively. The rockmass here is assumed to be impermeable. HF has been widely used to increase reservoir permeability during shale gas extraction, and has also been investigated as a method of enhancing fragmentation in block caving operations (van As & Jeffrey 2000) and to facilitate stress relief ahead of mine advances (Gambino 2014).

In contrast, the application proposed in the current research would involve a separate process, hydraulic shearing (HS), whereby slip is triggered along pre-existing discontinuities to release stored stress and strain energy. HS has been widely used to increase reservoir permeability in Enhanced Geothermal System projects (McClure & Home 2014), through overriding fracture asperities serving to prop open the fracture. In this case, the fluid pressure,  $p_f$ , reduces the effective normal stress acting on the fault, diminishing its overall shear strength until the fault slips via the Mohr-Coulomb shear failure condition:

$$|\tau| \geq (\sigma_n - p_f) \tan \phi \quad [2]$$

where  $\tau$  is the shear stress and  $\sigma_n$  is the normal stress acting on the fault, and  $\phi$  is the friction angle of the fault surface.

In practice, the fluid pressure required to trigger HS (criterion [2]) is usually less than that required for HF

(criterion [1]). This suggests that hydraulic stimulation could be used to induce slip along a critically-stressed fault plane without significantly damaging the surrounding rock. In this manner, fault-slip events could be triggered at planned intervals in advance of mining when there is reduced risk to personnel.

## Methodology

An integrated numerical modelling and lab testing study was undertaken with the following objectives:

1. Determine if triggering slip via hydraulic stimulation can release stored strain energy along critically-stressed faults in advance of mining.
2. Determine optimal fluid injection parameters (volume, rate, length of packed interval, etc.) required to initiate HS and trigger slip.

To investigate the first objective, the 2-D distinct element code UDEC (Itasca 2014) is used to simulate the rock mass response to a field scale hydraulic stimulation trial in a hypothetical deep mining environment. Initial results show that a significant release of shear stress accompanies fault slip events generated in the model (Figure 1).

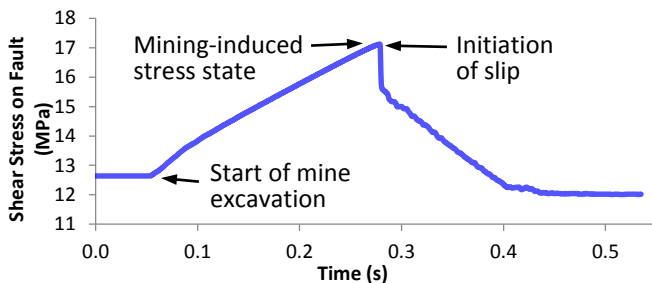


**Figure 1: Shear stress history of a slipping fault adjacent to an excavation modelled in UDEC**

The second objective is studied through a series of laboratory HS tests. Granite samples with angled saw cuts are loaded in triaxial compression, and pressurized water is injected to trigger a HS event. Tests are monitored using a state-of-the-art acoustic emission system, which consists of six piezoelectric sensors mounted to the outside of the specimens. The system is capable of monitoring the location, source mechanism and magnitude of slip induced by HS, allowing the results of different injection trials to be compared. A typical test setup is shown in Figure 2.

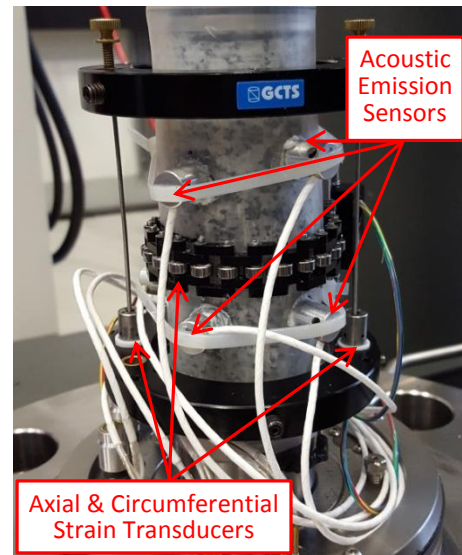


**Figure 2: Typical hydraulic stimulation test setup**

## Conclusions

Hydraulic stimulation offers a promising risk mitigation technique for fault-slip rockbursts to reduce harm to mine personnel. Research is being conducted on the feasibility of using this technique to relieve stored strain energy in a controlled manner in advance of mining. Ultimately this research will contribute to improvements in the safe mining of deep orebodies.

## References

- Blake, W., & Hedley, D. G. F. 2003. *Rockbursts: Case Studies from North American Hard-Rock Mines*. Littleton: Society for Mining, Metallurgy, and Exploration, Inc.
- Gambino, G. F. 2014. *An Assessment of Unpredictability in the Design of Hydraulic Fractures for Stress Amelioration around Underground Excavations*. M.A.Sc. thesis, University of Toronto.
- Itasca Consulting Group Inc. 2014. *UDEC version 6.0*.
- McClure, M.W. & Home, R.N. 2014. An investigation of stimulation mechanisms in Enhanced Geothermal Systems. *Int. J. Rock Mech. Min. Sci.*, 72: 242–260.
- McGarr, A., Bicknell, J., Sembera, E., & Green, R. W. E. 1989. Analysis of exceptionally large tremors in two gold mining districts of South Africa. *Pure and Applied Geophysics*, 129(3/4): 295–307.
- Preisig, G., Eberhardt, E., Gischig, V., Roche, V., et al. 2015. Development of connected permeability in massive crystalline rocks through hydraulic fracture propagation and shearing accompanying fluid injection. *Geofluids*, 15(1-2): 321–337.
- van As, A., & Jeffrey, R. G. 2000. Caving induced by hydraulic fracturing at Northparkes Mines. In Girard et al. (eds.), *Pacific Rocks 2000*. Rotterdam: Balkema.

## Influence of macroporosity in northern Quebec tills



M. Malenfant-Corriveau  
 Hatch, Fredericton  
[manuel.malenfant@hatch.com](mailto:manuel.malenfant@hatch.com)

### Introduction

Several rock-filled dams have been built in northern Quebec in the last 50 years. Tills have been used as hydraulic barriers for the construction of the impervious core of the dams because of their hydraulic and mechanical properties and their availability nearby the construction sites. They usually have low compressibility, high shear strength and low hydraulic conductivity when compacted (Loiselle & Hurtubise, 1976). The aim of this paper is to assess the effect of compaction conditions and macroporosity on the fabric and the hydraulic conductivity of northern Quebec tills.

### Influence of compaction conditions

In cohesive soils, the compaction conditions (water content and dry density) influence the hydraulic conductivity, the fabric and the pore-size distribution. Watabe et al. (2000) and Leroueil et al. (2002) showed that the compaction conditions can also have a significant influence on the hydraulic conductivity and fabric of compacted tills, even in nonplastic ones.

Fig. 1 shows the relationships between the saturated hydraulic conductivity and the compaction degree of compaction of three typical clays (Mitchell et al. 1965) and one typical till (Watabe et al. 2000). The behaviour associated with tills is very similar to the one associated with clays, where an important reduction of hydraulic conductivity is observed in the specimens compacted at compaction degree of saturation higher than that at the optimum (wet side,  $S_{r0} > S_{r-opt}$ ).

Tills compacted on the wet side of optimum usually have homogeneous fabric and lower hydraulics conductivities of up to four orders of magnitude in comparison with those compacted at  $S_{r0} \leq S_{r-opt}$  (dry side) (Leroueil et al. 2002). However, it was shown that the compaction degree of saturation of a till with very low clay-size content poorly influences the fabric and the hydraulic conductivity (Malenfant-Corriveau et al. 2016). Higher suction in the specimen during compaction on the dry side results in particles aggregation, which causes the development of macroporosity and aggregated fabric (Leroueil & Hight, 2013).

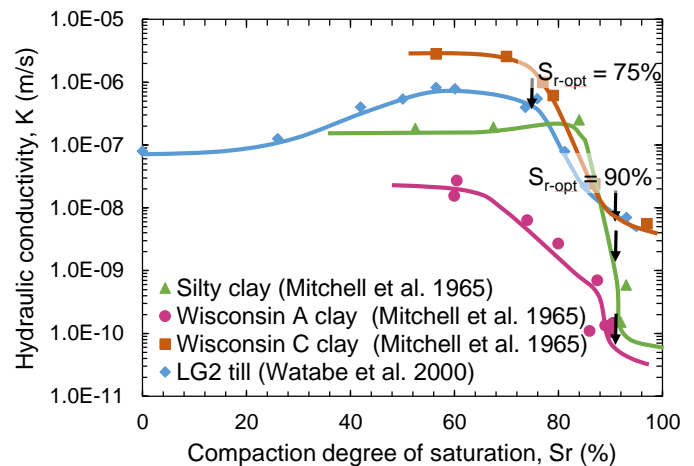


**Fig. 1. Compaction degree of saturation of a function of hydraulic conductivity**

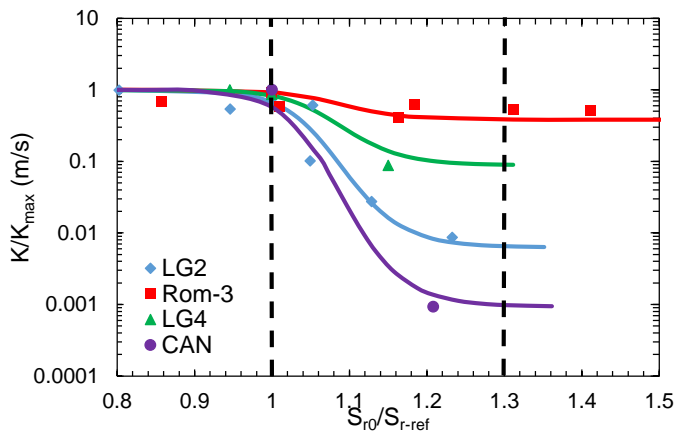
### Influence of macroporosity model

Fig. 2 shows the relationship between the normalised saturated hydraulic conductivity ( $K/K_{max}$ ) and the normalised compaction degree of saturation ( $S_{r0}/S_{r-ref}$ ), in order to illustrate the influence of

macroporosity on hydraulic conductivity. The reference degree of saturation ( $S_{r-ref}$ ) is the point where the hydraulic conductivity begins to abruptly decrease and the hydraulic conductivity is generally at its maximum level. It represents the point where the soil fabric begins to change from aggregated state towards homogeneous state. The experimental results from Leroueil et al. (2002) (LG2, LG4, CAN) and Malenfant-Corriveau et al. (2016) (Rom-3) shown in Fig. 2 are described by a sigmoid equation [Eq. 1] developed by Hébert (2016).

$$K_{sat} = 10 \left[ \frac{\log_{10} \left( \frac{K_{max}}{K_{min}} \right)}{1 + \left( \frac{x_0 + x_1}{S_r / S_{r-ref}} \right)^{-p}} \right] \quad \begin{array}{l} x_0 = 1.011 \\ x_1 = 1.173 \\ p = 28.007 \end{array} \quad [1]$$

Where  $K_{max}$  and  $K_{min}$  are respectively the maximum and minimum hydraulic conductivities measured at a representative void ratio and  $x_0$ ,  $x_1$  and  $p$  are constants.



**Fig. 2. Normalized compaction degree of saturation as a function of the normalized hydraulic conductivity**

As illustrated in Fig. 2, the hydraulic conductivity of the Rom-3 till doesn't decrease significantly once the optimum compaction degree of saturation is reached as opposed to the LG4 till that decreased by one order of magnitude, LG2 till that decreased by two orders of magnitude and Caniapiscou till (CAN) that decreased by three orders of magnitude. It shows that the hydraulic conductivity of the Rom-3 till is poorly influenced by the compaction degree of saturation.

It is observed that influence of the compaction degree of saturation on the soil fabric and the hydraulic conductivity depends mostly on the grain-size distribution. For instance, the compaction degree of saturation of a till with higher clay-size particle content, such as the Caniapiscou till (12.5%) have a

higher influence on the hydraulic conductivity than a till with lower clay-size particle content, such as the till from Rom-3 (0.70 %) (Malenfant-Corriveau et al. 2016). LG4 till have a clay-size content of 2.5% and LG2 of 6.9%. Thus, an increase in the clay-size content causes an increase of the hydraulic conductivity dispersion, meaning an increasing influence of macroporosity.

Finally, it is observed that for  $S_{r0}/S_{r-ref} \leq 1$ , the fabric is assumed aggregated and the curve characterizing hydraulic conductivity is a plateau.

Between  $S_{r0}/S_{r-ref} = 1.0 - 1.3$ , the soil fabric is in a transition zone from aggregated towards homogeneous state, but the fabric is still considered aggregated. At  $S_{r0}/S_{r-ref} \geq 1.2$ , the hydraulic conductivity stops to decrease abruptly, but decreases poorly up to  $S_{r0}/S_{r-ref} = 1.3$  until the hydraulic conductivity is stabilized and another plateau is reached. From  $S_{r0}/S_{r-ref} \geq 1.3$ , hydraulic conductivity stops to decrease and the soil fabric is considered homogeneous.

## References

- Hébert, É. 2016. Analyse géostatistique quasi-3D des propriétés hydrauliques d'un noyau de barrage en remblai *Thèse (M.Sc.), Université Laval*.
- Leroueil, S., Le Bihan, J.-P., Sebaihi, S., & Alicescu, V. 2002. Hydraulic conductivity of compacted tills from northern Quebec. *Canadian Geotechnical Journal*, 39(5), 1039-1049.
- Leroueil, S. and Hight, D. 2013. Invited Lecture. Compacted soils: from physics, to mechanics to hydraulic and mechanical behaviour. *First Pan-American Conf. on Unsaturated Soils*, Cartagena de Indias, Colombia. 41-59.
- Loiselle, A.A., and Hurtubise, J.E. 1976. Properties and behaviour of till as construction material. In *Glacial till an interdisciplinary study. Edited by R.F. Legget. Royal Society of Canada*, Ottawa, 346-363.
- Malenfant-Corriveau, M., Côté, J. and Konrad, J.M. 2016. Hydraulic conductivity of compacted till with low clay-size particle content. *Proceedings of the 69th Canadian Geotechnical Conference*, Vancouver, Canada, October 2-5.
- Mitchell, J.K., Hooper, D.R., and Campanella, R.G. 1965. Permeability of compacted clays. *Journal of the Soil Mechanics and Foundations Division, ASCE*, 91(SM4): 41-65.
- Watabe, Y., Leroueil, S. & Le Bihan, J.-P. 2000. Influence of compaction conditions on pore-size distribution and saturated hydraulic conductivity of a glacial till. *Canadian Geotechnical Journal*, 37(6), 1184-1194.

# Impact of tetrahydrofuran hydrate veins on the shear strength of hydrate-bearing fine-grained soil specimens



J. Wu  
University of Calgary, Calgary  
[jiechun.wu@ucalgary.ca](mailto:jiechun.wu@ucalgary.ca)

J. A. Priest  
University of Calgary, Calgary  
[japriest@ucalgary.ca](mailto:japriest@ucalgary.ca)

J. L.H. Grozic  
University of Calgary, Calgary  
[jgrozic@ucalgary.ca](mailto:jgrozic@ucalgary.ca)

## Introduction

Gas hydrates are ice-like compounds formed of methane gas and water that are stable under certain temperature and pressure conditions that exist within the sediments on the continental margins of the world's oceans and beneath permafrost areas in Arctic. In the recent years, gas hydrate has attracted considerable attention due to its potential as a significant future energy source, a driver for global

climate change and a trigger for geotechnical hazards, since hydrate dissociation can significantly reduce the strength of sediments.

The physical properties of hydrate-bearing sediments and the changes in sediment behavior when the hydrate dissociates is heavily dependent on the hydrate morphology and where it forms within the sediment. It is now commonly assumed that hydrate formation occurs within the pore space of sediments when upward migrating methane saturated pore water reaches the conditions for hydrate stability. However, for fine-grained sediments the small pore size can inhibit hydrate formation within the pore space, leading to localized and discrete hydrate formation in places where larger pore sizes are available, such as along fractures and faults within the host sediment. The inclusion of hydrate veins in fine-grained soils appears to prevent normal consolidation processes, which may lead to significant reduction in sediment strength if the hydrate were to dissociate, and potentially lead to failure of the soil. However, the influence of hydrate veins on soil behavior is not clearly understood, and therefore the impact of subsequent hydrate dissociation on soil behavior and the potential hydrate being a geohazard cannot be assessed properly.

## Research Program

In this paper we report on a series of triaxial compression tests carried out using a temperature controlled triaxial cell to determine the shear strength of fine-grained soil specimens containing vertical cylindrical veins of tetrahydrofuran (THF) hydrate. THF is used as a substitute for methane gas in our laboratory studies to determine the behavior of hydrate-bearing soils. Advantages of using THF are that it is completely miscible in water and can be formed at atmospheric pressure at a relatively low temperature (below 4.13°C). Thus, THF hydrate can be readily formed in fine-grained soils, overcoming the issue with methane gas phase in low permeability soil. In addition, the stability conditions for THF hydrate enables experiments to be achieved using standard laboratory apparatus. Although THF might not be the perfect analog for methane, it is suggested

that the differences between THF and methane during hydrate formation are minor compared to the influence of formation history, laboratory techniques utilized and the distribution of hydrate in the pore space.

Preliminary baseline triaxial tests were carried out on non-hydrate bearing fine-grained soil specimens and a series of compression tests were carried out on standalone, vertical, cylindrical THF hydrate veins to quantify the inherent strength of the two materials. Consolidated undrained triaxial compression tests were then carried out on soil specimens with hydrate veins of varying diameters located in the center of the soil specimens in order to better understand the inclusion of hydrate veins on the consolidated undrained strength of the soil. The stress-strain response of hydrate-bearing fine-grained soil specimens were investigated as a function of hydrate vein size and effective stress.

### Conclusion

Results showed that the shear strength of the hydrate-bearing fine-grained specimen was increased as the vein size increased. Furthermore, soil strength was increased above its baseline value once the vein size was above a threshold diameter, but reduced when the vein diameter was below the threshold. In addition, the shear strength was found to increase with effective stress, while the increase in shear strength with effective stress was reduced with increasing vein diameter. These results suggest that natural hydrate-bearing sediments where hydrate veins were formed when the sediment was under low effective stresses, may experience significant settlement and loss of strength if the hydrate were to dissociate.

### References

- Boswell, R. and Collett, T.S. 2011. Current perspectives on gas hydrate resources, *Energy & environmental science*, 4(4):1206-1215.
- Chuvilin, E.M., Makhonina, N.A., Titenskaya, O.A. and Boldina, O.M., 2002. *Petrophysical Investigations on Frozen Sediments Artificially Saturated by Hydrate*.
- Grozic, J.L.H. 2010. Interplay between gas hydrates and submarine slope failures, in *Submarine Mass Movements and their Consequences*, Springer Netherlands, 11-30.
- Helgerud, M. B., Dvorkin, J., Nur, A., Sakai, A. and Collett, T. (1999). Elastic-wave velocity in marine sediments with gas hydrates: effective medium modeling. *Geophys. Res. Lett.* 26: 2021-2024.
- Hyodo, M., Li, Y., Yoneda, J., Nakata, Y., Yoshimoto, N., Nishimura, A. & Y. Song 2013. Mechanical behaviour of gas-saturated methane hydrate-bearing sediments. *Journal of Geophysical Research*, 118, 5185-5194, doi:10.1002/2013JB010233.
- Kayen, R.E. and Lee H.J. 1991. Pleistocene slope instability of gas hydrate-laden sediment on the Beaufort sea margin, *Marine Georesources & Geotechnology*, 10:125-141.
- Kvenvolden, K.A. 1993. Gas hydrates-geological perspective and climate change, *Reviews of Geophysics*, 31(2): 173-187.
- Lee, J.Y., Yun, T.S., Santamarina, J.C. and Ruppel, C., 2007. Observations related to tetrahydrofuran and methane hydrates for laboratory studies of hydrate-bearing sediments. *Geochemistry, Geophysics, Geosystems*, 8(6).
- Lee, J.Y., Santamarina, J.C. and Ruppel, C., 2008. Mechanical and electromagnetic properties of northern Gulf of Mexico sediments with and without THF hydrates. *Marine and Petroleum Geology*, 25(9), pp.884-895.
- Nimblett, J.N., Shipp, R.C., and Strijbos, F. 2005. Gas hydrate as a drilling hazard: examples from global deepwater settings, *Offshore Technology Conference*, Houston, Texas, USA, 17476: 1-7.
- Rees, E.V., Priest, J.A. and Clayton, C.R.I. 2011. The structure of methane gas hydrate bearing sediments from the Krishna-Godavari Basin as seen from Micro-CT scanning, *Marine and Petroleum Geology*, 28(7): 1283-1293.
- Priest, J.A., Best, A.I. and Clayton, C.R., 2005. A laboratory investigation into the seismic velocities of methane gas hydrate-bearing sand. *Journal of Geophysical Research: Solid Earth*, 110(B4).
- Priest, J.A., Rees, E.V. and Clayton, C.R., 2009. Influence of gas hydrate morphology on the seismic velocities of sands. *Journal of Geophysical Research: Solid Earth*, 114(B11).
- Sloan, E.D., Jr., and Koh, C. 2007. *Clathrate hydrates of natural gases*. CRC press.
- Smith, W.E. 2016. *The Influence of Tetrahydrofuran Hydrate Veins on Fine-Grained Soil Behaviour (Master's Dissertation)*
- Yun, T.S., Narsilio, G.A. and Santamarina, J.C. 2006. Physical characterization of core samples recovered from Gulf of Mexico, *Marine and Petroleum Geology*, 23(9): 893-900.
- Yun, T.S., Santamarina, J.C., Ruppel, C. 2007. Mechanical properties of sand, silt, and clay containing tetrahydrofuran hydrate, *Journal of Geophysical Research: Solid Earth* (1978-2012), 112(B4).

# Cisaillement annulaire à volume constant des argiles sensibles



H. Michaud, A. Locat  
 Dép. de génie civil, Université Laval, Qc.  
[hubert.michaud.1@ulaval.ca](mailto:hubert.michaud.1@ulaval.ca), [ariane.locat@gci.ulaval.ca](mailto:ariane.locat@gci.ulaval.ca)

## Introduction

Un nouvel appareil de cisaillement annulaire est mis au point afin de déterminer la résistance intacte et à grande déformation des argiles sensibles. Ce résumé décrit les principes de cet essai et les résultats préliminaires du premier essai réalisé sur un échantillon d'argile sensible de Saint-Alban, Qc.

## Description de l'appareil

Les figures 1 et 2 montrent une vue détaillée et une vue générale de l'appareil. Une boîte de cisaillement (5) est utilisée pour contenir l'échantillon (16), ayant une épaisseur de 20 mm, et cisailier l'échantillon en son centre sur un plan de cisaillement horizontal. Elle est composée de quatre anneaux (12 à 15) et d'une pierre poreuse (17). Les anneaux intérieurs ont un diamètre intérieur de 70 mm tandis que les anneaux extérieurs ont un diamètre intérieur de 100 mm. Les anneaux supérieurs sont immobiles pendant le cisaillement. Les anneaux inférieurs sont fixés sur un disque d'entraînement (11) qui tourne lors du cisaillement grâce à un servomoteur (7). Deux positionneurs

verticaux (6) permettent de soulever les anneaux supérieurs pour créer une ouverture au niveau du plan de cisaillement. Une charge verticale est appliquée sur le haut de l'échantillon à l'aide d'un vérin électrique (1). Une cellule de charge (2) mesure cette charge. Un potentiomètre (3) mesure la position verticale de l'échantillon. Deux aiguilles reliées à des capteurs de pression interstitielle (4) sont insérées dans l'échantillon. Un couplemètre (8) mesure le couple à l'échantillon, qui est convertie en valeur de résistance au cisaillement. Une vis sans fin (9) transmet la rotation. Un encodeur (10) mesure la position angulaire de l'échantillon.

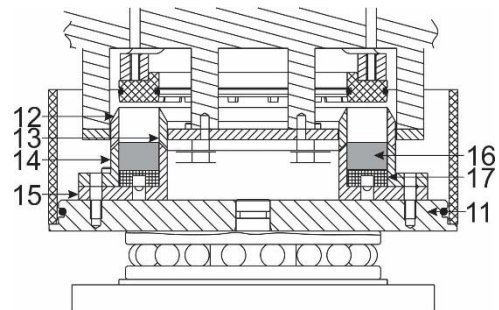


Figure 1 – Vue détaillée de l'appareil

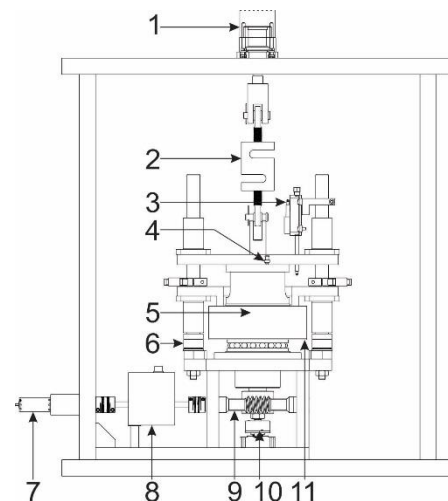


Figure 2 – Vue générale de l'appareil

La taille de l'échantillon est réalisée à même la boîte de cisaillement. Ceci permet, grâce à un bâti indépendant expressément conçu à cet effet, de conserver l'état intact de l'échantillon.

## Déroulement de l'essai

L'échantillon est d'abord consolidé sous une contrainte appliquée par le vérin. Les anneaux supérieurs sont ensuite soulevés afin de minimiser le frottement le long du plan de rupture. Par la suite, le moteur est actionné afin d'appliquer une vitesse de déformation angulaire constante sur l'échantillon et de débiter le cisaillement. La contrainte verticale appliquée par le vérin est alors contrôlée de façon à ce que la hauteur de l'échantillon demeure constante. Ainsi, puisque l'échantillon est confiné latéralement par les anneaux, son volume demeure constant. Ceci a pour effet de simuler des conditions de cisaillement non drainé similaires à celles décrites par Stark et Contreras (1996).

## Résultats préliminaires

Un essai a été réalisé sur un échantillon d'argile sensible prélevé à une profondeur de 6 m à l'aide de l'échantillonneur Laval sur le site de St-Alban, Qc. Selon le profil géotechnique présenté par Leroueil (1985), il s'agit d'une argile silteuse très sensible ayant une limite de plasticité de 20%, une limite de liquidité de 41%, une teneur en eau de 65%, une résistance au cisaillement non drainé mesurée au scissomètre de 22 kPa et un degré de surconsolidation de 2,3. La contrainte verticale de consolidation utilisée lors de l'essai était de 30 kPa. La vitesse de rotation utilisée était de 0,00765 mm/min. La figure 3 présente le comportement contrainte-déformation, à gauche, et le cheminement de contrainte, à droite.

## Discussion et conclusion

D'après la courbe contrainte-déformation, l'argile a un comportement anti-écrouissant. Un pic bien défini est atteint à une contrainte de cisaillement de 17,3 kPa et à un déplacement de 0,46 mm, ce qui représente 2,3% de la hauteur de l'échantillon. Le fait que le pic a été atteint à un faible déplacement témoigne de l'efficacité de la taille de l'échantillon à minimiser le remaniement de l'argile (Leroueil, 1997). Le cisaillement s'est poursuivi jusqu'à un déplacement de 11,38 mm, ce qui représente 56,9% de la hauteur de l'échantillon. La contrainte de cisaillement à ce moment était de 5,3 kPa. Il semble que le déplacement nécessaire à l'atteinte de conditions de résistance résiduelle n'a pas été atteint puisque la résistance semble encore diminuer à la fin de l'essai. De plus, un bruit de  $\pm 5\%$  est observé sur

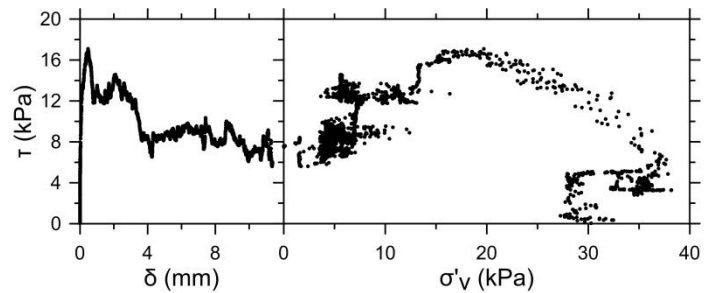


**Figure 3 - Contrainte de cisaillement en fonction du déplacement tangentiel et de la contrainte verticale effective**

les valeurs de contrainte de cisaillement. Ce bruit est dû au fait que la mesure du couple est réalisée avant la vis sans fin. L'indentation de cette pièce crée donc une oscillation du signal de la mesure. Relocaliser le couplemètre entre la vis sans fin et l'échantillon pourrait amenuiser le bruit. D'après le cheminement de contrainte (Figure 3), la contrainte verticale effective a diminué lors du cisaillement, passant de 30 kPa, soit la contrainte de consolidation, à 1,3 kPa. Cela signifie que l'échantillon présente un comportement contractant lors du cisaillement. Une dispersion importante est observée sur les valeurs de contrainte verticale effective. Ce problème est attribué à une instabilité du potentiomètre lors du cisaillement à volume constant qui sera corrigé lors des prochains essais. Ces résultats sont prometteurs. Une fois les modifications apportées, de nouveaux essais seront réalisés sur des échantillons d'argile sensible prélevés avec l'échantillonneur Laval à St-Jude, Qc, près du glissement de 2010 (Locat *et al.*, 2010). Les résultats seront utilisés afin de mieux comprendre le mécanisme de rupture progressive survenant le long de la surface de rupture lors des glissements de terrain dans les argiles sensibles.

## Références

- Leroueil, S. (1985). Remblais sur argiles molles. *Éditions Lavoisier*, Paris, France, p. 126.
- Leroueil, S. (1997). Geotechnical characteristics of eastern Canada clays. *Workshop on soft clays*, Yokosuka, Japon, 30 p.
- Locat, P., Fournier, T., Robitaille, D. et Locat, A. (2011). Glissement de terrain du 10 mai 2010 Sainte-Jude, Montérégie. Rapport sur les caractéristiques et les causes. *Ministère des Transports du Québec*, Rapport MT11-01, 77p.
- Stark, T. D. et Contreras, I. A. (1996). Constant volume ring shear apparatus. *Geotechnical Testing Journal*, 19(1) : 3-11.

# Dynamic response of rigid barrier under boulder-entrained debris flow impact



D. Song,  
C. W. Wai Ng,  
C. E. Choi,  
The Hong Kong University of Science and  
Technology, Hong Kong  
[dsong@connect.ust.hk](mailto:dsong@connect.ust.hk)

H. Y. Sze,  
Geotechnical Engineering Office, Civil Engineering  
and Development Department, Hong Kong SAR  
Government

## Introduction

Debris flows surge downslope with large momentum and comprise particles ranging from clay to boulder size. To intercept these hazardous flows, rigid reinforced concrete barriers are commonly installed along the predicted flow path (Kwan 2012). For simplicity, the design of rigid barriers treats the flow and boulder separately. Without a clear understanding of how boulders influence the mechanical response of a rigid barrier, there is little optimism for optimizing design guidelines.

Zhang (1993) and Hu *et al.* (2011) carried out field monitoring of natural debris flows and found that the large impulse loads on instrumented rigid obstacles

were mainly induced by the boulders. Likewise, at a smaller scale, flume modelling has been extensively used to investigate debris flow impact on structures (Scheidl *et al.* 2013; Choi *et al.* 2015; Cui *et al.* 2015). Soil-water mixtures with particle sizes ranging from 0.1–50 mm were adopted in these impact tests. However, it is evident that the distribution and contribution of the boulders on impact are not well understood and merit further investigation.

## Methodology

Centrifuge modelling allows the stress state of the flowing sediment, impact energy, and source volume to be scaled appropriately. In centrifuge modelling, the gravitational acceleration increases  $N$  times and linear dimensions (*e.g.* diameter of boulder and flow length) reduce  $N$  times, resulting in a scale factor of unity for velocity. The impact force  $F$  on the barrier has a scale factor of  $1/N^2$  (Ng *et al.* 2016). In addition, centrifuge tests can be carried out in a reliable and systematic manner, and eliminate the natural idiosyncrasies of a natural setting which are inevitable for field monitoring or large-scale tests (Iverson 2015).

The Geotechnical Centrifuge Facility at the Hong Kong University of Science and Technology (Ng *et al.* 2001) is used to study boulder-entrained debris impact against a 200 mm high model barrier. A similar model setup is introduced in Ng *et al.* (2016). The magnesium alloy model barrier has a Young's modulus (40 GPa) close to that of a reinforced concrete walls. One load cell was fixed behind the rigid barrier to measure the total impact load. A sampling rate of 20 kHz was adopted to capture the impact process. Both glass spheres and glass sphere-sand mixtures were adopted to simulate boulder-entrained debris flows impacting the rigid barrier. The glass spheres with diameters of 3 mm, 10 mm, 22 mm and 39 mm were tested. The 39 mm in model scale is equivalent to a 0.9 m prototype boulder under a gravitational level of 22.4  $g$ .

## Test results

Results reveal that for boulder diameters of 0.07 m in prototype (*i.e.* 3 mm in model scale) and 0.22 m (10 mm), the rigid barrier exhibits a hardening impact response without obvious individual impulses.

However, as the boulder diameter increase in size up to 0.50 m (22 mm), successive impulses from individual particles dominate the loading behavior.

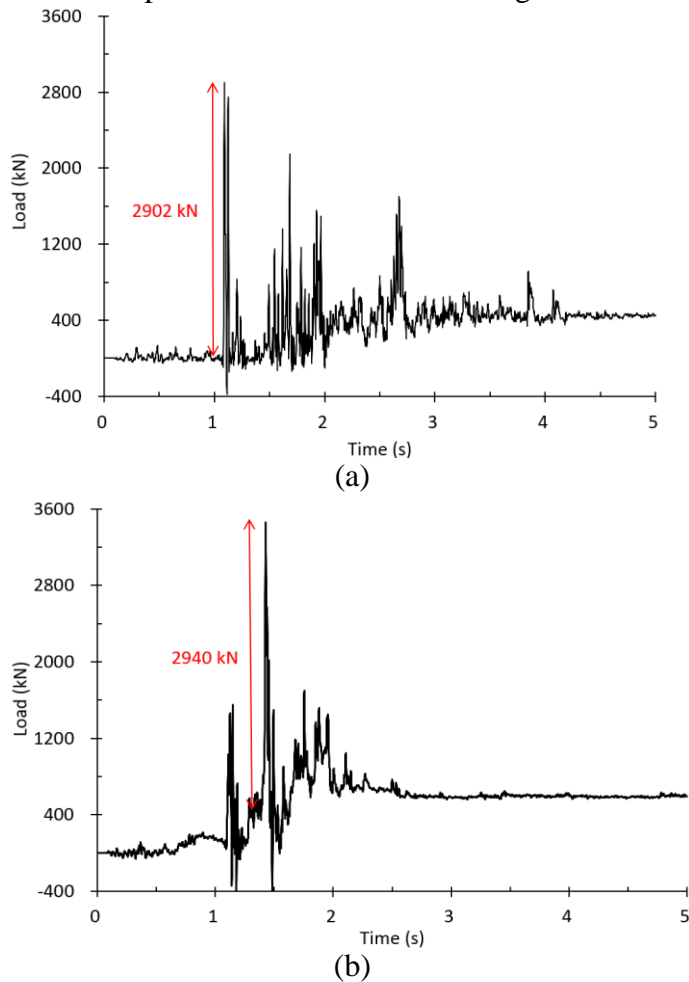


**Fig. 1: Measured impact loads: (a) 39 mm glass sphere and (b) 39 mm glass sphere-sand mixture**

Figure 1(a) shows the impact load induced from 0.9 m (39 mm) boulders. It is clear that the maximum discrete impulse loads correspond to the impact from the flow front. The peak load is about 5 times that of the static load. The time-history of the glass sphere-sand mixture impact is shown in Fig. 1(b). Less impulse loads are observed as the sand cushions the barrier from the boulders at impact. However, the peak load induced by the glass sphere-sand mixture is higher than that of pure glass sphere impact. This phenomenon is likely attributed to reverse segregation which means the larger particles are found in the upper layers of the flow. However, the chance of simultaneous impact of more than one 39 mm glass spheres resulting in the higher peak load cannot be precluded.

## Summary and conclusions

In this study, the response of rigid barrier under boulder-entrained flow impact is reported and preliminary results are discussed. Compared with pure glass sphere impact, glass sphere-sand mixtures exhibit less obvious impulse load. This may reflect the cushioning effect of the sand.

## Acknowledgment

The authors are grateful for financial support from research grant T22-603/15N provided by the Research Grants Council of the Government of Hong Kong SAR, China. This paper is published with the permission of the Head of the Geotechnical Engineering Office and the Director of Civil Engineering and Development, Hong Kong SAR Government.

## References

- Choi, C. E., Au-Yeung, S. and Ng, C. W. W. 2015. Flume investigation of landslide granular debris and water runup mechanisms. *Géotechnique Letters* 5(1): 28-32.
- Cui, P., Zeng, C., & Lei, Y. 2015. Experimental analysis on the impact force of viscous debris flow. *Earth Surface Processes and Landforms* 40(12), 1644-1655.
- Hu, K., Wei, F., & Li, Y. 2011. Real - time measurement and preliminary analysis of debris - flow impact force at Jiangjia Ravine, China. *Earth Surface Processes and Landforms* 36(9), 1268-1278.
- Iverson, R. M. 2015. Scaling and design of landslide and debris-flow experiments. *Geomorphology* 244, 9-20.
- Kwan, J. S. H. 2012. Supplementary Technical Guidance on Design of Rigid Debris-resisting Barriers. *GEO Report No. 270*. Geotechnical Engineering Office, HKSAR Government.
- Ng, C. W. W., Song, D., Choi, C. E., Koo, R. C. H., and Kwan, J. S. H. 2016. A novel flexible barrier for landslide impact in centrifuge. *Géotechnique Letters*. DOI: 10.1680/jgele.16.00048
- Ng, C.W.W., Van Laak, P.A., Tang, W.H., Li, X.S., & Zhang, L.M. 2001. The Hong Kong geotechnical centrifuge. In *Proceedings of the 3rd International Conference on Soft Soil Engineering*, pp. 225-230.
- Scheidl, C., Chiari, M., Kaitna, R., Müllegger, M., Krawtschuk, A., Zimmermann, T., and Proske, D. 2013. Analysing debris-flow impact models, based on a small scale modelling approach. *Surveys in Geophysics* 34(1): 121-140.
- Zhang, S. 1993. A comprehensive approach to the observation and prevention of debris flows in China. *Natural Hazards* 7(1), 1-23.

# Freezing characteristics of fluid fine tailings and their relation to unsaturated soil properties



H.L. Schafer  
University of Alberta, Edmonton  
[hvandalf@ualberta.ca](mailto:hvandalf@ualberta.ca)

N.A. Beier  
University of Alberta, Edmonton  
[nabeier@ualberta.ca](mailto:nabeier@ualberta.ca)

## Introduction

In order to produce oil, bitumen is extracted from mined oil sands ore through water-based processes, which result in the production of a tailings slurry. The tailings slurry is composed of water, sands, fines, and a small amount of residual bitumen (Sorta et al. 2013). The tailings are discharged to a settling basin, which allows the sand fraction to settle quickly near the entrance points with the remaining fluid fine tailings (FFT) settling in the center (Kabwe 2014). FFT is considered non-trafficable as it is essentially in the liquid state with no shear strength (Sorta et al. 2012). The FFT must be sufficiently de-watered in order to develop shear strength for the creation of trafficable land that would support equipment and allow

reclamation activities to progress. Many methods are currently being employed to dewater the FFT and promote the development of shear strength, including atmospheric drying.

Atmospheric drying requires the unsaturated soil properties to be known in order to predict the rate of dewatering and magnitude of strength gain. These properties can be estimated using the soil water characteristic curve (SWCC). The current methods for determining the SWCC are time consuming and challenging (Liu et al. 2012). As a result, it is becoming increasingly important to develop alternative methods to estimate and measure the SWCC. One such method is to estimate the SWCC based on the soil freezing characteristic curve (SFCC). The objective of the research is to evaluate the applicability of using the SFCC to determine the SWCC in different tailings materials. The oil sands tailings that will be tested are thickened tailings, and centrifuge tailings. Gold tailings will also be tested for comparison to the oil sands tailings. The validity of the apparatus and testing method will be confirmed by testing Devon Silt and comparing the results to Azmatch et al. (2012).

## *Similarity between the SWCC and SFCC*

It is possible to estimate the SWCC from the SFCC of a particular soil because the forces that prevent water from draining also prevent it from freezing (Spaans and Baker 1996). This is due to the fact that the process of wetting and drying in unfrozen soils is similar to the process of freezing and thawing in frozen soils (Lui et al. 2012). When a soil dries, water is removed and replaced by air, which decreases the matric potential of the remaining water (Azmatch et al. 2012). This process also occurs when a soil freezes where the water changes phase and becomes ice (Azmatch et al. 2012). The SFCC will be determined using time domain reflectometry (TDR) probes and resistance temperature detectors (RTDs). The TDR probes will be used to determine the unfrozen volumetric water content and the RTDs will be used to determine the temperature (Azmatch et al. 2012). The temperature measurement will be used to estimate the

suction in the soil at various unfrozen volumetric water contents using the Clapeyron equation (Azmatch et al. 2012). To determine the validity of the SFCC to estimate the SWCC, conventional SWCC measurement techniques will be conducted on the FFT samples.

#### *Influence of Salinity on the SFCC*

When a salt is added to the pore fluid of a soil, the freezing point of the pore fluid will be depressed (Williams 1964). The freezing point depression from salts present in the pore fluid is approximately proportional to the concentration of the salt (Williams 1964). As the soil freezes and ice forms, the salt is rejected resulting in an increase in salt concentration in the pore fluid (Banin and Anderson 1974). This will increase the freezing point depression and will impact the unfrozen water content and thus the SFCC. As a result, geochemical analyses will also be conducted on the tailings to evaluate the influence of pore fluid chemistry on the SFCC.

#### **Expected Results**

Work is ongoing to review and improve the testing apparatus and update it as needed. It is expected that the results from the SFCC testing on the Devon Silt will be similar to the results attained from Azmatch et al. (2012) as shown in Figure 1. This shows a close match between the SFCC and SWCC for Devon Silt consolidated to a pressure of 50 kPa and 100 kPa with no salinity.

Azmatch et al. (2012) also conducted testing to evaluate the impact of salinity on the SFCC by testing Devon Silt with a salinity of 5 g/L to a pressure of 50 kPa. As shown in Figure 1, this had substantial impacts on the SFCC due to the freezing point depression. The SWCC is not impacted by the influence of solutes in the pore fluid. As a result, there is a mismatch between the SFCC and the SWCC. This effect is not expected to be as extreme for the oil sands tailings as the salinity is much lower in these materials.

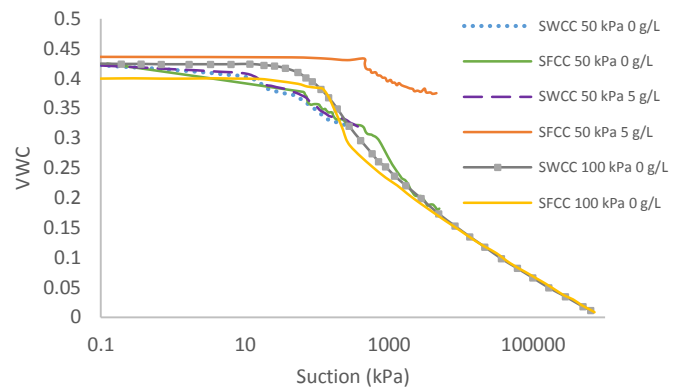


**Figure 1: Expected results for Devon Silt (adapted from Azmatch et al. 2012)**

#### **References**

- Azmatch, T.F., Segoo, D.C., Arenson, L.U. and Biggar, K.W. 2012. Using Soil Freezing Characteristic Curve to Estimate the Hydraulic Conductivity Function of Partially Frozen Soils. *Cold Regions Science & Technology* 83-84: 103-109.
- Banin, A., Anderson, D. M. 2012. Effects of salt concentration changes during freezing on the unfrozen water content of porous materials. *Water Resources Research* 10(1): 124-127.
- Kabwe, L.K., Scott, J.D., Wilson, G.W. and Sorta, A.R. 2014. From fluid to solid: Oil sands fluid fine tailings. *7<sup>th</sup> International Congress on Environmental Geotechnics; Proc. Intern. Congress, Melbourne, Australia, 10-14 November 2014.*
- Liu, Z., Zhang, B., Yu, X., Zhang, B., and Tao, J. 2012. A New Method for Soil Water Characteristic Curve Measurement Based on Similarities Between Soil Freezing and Drying. *Geotechnical Testing Journal* 35(1): 1-9.
- Sorta, A.R., Segoo, D.C. and Wilson, G.W. 2013. The Behaviour of Oil Sands Fines-Sand Mixture Tailings. *Canadian Institute of Mining* 4(4): 265-280.
- Sorta, A.R., Wilson, G.W. and Segoo, D.C. 2012. Effect of Thixotropy and Segregation on Centrifuge Modelling. *International Journal of Physical Modeling in Geotechnics* 12(4): 143-161.
- Spaans, E.J.A., and Baker, J.M. 1996. The soil freezing characteristic: Its measurement and similarity to the soil moisture characteristic. *Soil Science Society of America*, 60(1): 13-19.
- Williams, P. J. 1964. Unfrozen Water Content of Frozen Soils and Soil Moisture Suction. *Geotechnique* 14(3): 231-246.

# Technical Session 2

# Geohazards and Slope Stability

## Preliminary synthesis of spreads in Canadian sensitive clays



A. Locat  
Département de génie civil et de génie des eaux,  
Université Laval, Québec  
[ariane.locat@gci.ulaval.ca](mailto:ariane.locat@gci.ulaval.ca)

### Introduction

Spreads are one type of large landslides occurring in Canadian sensitive clays. They are characterized by the extremely rapid lateral spreading of a series of coherent clay blocks, having horsts and grabens shapes and moving on a layer of remoulded clay as presented in Fig. 1 (Hung et al. 2014). They constitute 37% of the 108 large landslides inventoried by the Ministère des Transports du Québec (MTQ) in Quebec (Demers et al. 2013). Based on witnesses, spreads generally occur rapidly, without any apparent warning sign, and cover large areas (> 1 ha). In addition, conventional stability analyses give too large safety factors when applied to this landslide type. Spreads are therefore serious threats to population and infrastructures on sensitive clays and the need for tools enabling their prediction and mitigation is quite necessary.

In the past decades, Université Laval and MTQ have collaborated on detailed geotechnical investigations of 7 cases of spreads in sensitive clays.

This paper presents an overview of the preliminary synthesis of these detailed case studies and also incorporates partial information from other cases of spreads from the literature and MTQ's database. The details of this study are presented in Locat et al. (2016).

### Methodology

For most cases, topographic data from before and after the landslide were obtained from aerial photographs and Light Detection and Ranging surveys (LIDAR). Careful examination of photographs taken on site soon after each event (from literature and MTQ's database) and site visits, when possible, was useful to obtain information on the morphology and the particular debris of these landslides. Boreholes, cone penetration tests with pore pressure measurement (CPTUs), vane shear tests and piezometer data were obtained for most of these cases. In addition, geotechnical properties as plasticity index ( $I_p$ ), liquidity index ( $I_L$ ), clay content (< 2  $\mu\text{m}$ ), intact and remoulded shear strength ( $S_u$  and  $S_{u,r}$ ) and overconsolidation ratio (OCR) were also obtained for most cases.

### Morphology of spreads

Study of spreads shows their retrogression distance varies from 80 to 580 m. Their width varies from 140 to 1045 m. Their width is generally larger than their retrogression distance. They typically have a rectangular or half-circular shape (see Fig. 1a). However, their shape can somewhat vary if they are constrained by topographic barriers (ex: deep gullies or older landslide scar). Generally, craters of spreads are filled with several ridges created by horsts separated by grabens, as can be seen on Fig. 1b presenting a photograph of the debris of the spread that occurred at Saint-Luc-de-Vincennes on September 25<sup>th</sup> 1986. Horsts are blocks of more or less intact clay having sharp tips pointing upward. Grabens are blocks of more or less intact soil having flat horizontal tops with trees that can still stand straight after the movement. Horsts and grabens are generally separated by other debris more disturbed or strongly remoulded.

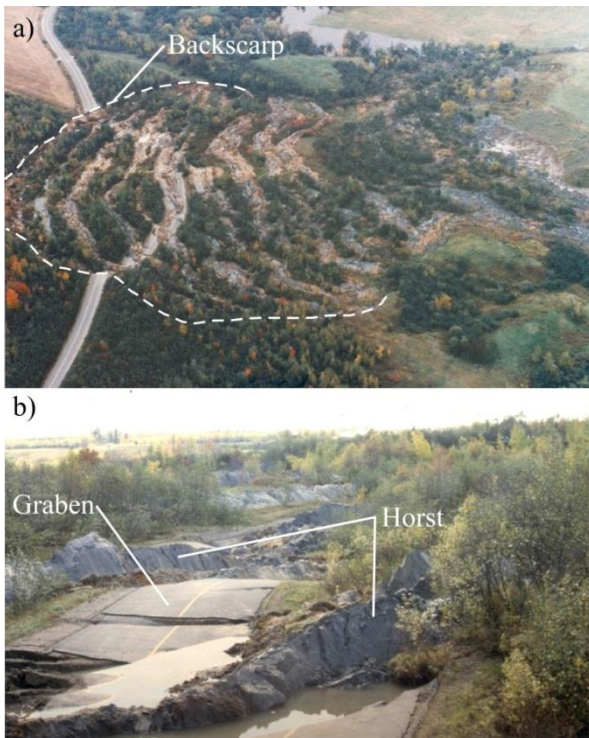


**Figure 1: Photograph of the spread that occurred at Saint-Luc-de-Vincennes showing: a) an oblique general view of the landslide and b) horsts and grabens in the debris (photos courtesy of MTQ).**

### Failure surface location

Failure surface in clayey material can be located by comparing CPTU tip resistance ( $q_t - \sigma_v$ , where  $q_t$  is the CPTU tip resistance corrected for water pressure and  $\sigma_v$  is the total vertical stress) performed in intact soil near the landslide and inside the landslide scar. The failure surface was located for the 12 spreads studied (Locat et al. 2016). It was found to be almost horizontal and located at the elevation of the toe of the slope, or 1 to 2.5 m above or below it.

Investigation of the landslide that occurred at Saint-Jude on May 10<sup>th</sup> 2010 shows that the failure surface developed at an elevation 2.5 m below the river bed and propagated 100 m horizontally and then went up by about 10 m to propagate an additional 50 m. The presence of more than one level of failure surface was also detected for the spreads that occurred at Brownsburg and Casselman and at some other sites investigated by MTQ (Locat et al. 2016). These cases indicate the occurrence of several failure events during these landslides and reveal that spreads can be complex and need detailed investigations in order to understand the kinematics involved during failure.

### Geotechnical properties of the soil involved

The detailed synthesis of spreads from Locat et al. (2016) shows that most spreads occurred in silty clays ( $< 2 \mu\text{m}$  between 27 to 87%) having  $I_p$  varying from 3 to 40% and  $I_L$  varying from 1.0 to 5.0. Remoulded shear strength is consistent with  $I_L$  values and can be lower than 0.07 kPa. Most of the spreads studied occurred in nearly normally consolidated soft clays ( $10 \text{ kPa} < S_u < 35 \text{ kPa}$  and  $\text{OCR} \approx 1.1$ ), as seen for the spread that occurred at Brownsburg. However, the spreads that occurred at Saint-Boniface and Saint-Barnabé occurred in firm overconsolidated clay ( $S_u > 50 \text{ kPa}$  and  $\text{OCR} > 1.3$ ). Geotechnical properties at the elevation of the failure surface are similar to the ones in the soil mass above it. It is worth noting that no softer or more sensitive soil layer has been observed at the level of the failure surface.

### Conclusion

The concluding remarks concerning spreads resulting from this synthesis are:

- Contrary to flowslides, spreads' craters are filled with more or less remoulded debris having horsts and grabens shapes;
- Stratifications in horsts and grabens are generally horizontal, indicating translation with only little rotation of the debris;
- Failure surface is generally continuous along several tens of meters and close to the horizontal.
- Weak layers cannot explain failure surfaces location in the cases mentioned in this study;
- Spreads occur in clays having a range of geotechnical properties. There does not seem to have a given set of geotechnical properties that can define their occurrence.

Given this study, earthflows cannot be considered the only landslide type occurring in sensitive clays.

### References

- Demers D., Locat P., Robitaille D., Potvin 2013. Inventory of Large Landslide in Sensitive Clay in the Province of Québec, Canada : Preliminary Analysis. In *Landslides in Sensitive clays – From Geosciences to Risk Management*, L'Heureux et al. eds. Springer, p. 77-89.
- Hungr, O., Leroueil, S. and Picarelli, L. 2014. The Varnes classification of landslide types, an update. *Landslides*. 11: 167-194.
- Locat A., Demers D. and Leroueil S. 2016. Spreads in Canadian sensitive clays. In: Proceedings of the 12<sup>th</sup> International Symposium on Landslides. Napoli, Italy, June 12<sup>th</sup>-19<sup>th</sup> 2016. 8p. In press.

## Emergency riverbank stabilization of Lyndale Drive in Winnipeg, Manitoba



M. J. Van Helden  
TREK Geotechnical Inc., Winnipeg, MB  
[mvanhelden@trekgeotechnical.ca](mailto:mvanhelden@trekgeotechnical.ca)

### Introduction

Lyndale Drive is a local residential collector street and primary flood protection dike that runs adjacent to the Red River in Winnipeg, Manitoba. In 1976, about 575 m of the riverbank was regraded (flattened) and a timber pile retaining wall was installed along the top of bank to isolate the roadway from riverbank movements. In 2000, the timber pile wall was extended about 100 m downstream with longer timber piles and tie-back anchors for enhanced stability.

In April 2013, about 300 mm of horizontal movement and 100 mm of settlement occurred within the pavement of Lyndale Drive at the downstream end of the 1976 wall, as shown in Figure 1. TREK was retained by the City of Winnipeg to provide riverbank monitoring as well as emergency design and construction of riverbank stabilization measures.



Figure 1 – Upper Bank Head Scarp

### Failure Mechanism

As part of the design phase, riverbank instrumentation including vibrating wire piezometers and slope inclinometers were installed on both sides of the timber pile wall to evaluate groundwater conditions and to delineate the failure mechanism. Sub-surface stratigraphy consists of a thin layer of clayey silt overlying about 15 m of high-plastic lacustrine clay and dense silt till.

The interpreted failure mechanism consisted of a loss of passive resistance on the downslope side of the retaining wall due to deep-seated riverbank movements, followed by the development of a failure wedge behind the wall and into the pavement. Rotation and lateral displacement of the retaining wall was apparent, which supports this interpretation.

### Stabilization Design

Emergency stabilization works were designed in July, tendered in August and constructed in September and October, 2013. Soil replacement in the form of rockfill columns were used to increase the factor of safety of the riverbank instability. Rockfill columns have been used extensively and successfully in the Winnipeg and surrounding areas for stabilization of riverbanks since the 1980's. Research conducted at the University of Manitoba including large-scale direct shear testing of crushed limestone rockfill and scale models (Kim, 2007; Abdul Razaq, 2007) and full-scale field testing (Thiessen et al, 2008) has advanced local knowledge and improved design and construction techniques. Although large-scale direct-

shear testing of well-compacted rockfill suggests that a peak friction angle of up to  $\phi' = 65^\circ$  is possible, design was based on a conservative value of  $\phi' = 45^\circ$ , attributed to potential construction difficulties and uncertainty in the degree of rockfill compaction.

A back-analysis of the observed instability was used to establish shear strength parameters for the various soil layers. The Lacustrine clay layer was divided into three distinct zones based on various degrees of observed movement as shown in Figure 2. Increased shear strains can be associated with increased strain-softening (weakening) of the otherwise intact clay. The back-analysed shear strength parameters within the zone of the observed instability (down-slope of the wall) are representative of residual strengths for Winnipeg clays.

The rockfill columns were represented in the limit-equilibrium slope stability model as a series of trench shear keys, each representing a row of columns, in order to determine the area replacement ratio (in plan view) required to achieve a minimum improvement of 30% relative to existing stability ( $FS = 1.30$ ). As shown in Figure 2, a 4.5 m wide equivalent shear key combined with fill placement (required to eliminate the retaining wall) achieved the target factor of safety.

The rockfill column layout required to achieve an area replacement of 4.5 m<sup>2</sup> per lineal metre of riverbank consists of 4 rows of 2.1 m diameter rockfill columns with a clear (edge to edge) spacing of 0.9 m, as shown in Figure 3.

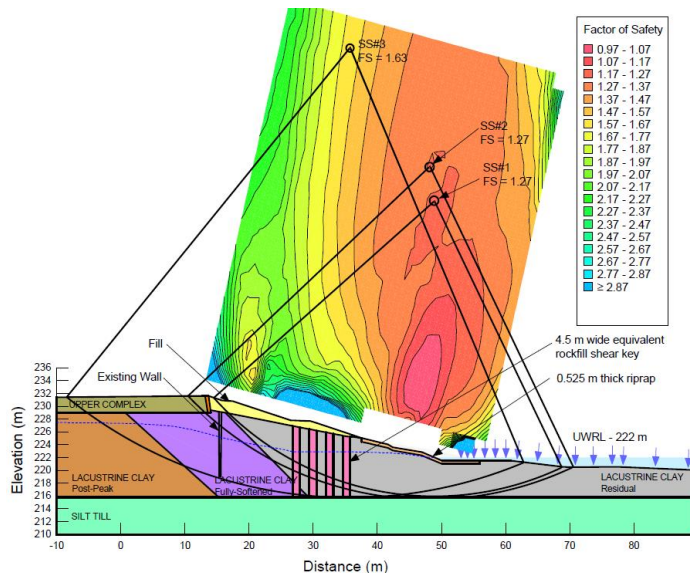


Figure 2 – Proposed Stabilization Works

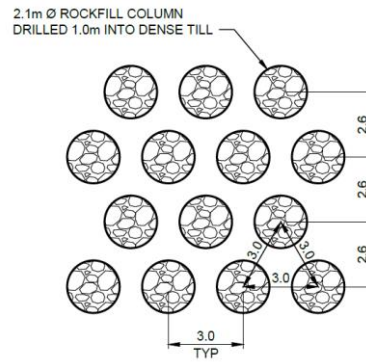


Figure 3 – Rockfill Column Layout

Displacement rates prior to stabilization were up to 200 mm per week. Monitoring results after construction (Figure 4) indicate that the rate of displacement in slope inclinometers quickly reduced following the installation of rockfill columns. Ongoing movements of about 5 mm per year continue to occur. Placement of the fill to eliminate the wall is planned for the spring of 2017.

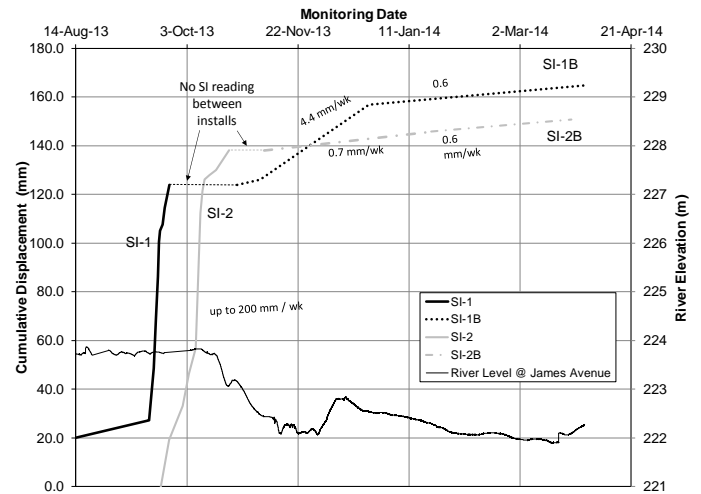


Figure 4 – Post-Construction Monitoring Results

## References

- Thiessen, K., Alfaro, M. and Blatz, J. 2008. Monitoring Results from a Full-Scale Field Test of Rockfill Columns, *Geo-Edmonton '08, Canadian Geotechnical Conference*: Edmonton, Alberta, Canada.
- Abdul Razaq, W.F. 2007. Evaluation of Riverbank Stabilization using Rockfill and Soil-Cement Columns. Ph.D., University of Manitoba.
- Kim, C.S. 2007. Evaluating Shear Mobilization in Rockfill Columns Used for Riverbank Stabilization. M.Sc., University of Manitoba, Winnipeg.

# Building a rockfall database using remote sensing data: Applications for hazard management in Canadian rail corridors



M. van Veen, D. J. Hutchinson  
Queen's University, Kingston ON  
[m.van.veen@queensu.ca](mailto:m.van.veen@queensu.ca)

M. Lato, D. Gauthier  
BGC Engineering Inc., Ottawa/Kingston ON

T. Edwards  
CN Rail, Edmonton AB

## Introduction

Railways in Western Canada are subject to frequent rockfall hazards, which have the potential to cause disruptions to service, damage to infrastructure, and can present risk to railway personnel working on these slopes. The section of railway between Ashcroft and Hope, in British Columbia is especially susceptible to these hazards and the proximity of the railway to the Fraser and Thompson rivers limits the ditch retention capacity for rockfall.

The use of a rockfall database can aid in the management of the railway in these hazardous settings, and can help to determine the return period for certain volume of failure. While traditional rockfall inventories may contain approximate estimates of rockfall event timing and volumes, these records are often incomplete for slopes where rock fall activity is frequent. We present a case study where remote sensing techniques are used to create a database of rockfall events.

The study site, known as the White Canyon, is located approximately 250 km north-east of Vancouver, near the town of Lytton (Figure 1). It is possible to see rockfalls and slides of varying magnitudes and failure mechanisms in the canyon as the fracturing and alteration exist on many different scales (Gauthier et al. 2012). Terrestrial LiDAR has been collected at the site since 2012 and rockfalls ranging in size from 0.01 to 2600 m<sup>3</sup> have been identified using these methods.

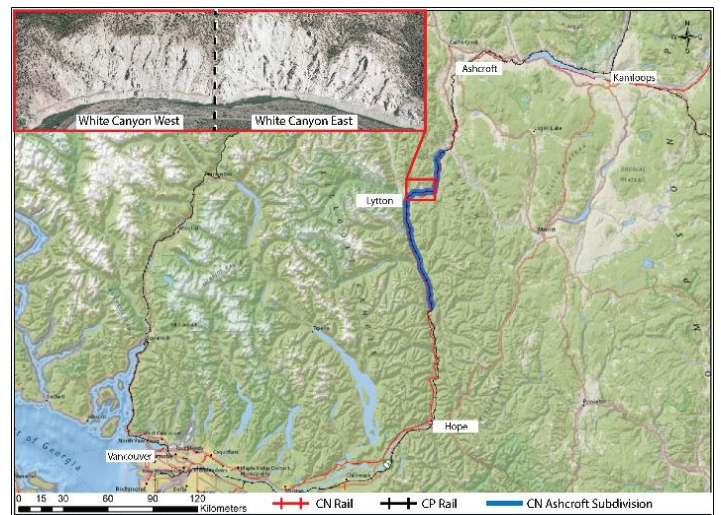


Figure 1: Site location of the White Canyon

## Data and Methods

The data collected at the site includes four years of terrestrial LiDAR data (collected every few months) as well as photogrammetry data for select dates. The LiDAR data is aligned to a common reference frame such that change detection can be performed to identify rockfall events. Photogrammetry data is used to create a 3D model of the slope which can be classified in terms of lithological units to create a fully

3D model of the slope, which can also be aligned to the LiDAR datasets.

Using the measured change between sequential LiDAR scans, we can automatically identify thousands of rockfall events on the slope based on methods outlined in Carrea et al. (2014) and Tonini and Abellan (2014), and use this data to build a database of events including rockfall locations and magnitudes. We can automatically relate these events to the classified photogrammetry model to determine the lithology of each event. Photos that were taken at the same time as the LiDAR scans help us to validate the rockfall events and to evaluate the structural conditions of the rockmass. An example of a 15 m<sup>3</sup> rockfall (that occurred about 10 m above the tracks) identified using this process is shown in Figure 2.

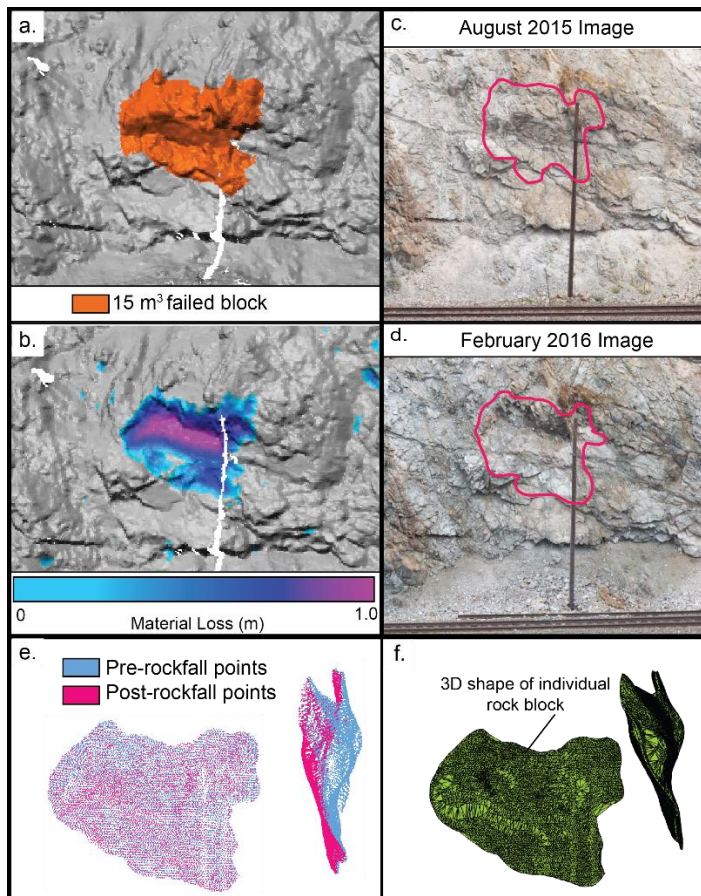


**Figure 2: Identification of 15 m<sup>3</sup> rockfall**

### Outcomes

Once the database has been populated, the information can be used to understand the frequency-magnitude relationship for the slope, and therefore to estimate the return period for rockfall events of varying sizes. In addition, the 3D nature of our data allows us to understand spatially where rockfalls of different

magnitudes are occurring and how these patterns vary over time. These patterns are useful to the railway for planning maintenance activity (scaling of rock sheds, and clearing of ditches). Input of the information from this database (source zone locations, block sizes and shapes) into rockfall models can aid in the planning of future mitigation options such as the installation of new rock sheds, fences or mesh along the slope.

Separation of the rockfall events into their respective lithologies and comparing the frequency of events to the area of each unit can help us to understand the relative frequency of rockfalls for different areas of the slope. We can also relate these rockfall events to triggering factors such as precipitation and freeze-thaw activity. Separation of rockfalls into their respective lithologies during this process may help future understanding of how units may differ in terms of failure kinematics.

While many of the rockfalls we identify are small enough in volume that they likely wouldn't present a hazard to the rail network, Kromer et al. (2015) identified that large failures can be preceded by a series of smaller precursor events, as well as deformation of the rockfall sources. Therefore, it is important to not discount these small failures for the safe operation of the railway.

This method of collecting rockfall data provides significant advantages over traditional methods of inspection and monitoring, including the rockfall slide detector fences, in building a complete database of rockfall events for hazard management.

### References

- Carrea, D., A. Abellan, M.-H. Derron, and M. Jaboyedoff. 2014. Automatic rockfall volume estimation based on terrestrial laser scanning data. *Engineering Geology for Society and Territory* 2: 425-428.
- Gauthier, D., M. Lato, T. Edwards, and D. Hutchinson. 2012. Rockfall and talus accumulation from serial LiDAR scans: a railway case study from the White Canyon, Thompson River, BC. *GeoManitoba*. Winnipeg, MB, Canada.
- Kromer, R., D.J. Hutchinson, M. Lato, D. Gauthier, and T. Edwards. 2015. Identifying rock slope failure precursors using LiDAR for transportation corridor hazard management. *Engineering Geology* 195: 93-103.
- Tonini, M., and A. Abellan. 2014. Rockfall detection from terrestrial LiDAR point clouds: a clustering approach using R. *Journal of Spatial Information Sciences* 8: 95-110.

# A forensics study of the deformation and structural controls on rockfalls in White Canyon using terrestrial LiDAR



E. Rowe  
Queen's University, Kingston ON  
[emily.rowe@queensu.ca](mailto:emily.rowe@queensu.ca)

D. J. Hutchinson, R.A Kromer  
Queen's University, Kingston ON

## Introduction

Rockfalls are a major hazard in the mountain ranges of western Canada, posing a risk to human populations, infrastructure, and the natural environment. This type of landslide is characterized by the detachment of an intact unit of rock material followed by a rapid downward movement driven by gravity (Higgins et al. 2012). Rockfall blocks can take on a range of shapes and sizes, with no well-defined upper limit on a rock block's maximum volume (Higgins et al. 2012).

This type of hazard is especially pronounced in the rocky slopes of White Canyon, situated on the Thompson River (Figure 1). Canadian National (CN) and Canadian Pacific (CP) Railways share two rail lines that pass through this corridor. The rock masses in White Canyon are weak and highly foliated, making

them prone to frequent rockfalls. With a limited ditch capacity adjacent to the rail tracks, these rockfalls often deposit material directly on the tracks, leading to an increased risk of train derailment.

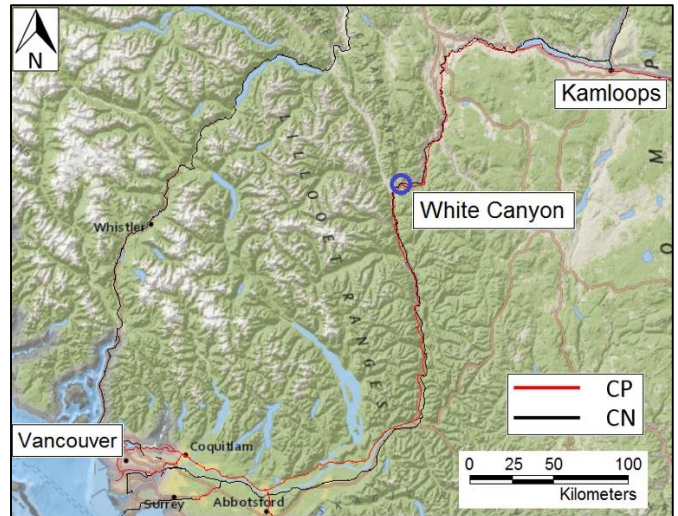


**Figure 1. Map of southwestern British Columbia highlighting CN and CP routes; note White Canyon study area circled in blue**

The primary objective of this study is to gain an improved understanding of the pre-failure deformation patterns experienced by rockfall source zones as constrained by structural discontinuity planes.

## Data and Methods

In the present study, a stationary terrestrial LiDAR device is used to collect three-dimensional point cloud data of the White Canyon (Figure 2). Laser scanning at this site has been carried out episodically at time intervals ranging from days to months since 2012 as part of the Railway Ground Hazard Research Program (RGHRP).

The data is first processed to remove vegetation or parts of the slope captured in the LiDAR scan that are not intended to be part of the analysis. Change detection is then executed by aligning individual scans to a reference dataset using InnovMetric PolyWorks software. Polyworks then computes a shortest distance measurement between points of the reference and aligned scan to produce a coloured change detection map. In this image, areas of material loss and accumulation are highlighted and thus rockfalls may be identified.

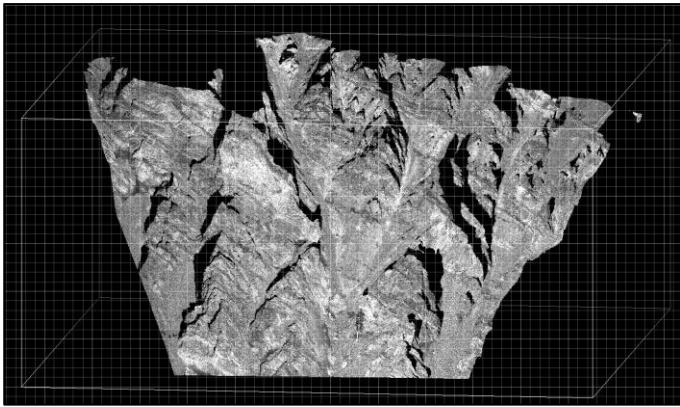


**Figure 2. LiDAR point cloud dataset of White Canyon collected February 18, 2016.**

Once a rockfall has been detected, the volume may be determined (van Veen 2016) and earlier scans of the rockfall source area may be studied to better understand the mechanisms that led to failure. An algorithm developed by Kromer et al. (2014) based on the methods of Oppikofer et al. (2009) was implemented for this purpose. This algorithm calculates the precise translations and rotations that the rock block underwent between the time of the reference dataset (in this case a dataset from 2013) and a more recent dataset. This calculation is repeated for multiple successive scans between 2013 and the failure date to quantify the cumulative deformation experienced by the rockfall source zone before failure occurred.

The post-failure dataset is also studied to observe the structural discontinuities exposed after the block has detached from the surface. The orientation of these planes is calculated and plotted on a stereonet to determine the type of failure mechanism experienced by the rock block.

## Results

Preliminary deformation analyses reveal that rock blocks typically displace several centimeters prior to failure (Kromer et al. 2014).

One rock block that fell between June and August 2015 was classified as a planar slide failure and sustained approximately 2 cm of deformation before failure. The orientation of structural discontinuities constraining this block suggest that wedge failure mechanisms were also possible; however, a closer

visual inspection of the LiDAR data affirms that planar sliding was likely the dominant mechanism in this case.

## Next Steps

By conducting repeated analyses as described above, a database of rockfalls with their deformation and failure mechanism trends will be created. Once populated, this database will allow for further investigation of the relationships between deformation and structural constraints of rockfalls in White Canyon.

## References

- Higgins, J.D. and Andrew, R.D. 2012. Rockfall: Characterization and Control. National Academy of Sciences, Washington D.C.
- Kromer, R.A., Hutchinson, D.J., Lato, M.J., Gauthier, D., and Edwards, T. 2014. Identifying rock slope failure precursors using LiDAR for transportation corridor hazard management. *Engineering Geology*, 195: 93-103.
- Oppikofer, T., Jaboyedoff, M., Blikra, L., Derron, M-H., and Metzger, R. 2009. Characterization and monitoring of the Aknes rockslide using terrestrial laser scanning. *Natural Hazards and Earth System Sciences*, 9: 1003-1019.
- van Veen, M. 2016. Building a Rockfall Database using Remote Sensing Data: Applications for Hazard Management in Canadian Rail Corridors. In *Proceedings of the Canadian Young Geotechnical Engineers & Geoscientists Conference, Whistler, B.C., 29 Sept. – 1 Oct. 2016.*

## The August 6, 2010 Mount Meager landslide



C.A. Lau  
Simon Fraser University  
BGC Engineering Inc.  
[carieann\\_lau@sfu.ca](mailto:carieann_lau@sfu.ca)

### Introduction

We started the field day in Pemberton as we had many before, rising early to avoid the expected hot weather in the afternoon. However, as we drove up the Lillooet Forest Road, that day would prove to be anything but normal. As we rounded a corner near Mount Meager, we encountered a newly washed out bridge and an impassable road. While we knew landslides were common in this valley, we did not know that we had encountered the hours-old deposit of one of Canada's largest landslides.

This paper provides an overview of the landslide event, observations of the effects of the landslide induced sediment pulse, and hazard implications for the Pemberton Valley.

### August 6, 2010

#### *The Landslide*

At 0327h PDT on August 6, 2010 the southern summit of the Mount Meager volcanic massif collapsed and

fell approximately 500 m onto the talus slope on the flank below (Guthrie et al. 2012). The saturated talus slope fluidized into a rock avalanche and flowed down Capricorn Creek towards the Lillooet River Valley. As the debris transformed into a massive debris flow, it averaged speeds of 67 m/s (Guthrie et al. 2012). Upon reaching the valley confluence with Meager Creek, the debris flow ran 270 m up the opposite valley wall, deposited a 30-50 m high wedge of sediment, and created a landslide dam. The flow then spread across the Lillooet River Valley for a run out distance of approximately 12 km (Fig.1).

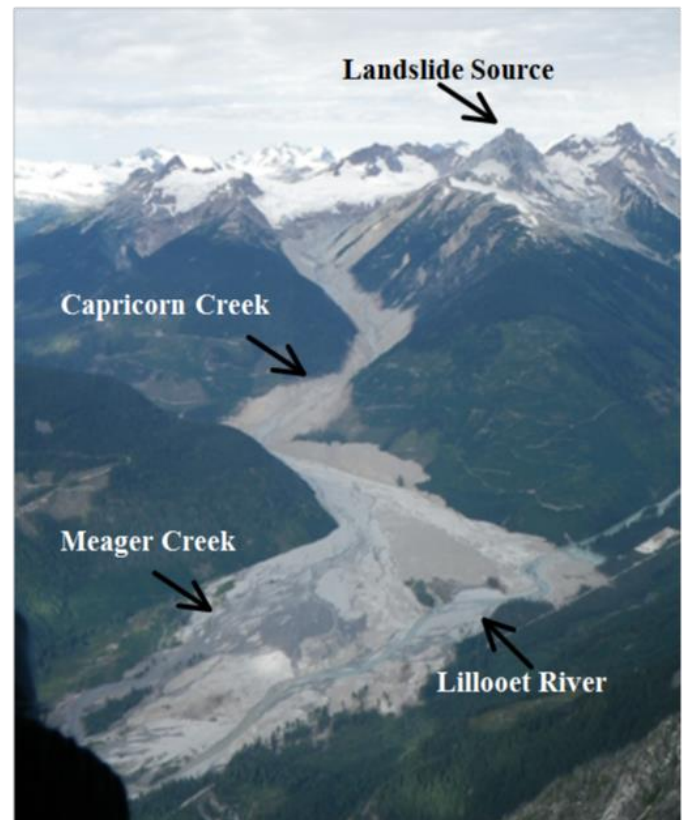


**Figure 1: An overview of the Mount Meager landslide. Photo taken on August 29, several weeks after the landslide dam had been breached. Subsequent water and debris flows eroded large sections of the landslide deposit.**

The cause of this landslide has been attributed to high groundwater conditions from a prolonged heat spell, glacial debuttressing of the massif since the Little Ice Age, and the weak nature of the volcanic rock due to hydrothermal alteration (Guthrie et al. 2012). The rock avalanche volume was estimated as 48.5 Mm<sup>3</sup>

(Guthrie et al. 2012). However, recent work suggests this may be an underestimation of the source volume (G. Roberti, pers. comm. 2016). The size of this landslide is comparable to the 1965 Hope landslide, the largest historical landslide in Canada.

### *Downstream Effects*

The landslide had a profound impact on the proximal and downstream river systems in the valley. The deposit partially blocked the Lillooet River for a short time and fully blocked Meager Creek for approximately 19 hours (Roche et al. 2011). As the landslide dam on Meager Creek was breached, it created a small flood wave that flowed downstream towards Pemberton. The landslide deposit introduced a large sediment pulse into the Lillooet River, an aggrading wandering gravel river system already near transport capacity (Fig. 2). Large volumes of gravel and sand were transported downstream during a rainfall-induced flood on September 28, 2010 (Lau 2011). During subsequent field investigations large gravel bars, numerous avulsion channels, and severe erosion of the forest road network were observed upstream of Pemberton. The sediment pulse potentially increased downstream flood hazards in the Mount Currie First Nations community due to the decreased river gradient from the accommodation of excess sediment (Roche et al. 2011).

### **Discussion**

There have been more than 25 prehistoric and historic landslides from the Mount Meager volcanic complex. Three of these prehistoric landslides travelled tens of kilometres downstream and reached the present location of Pemberton village (Friele et al. 2008). Additionally, Mount Meager is an active stratovolcano that last erupted approximately 2,300 years ago. Given these hazards, the Mount Meager valley was coined as the “most active and dangerous valley in the Canadian Cordillera” (Read 1990). Thankfully, during the 2010 event there were no recorded casualties and no buildings were damaged downstream in the communities of Pemberton Meadows, Pemberton, or Mount Currie. However, the destructive nature of this landslide and the evidence of larger prehistoric events demonstrate the high societal risk that Pemberton Valley residents face from Mount Meager landslides (Friele et al. 2008).



**Figure 2: Looking east downstream from the distal edge of the landslide (visible in lower right) towards the Pemberton Valley.**

### **References**

- Friele, P., Jakob, M., and Clague, J. 2008. Hazard and risk from large landslides from Mount Meager volcano, British Columbia, Canada. *Georisk* 2(1):48-64.
- Guthrie, R.H., Friele, P., Allstadt, K., Roberts, N., Evans, S.G., Delaney, K.B., Roche, D., Clague, J.J., and Jakob, M. 2012. The 6 August 2010 Mount Meager rock-slide-debris flow, Coast Mountains, British Columbia: characteristics, dynamics, and implications for hazard and risk assessment. *Natural Hazards and Earth System Sciences* 12:1277-1294.
- Lau (née Hancock), C.A. 2011. Geomorphic changes to Lillooet River due to the 2010 Mount Meager landslide. *Unpublished BSc.(Hons) thesis*. Simon Fraser University Department of Earth Sciences. 63 pages.
- Read, P.B, 1990. Mount Meager Complex, Garibaldi Belt, Southwestern British Columbia. *Geoscience Canada* 17 (3):167-170.
- Roche, A.D., Guthrie, R.H., Roberts, N.J., Ellis, E., and Friele, P. 2011. Once more into the breach: A forensic analysis of the August 2010 landslide dam outburst flood at Meager Creek, BC. *Proceedings of the 5<sup>th</sup> Canadian Conference on Geotechnique and Natural Hazards*. Canadian Geotechnical Society, May 15-17, 2011. Kelowna, BC.

# Technical Session 3

## Planning and Guidelines

## A call to arms: Sustainability in geotechnical engineering



S. McKean, P.Eng.  
University of Calgary  
[scott.mckean@ucalgary.ca](mailto:scott.mckean@ucalgary.ca)

### Introduction

The collision of geoenvironmental engineering and sustainability is inevitable. This paper and presentation review sustainability in infrastructure projects. It calls on young geotechnical practitioners to become skilled in sustainability and lead our clients, regulators, and vendors into a resilient world.

Sustainable development is an ancient concept embodied in a new term. The term was classically defined in *Our Common Future* as “development that meets the needs of the present without compromising the ability of future generations to meet their own needs” (Brundtland 1987). Yet, the concepts of environmental consciousness and stewardship already existed in Indigenous cultures for centuries (Beckford et al. 2010).

As engineers, we are tasked with building our environment, protecting the public, and providing resources for society’s growth. Our methods for

achieving this have rapidly improved due to advances in investigation techniques, predictive design methods, and monitoring technology. But economical designs that perform well are no longer enough. We need to operate within the larger framework of sustainable development and build sustainable infrastructure.

### Sustainable Infrastructure

The concept of sustainability has been in widespread use since the 1970s (Caradonna 2014), but it has only recently been applied to design and engineering. Quantitative rating systems that allow transparent communication of a project’s level of environmental performance following a well-defined methodology (Berardi 2012) have brought sustainable design into mainstream practice. These rating systems were limited to buildings (and their effects on occupants and the surrounding environment) but new rating systems have now been developed to quantify the impact of infrastructure projects on the environment, the economy, and society (i.e. the triple bottom line).

One of these systems, ENVISION®, was developed for infrastructure projects such as roads, pipelines, dams, and industrial facilities (it avoids occupant oriented buildings addressed in other systems). It can be used to evaluate social wellbeing and create a stronger social license to operate. In considering changing environmental conditions, it makes our designs more resilient and economical over the long term. It challenges us to restore our natural resources and ecosystems instead of contributing to their degradation. The system provides guidance for risk assessment beyond failure and serviceability, towards lifecycle of assessment of a whole project from cradle to grave. Innovation is transformed from simply designing better foundations to being the foundation for design itself (Institute for Sustainable Infrastructure and Zofnass Program for Sustainable Infrastructure 2015).

### Sustainable Engineering

Geotechnical engineering can easily promote sustainability due to its early involvement in a project’s lifecycle and influence on site selection and

earthworks. We cannot outsource sustainable design to our clients or external experts – we must take responsibility for it during the design process. It could be argued that every geotechnical design is sustainable because we strive to create the most economical design within the realm of acceptable risk and safety, but this isn't always the case.

The subsurface is infinitely complex, necessitating empirical and observational design approaches (Peck 1969). These methods, when coupled with powerful numerical resources, can be used within a sustainability-based framework to revolutionize how we design for the environment. For example, detailed terrain analysis using aerial geophysics and LIDAR can greatly assist in terrain avoidance when constructing linear infrastructure, which also reduces excessive erosion and material needs. Automated data collection, powerful computers with advanced algorithms and numerical models that move past simplified continuum mechanics into discrete elements or individual grain-based models can provide much more realistic predictions of ground response. We can investigate and evaluate project risks probabilistically instead of experientially.

Several fundamental changes are required to merge emerging technologies and design practices with sustainability. Geotechnical practitioners need to become conversant with sustainability and use it as a standard practice to push innovation. Advanced technology needs to be fully incorporated into drilling and construction methods (not only in design and modeling). Contracts for consulting and construction services need to allow ways to reduce waste and encourage innovative solutions (beyond just providing legal assurance). Regulatory standards that hinder sustainable solutions need to be carefully reviewed and modified if possible. Finally, we need to push our materials beyond a 50-year design life, which will require more research into long-term durability and truly understanding how the ground and foundation materials interact over several generations of time.

## Conclusion

Sustainability could lead to the world's third major socio-economic transformation (after the Agricultural revolution 10,000 years ago and the Industrial revolution in the 1800/1900s) (Caradonna 2014). To achieve this we need to question our current design practices and identify the factors that resist innovation in order for our profession to evolve in a changing

world that desperately needs resilience, leadership, and innovation to thrive.

## References

- Beckford, Clinton L., Clint Jacobs, Naomi Williams, and Russell Nahdee. 2010. "Aboriginal Environmental Wisdom, Stewardship, and Sustainability: Lessons From the Walpole Island First Nations, Ontario, Canada." *The Journal of Environmental Education* 41 (4): 239–48. doi:10.1080/00958961003676314.
- Berardi, Umberto. 2012. "Sustainability Assessment in the Construction Sector: Rating Systems and Rated Buildings." *Sustainable Development* 20 (6): 411–24. doi:10.1002/sd.532.
- Brundtland, Gro H. 1987. "Our Common Future: Report of the World Commission on Environment and Development." doi:10.1080/07488008808408783.
- Caradonna, Jeremy L. 2014. *Sustainability: A History*. Oxford University Press.
- Institute for Sustainable Infrastructure, and Zofnass Program for Sustainable Infrastructure. 2015. "Envision Rating System for Sustainable Infrastructure." Washington, DC.
- Peck, Ralph B. 1969. "Advantages and Limitations of the Observational Method in Applied Soil Mechanics." *Geotechnique* 19 (2). Thomas Telford Ltd: 171–87.

## Development of gravel shear key design guidelines for slope stabilization



H.F. Gillen  
University of Alberta, Edmonton  
[gillen@ualberta.ca](mailto:gillen@ualberta.ca)

### Introduction and purpose

Major transportation corridors in the form of highways and railroads typically run thousands of kilometers, resulting in high exposure to the hazard posed by landslides. In Canada, the road network comprises over 1.4 million kilometers of roads and boasts one of the highest kilometers per capita in the world (Statistics Canada 2006). Meanwhile, Canada's railway network is responsible for the annual delivery of over 70% of all intercity surface goods moved in Canada and half of Canada's exports (Railway Association of Canada 2011). Altogether, the transportation industry in Canada contributed 6.3% to the GDP in 2000 (Statistics Canada 2006), which demonstrates the importance of the road and railway networks to the Canadian economy. As a result, the active management and remediation of landslides is a multibillion dollar industry with a long history.

Landslide mitigation techniques can be used to slow down movement or stop landslides altogether (Cornforth 2005). Gravel shear keys are one such technique that has been used for decades, to varying degrees of success. The purpose of this research is to develop reliability-based design guidelines for landslide remediation using gravel shear keys based on quantitative results from case studies.

### Gravel shear keys for slope stabilization

#### *Gravel shear keys*

A gravel shear key is a deep trench that is excavated below the sliding surface of a landslide before being backfilled with granular material. This granular material possesses greater internal shear strength than the native soils it is replacing (Cornforth 2005). The shear key is intended to increase shearing resistance along the sliding surface by either having it shear through the stronger shear key material or forcing it to follow a deeper, longer path through more competent materials (Abramson, et al. 2002). However, the complexities of landslide geometries and materials require the consideration of a wide range of design parameters. Several parameters that must be considered include the depth of the shear key beyond the sliding surface, the width of the shear key, the angularity of the gravel, the contrast between the properties of the gravel and the sliding material, and the depth of the water table.

#### *Current practice*

Current design approaches for gravel shear keys rely on limit equilibrium analyses (Wyllie and Mah 2004) and altering the dimensions until the target factor of safety is attained. This method can be time consuming, and cannot wholly capture the complexities of resistance mobilized by deformation. This can result in designs that do not perform as expected. Typically, poor performance is observed in the form of deformations that go on for extended periods of time after remediation, resulting in continued damage to infrastructure and additional costs.

On the other hand, compensating to avoid such deformations can result in designs that use more gravel than is necessary. However, hauling gravel can be one

of the largest components of the cost for this type of remediation (Transportation Alberta 2003), (Williams 2015). Thus, it is important for designs to be as effective as is practical and for gravel volume estimates to be accurate.

#### *Case studies*

A number of gravel shear keys have been constructed in Western Canada over the last 20 years; for example, those in the Harrowby Hills Slides west of Russell, MB (Yong, et al. 2003), in the Peace Region west of Fairview, AB (Alberta Transportation 2003), and along Highway 43 south of Sturgeon Lake (Alberta Transportation and Karl Engineering Consultants, Ltd. 2007). Borehole instrumentation has been used in many of these cases to monitor slope conditions, including the rate of movement and changes in the groundwater level to gauge the success of the installed support systems. The documentation of these details provides an opportunity to develop performance-based design guidelines to enhance design reliability.

#### *Performance-based design guidelines*

Design guidelines and nomograms developed through this research are intended to simplify the design process by potentially providing a quick and reliable method to estimate the size of the shear key and volume of gravel required for a safe design.

The outputs of these guidelines and nomograms could serve as a means of confirming designs or providing a reliable starting point for more detailed designs. These improvements could make the use of gravel shear keys more cost effective and reliable, with the potential for saving time and money while making transportation routes more secure.

#### **References**

- Abramson, L.W, Lee, T.S., Sharma, S. and Boyce, G.M. 2002. *Slope Stability and Stabilization Methods*, 2<sup>nd</sup> ed. New York: John Wiley & Sons, Inc.
- Alberta Transportation. 2003. Part B: 2003 Site Visit – Landslide Risk Assessment – Peace Region (Peace River Valley/High Level). Edmonton: Government of Alberta.
- Alberta Transportation and Karl Engineering Consultants Ltd. 2007. 2007 Slide Tour Report: (GP10) Hwy 43:06 South of Sturgeon Lake. Edmonton: Government of Alberta.
- Cornforth, D.H. 2005. *Landslides in Practice*. Hoboken: John Wiley & Sons, Inc.
- Railway Association of Canada. 2011. Rail Facts. Accessed June 1, 2016. <http://www.railcan.ca/education/facts>.
- Statistics Canada. 2006. *Human Activity and the Environment: Annual Statistics*. Accessed July 29, 2016. <http://www.statcan.gc.ca/pub/16-201-x/2006000/9515-eng.htm>.
- The Geological Society of America. 1977. *Reviews in Engineering Geology Volume III*. D.R. Coates (ed.). Boulder: The Geological Society of America, Inc.
- Willie, D.C. and Mah, C.W. 2004. *Rock Slope Engineering: Civil and mining*, 4<sup>th</sup> ed. New York: Spon Press.
- Yong, S., Martin, C.D., Sego, D.C. and Bunce, C. 2003. The Harrowby Hills Slides. In *Proceedings of the 3<sup>rd</sup> Canadian Conference on Geotechnique and Natural Hazards, Edmonton, 9-10 June 2003*: 219-226. Richmond: Canadian Geotechnical Society.

## Development of design guidelines for sheet pile walls for railway slope stabilization



J.R. Bartz, P.Eng.  
University of Alberta, Edmonton  
[jbartz@ualberta.ca](mailto:jbartz@ualberta.ca)

### Introduction

Landslides in Prairie river valleys are common, and the slope movement can have detrimental impact on the human use of the land. Such problems include the loss of property, damage to existing structures, and damage to linear infrastructure, such as pipelines, roads and railways. Railroad and pipeline companies continue to look for cost effective solutions for maintaining their infrastructure. Current mitigation techniques, such as regrading and reconstructing the site to a new geometry, constructing rockfill shear keys or rockfill columns, using geogrid slope reinforcement, and/or installing a row(s) of large diameter piles can be difficult or costly to install along some rail lines where access to the site is limited to rail. Many of the secondary rail lines in western Canada have limited access, and thus new slope stabilization techniques may provide solutions that are better suited for the unique conditions faced by railways.

This research project is currently being conducted to develop a methodology for the design of a slope stabilization technique utilizing sheet pile walls referred to as "Hardy Walls". Since the Hardy Wall slope stabilization technique is not a common or well-known method, there are currently no existing guidelines.

### Hardy Wall Landslide Stabilization

An unconventional slope stabilization method has been developed utilizing sheet pile walls installed oriented parallel to the movement of the landslide. This novel slope stabilization method is known locally in Edmonton, but has only seen limited application since it was first introduced by Dr. R. Hardy in the 1960s. Recently CN Rail utilized the method, referred to as "Hardy Walls", near the Birdtail Sioux First Nation in western Manitoba to slow or stop a landslide that was impacting its rail line.

### *Study Site at CN Mile 191.4 Rivers Subdivision*

CN Rail utilized the Hardy Wall landslide stabilization method at CN Mile 191.4 Rivers Subdivision near Birdtail Sioux First Nation in Western Manitoba. The site is located in the Assiniboine River valley along the outside bend of the river. Approximately 110 m of track was affected by the slow moving landslide as estimated by ongoing track maintenance prior to the construction of the Hardy Wall.

The stratigraphy at the study site consists of alluvial clay underlain by shale bedrock with a granular terrace at ground surface near the tracks. Three slope inclinometers (SI) were installed at the study site that identified a slide plane within the shale bedrock approximately 8 to 11 m below ground surface. Monitoring of the SIs in November and December of 2014 indicated a horizontal displacement rate of approximately 1.0 mm/day. The SI casings deformed beyond their functional limits prior to construction of the Hardy Wall.

The Hardy Wall was constructed over a period of approximately 40 days in June and July of 2015 and consisted of 37 sheet pile walls spaced 3.0 m apart and installed parallel to the direction of slope movement as shown in Figure 1. Each sheet pile wall is constructed

of 10 PZC-26 steel sheet pile sections with an overall length of approximately 7.08 m and installed to approximately 1.83 m (6 ft) below the shear plane. The sheet piles were installed by initially vibrating to a depth of approximately 5.5 m using a crane hoisted vibratory hammer and then driven to final elevation with a diesel hammer.



**Figure 1: Hardy Wall Installation at CN Mile 191.4 Rivers Subdivision.**

An additional slope inclinometer was installed after construction of the Hardy Wall and indicated horizontal displacement along the shear plane of 7 mm over 145 days between December, 2015 and May, 2016. The rate of horizontal displacement appears to have significantly decreased, however the available monitoring data from SIs is over irregular periods of time and does not provide consistent data from before, during and after construction of the slope stabilization works.

### **Ongoing Research**

Developing design guidelines involves studying the potential failure mechanisms of the moving soil mass above the landslide shear plane and the stable soil below the shear plane. The design guidelines developed as part of this research are intended to follow a similar methodology to existing guidelines (Poulos, 1995; Cornforth, 2005; Vessely, Yamasaki & Strom; 2007) for the design of a row of circular piles for slope stabilization with a de-coupled approach consisting of two-dimensional limit equilibrium slope stability analysis and laterally loaded pile analysis. The ultimate lateral soil resistance for sheet pile walls of a Hardy Wall system will be analyzed and the effect of sheet pile wall spacing and geometry will be evaluated by using numerical models.

This novel technique for track stabilization is relatively fast to install, appears to be cost effective and is ideally suited for railroad maintenance. The development of a design methodology for Hardy Walls would introduce a new landslide stabilization technique for civil engineering infrastructure projects in North America.

### **Acknowledgments:**

I would like to thank the partners of the Railway Ground Hazard Research Program (RGHRP) for their support. I would also like to thank my research supervisors, Dr. Derek Martin and Dr. Michael Hendry of the University of Alberta for their guidance in conducting this research. Lastly, I would like to thank CN and in particular, Tom Edwards and Melissa Ruel, for their cooperation and providing information regarding the study site.

### **References**

- Cornforth, D.H. 2005. *Landslides in Practice*, 413-417. Hoboken, New Jersey: John Wiley & Sons.
- Poulos, H.G. 1995. Design of reinforcing piles to increase slope stability. *Canadian Geotechnical Journal*, 32: 808-818.
- Vessely, A., Yamasaki, K. & Strom, R. 2007. Landslide stabilization using piles. *First North American Conference on Landslides; Proceedings, Vail, Colorado, 3-8 June 2007*, 1173-1183. Denver, Colorado: The Association of Environmental & Engineering Geologists.

# Integrated planning for mine closure supported by the use of digital elevation model surfaces



J.T.G. McGreevy  
BGC Engineering Inc., Vancouver  
[jmcgreevy@bgcengineering.ca](mailto:jmcgreevy@bgcengineering.ca)

R.B. Mooder & G.T. McKenna  
BGC Engineering Inc., Vancouver

## Introduction

Integrated planning provides an opportunity to improve a mine operator's ability to better set expectations for the reclaimed landscape and to deliver on those expectations. Most mines are not currently meeting their closure goal of receiving regulatory signoff on the reclaimed landscape and discharging their liability partly due to inadequacies in planning and design (McKenna et al. 2016). This paper discusses the use of digital elevation models (surfaces) to support integrated planning. Integrated planning incorporates next land use considerations and requirements, and ties the mine plan (mining advance plan, overburden disposal plan, tailings deposition plan, reclamation stockpile plan, and water management plan) to the closure plan (regrading plan, reclamation material placement plan, revegetation plan, monitoring and maintenance plan, wildlife plan, and relinquishment plan).

This paper focusses on lessons learned from work in the Alberta oil sands mining industry. The lessons learned are applicable in other mining districts.

## Background

Development of integrated planning has been ongoing at oil sands operators for over 20 years. During this time, more powerful computers, more powerful three dimensional tailings deposit planning software (e.g., Muck3D), and the greater use of geographic information system (GIS) software in mine planning has allowed for the use of larger data sets and higher resolution surfaces in planning (Alostaz et al. 2014). This paper proposes an update to the surface development technique presented in Hachey and Lanoue (2011) that takes advantage of advances in software and computing power and recent experience.

## Integrated Planning

Mine plans for operations in the oil sands provide the solids, bitumen, and water mass balances and schedules for mining. Generally, closure plans use mine plans as inputs and provide a conceptual description of the projected performance of the reclaimed mine site after the end of mining. Closure plans typically consider the end land uses, and the long term geotechnical, geochemical, hydrotechnical, hydrological, hydrogeological, and ecological post-mining conditions.

To foster integrated planning, the mine plan must be linked to the closure plan by a framework that supports mine planning mass balance tracking, while also providing the closure planning process with data to support landscape performance projections. This framework is achieved by developing multiple surfaces that represent the mine plan and that are used as inputs for closure plan designs and models.

## Geology

Understanding the geology is a key component of mine planning, including orebody delineation, geotechnical engineering, hydrogeology, and geochemistry. The anthropogenic mining deposits form part of the post-mining geology and can be classified by grain size, depositional environment, and

mineralogy, etc. Three dimensional geological models for pre-mining and post mining conditions are required, as a minimum. Intermediate geologic models of mining operations may also be useful to support operational mine planning. Post-mining geologic models that account for consolidation and erosion may be useful to predict reclaimed landscape performance.

### Mine Plan and Closure Surfaces

Table 1 describes each of the mine plan and closure surfaces used. While simple in concept, considerable effort has been put into defining these surfaces. Taken together, the set of surfaces link the mine plan to the closure plan through the mining material mass balances and landform designs. The mine plan surfaces when stacked together represent a solid model of the placed materials. The volume of material represented by the model contains the mine plan mass balances at planning densities. The closure surfaces contain the mass of reclamation material placed at planning densities. The surfaces can be used as inputs to evaluate landform stability, consolidation, wildlife habitat, vegetation, surface water, and groundwater.

**Table 1. Surface Descriptions**

Type	Surface	Description
Mine Plan Surfaces	Pre-disturbance	The pre-disturbance surface represents the topography before the beginning of mining development.
	Base-of-Pit	The base-of-pit surface represents the planned or constructed lowest mined extents of the mine pits. The base-of-pit surface is used to show where the original topography and geology units have been mined out.
	Planning Basis	The planning basis surface represents the as-built dumps and dykes topography, and tailings pond bathymetry dated to the beginning of the planning period.
	Tailings Storage Areas	The tailings storage areas surface represents the dyke and tailings area topography planned to be built over the life of mine.
	Waste Storage Areas	The waste storage areas surface represents the overburden storage area topography planned to be built over the life of mine.
Closure Surfaces	Ready for Reclamation	The ready for reclamation surface represents the mine site topography at the end of mining before reclamation material has been placed. The surface provides the topography the mine will build to meet the closure design.
	Reclaimed	The reclaimed surface represents the mine site topography at the end of mining with reclamation material placed.
	Long-term	The long-term surface represents a projection of what the mine site topography will be after long term consolidation of the materials in the reclaimed landscape.

### Closure Goals

Integrated mine and closure planning provides a framework for developing and meeting practical closure goals by linking mining with closure through the mine plan mass balance and material placement schedule. As a result, the projected reclaimed landscape performance presented by the closure plan reflects a realistic end case of the mine plan.

If the projected reclaimed landscape performance meets the closure goals, the integrated plan defines the path to achieve the goals. Conversely, if the projected performance does not meet the closure goals, then the mine plan is not aligned with the closure goals. In this situation, the mine operator can either adjust the mine plan, or work with local communities and regulators to adjust the closure goals to align with what is practically achievable. In practice, mine operators frequently do both.

### Conclusion

The use of surfaces provides a rigorous framework for providing an integrated plan joining the closure plan and the mine plan. The particular strength of the surface planning process is that it provides topography outputs that can be used to support the mass balance and material placement tracking of mined materials for the mine plan, and as inputs into closure plan models. Integrated planning allows mine operators to develop closure goals that reflect the reclaimed landscape that will be created by the integrated mine and closure plan.

### References

- Alostaz, M., McGreevy, J.T.G, Lee, D., McKenna, G.T., & Cooper, C. 2014. Mine Closure Design and Tailings Planning Tools: Synergies and Opportunities. *In the proceedings of International Oil Sands Tailings Conference 2014*. Lake Louise, Alberta, December 8-10, 2014.
- Hachey, L.N. & Lanoue, A.V. 2011. Use of three-dimensional topography as a tool for closure integration at Syncrude Canada Ltd.'s Mildred Lake and Aurora North Leases. *In the proceedings of Mine Closure 2011*. Lake Louise, Alberta, 18-21 September 2011.
- McKenna G, Straker J, and O’Kane M. 2016. Custodial transfer of reclaimed mines: barriers and opportunities. TRCR 40th Annual BC Mine Reclamation Symposium. Penticton, BC, Canada. September 2016. 12p.

# Technical Session 4

# Foundation Engineering

# Estimation of lateral pile capacity for design of soil-structure interaction experiments



K. H. Lamba, PhD Student  
 Iowa State University, Ames, IA 50010, USA  
[klamba@iastate.edu](mailto:klamba@iastate.edu)

J. C. Ashlock, Associate Professor  
 Iowa State University, Ames, IA 50010, USA  
[jashlock@iastate.edu](mailto:jashlock@iastate.edu)

## Introduction

The accurate prediction and computational simulation of 3D multi-modal dynamic soil-pile interaction remains a significant challenge. As part of an ongoing research project to advance fundamental knowledge on this subject, dynamic soil-pile interaction experiments will be performed on single piles and pile groups, and new computational continuum models will be developed for seismic applications. To help calibrate the computational models, full-scale field tests are being planned for a single pile and a 2x2 pile group, including lateral vibration tests with small soil strains and quasi-static cyclic loading to failure.

This paper describes the estimation of the ultimate lateral capacity of the single pile and 2x2 pile group at the selected project sites, required for designing the experiments.

## Planned Lateral Load Tests

Several series of multi-modal vibration tests will be performed using a servo-hydraulic inertial shaker and random vibration techniques. Following the vibration tests, the quasi-static lateral cyclic load tests will be performed on the single pile and 2x2 pile group at a project site in Ames, Iowa.

## Project Site Selection, Soil and Pile Parameters

Two sites were selected for the field tests, referred to as Sites 2 and 3. The soil profile for Site 2 was obtained from geophysical Multichannel Analysis of Surface Waves (MASW) tests performed by the authors and project team, and the soil profile for Site 3 was evaluated using data from previously conducted Cone Penetration Tests (CPTs). The resulting soil parameters are given in Table 1.

**Table 1: Soil profile parameters for Sites 2 and 3 ( $V_s$ : Shear Wave Velocity;  $\gamma$ : Unit weight;  $c_u$ : undrained shear strength;  $\phi'$ : friction angle;  $a$ : (FHWA 2002);  $b$ : (Kulhawy & Mayne 1990);  $c$ : (Kulhawy & Chen (2007))).**

Soil parameters for Site 2, located at intersection of East Lincoln Way and I-35, Ames, IA						
Soil Type	Depth (ft)	$V_s$ (ft/s)	$\gamma$ (pcf)	SPT ( $N_{60}$ ) <sup>a</sup>	$c_u$ <sup>b</sup> (psi)	$\phi'$ <sup>c</sup> (°)
Clay	0	530	112	11	2.5	-
	7.9	707	112	15	7.7	-
	14.6	720	119	15	8.3	-
	30.0	737	119	12	9.0	-
	47.4	790	119	15	11.8	-
Sand	64.4	1020	119	31	31.2	41
	82.8	1419	119	82	111.4	45
Soil parameters for Site 3, located near Spangler Geotechnical Laboratory at Iowa State University, Ames, IA						
Soil Type	Depth (ft)	$\gamma$ (pcf)	$c_u$ (psi)	$\phi'$ (°)		
Clay	35	130	20	-		
Clay	78	135	50	-		

**Table 2: Pile parameters for L-Pile analysis**

Case	1	2	3
Pile diameter (in.)	8.625	10.75	12.75
Wall thickness (in.)	0.322	0.365	0.375
Pile length (in.)		360	
Pile embedded length (ground surface to pile bottom) (in.)		300	
Pile unembedded length (ground sfc. to bottom of pile cap) (in.)		32	
Modulus of elasticity (lb/in.)		29 x 10 <sup>6</sup>	
Yield stress of pile (ksi)		50	

**Lateral Pile Capacity Analysis**

The lateral capacity of the single fixed-head pile for displacement-controlled field tests was determined using the L-Pile Plus (V5.0) software program. The results are detailed in Figures 1 and 2 and Table 3.

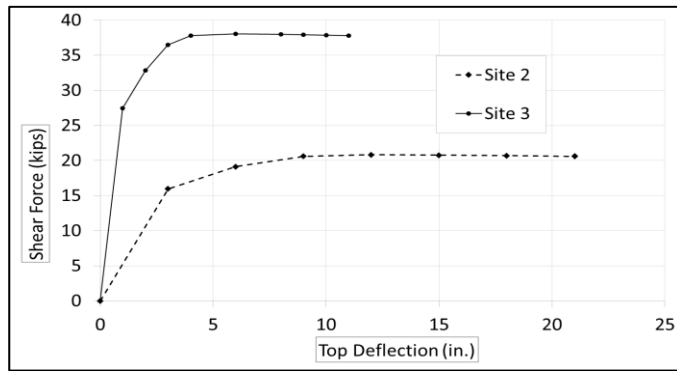


**Figure 1: Force-deflection at the bottom of pile cap for 8.625 in diameter steel pipe pile**

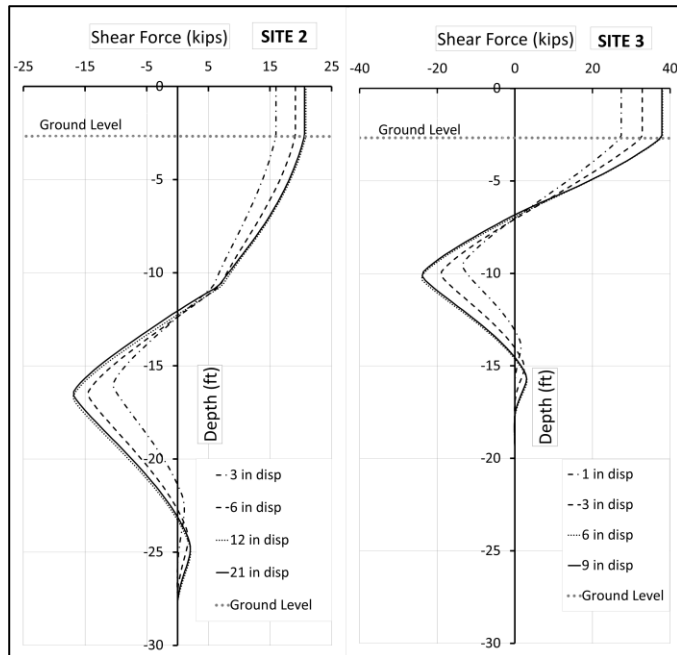


**Figure 2: Shear force profiles for increasing pile-head displacements for fixed head 8.625 in. diameter pipe pile**

**Table 3: Lateral Pile Analysis Results for Sites 2 and 3**

Site	Site 2			Site 3		
Pipe Pile Diameter (in)	8.625	10.75	12.75	8.625	10.75	12.75
Capacity of single pile <sup>1</sup> (kips)	21	28	39	38	60	80
Estimated capacity of pile group <sup>2</sup> (kips)	84	112	156	152	240	320
Top deflection at pile capacity (inches)	10.65	11.48	12.1	6.0	8.0	10
Maximum bending moment (in-kips)	1090	1930	2815	1100	1950	2800
Depth of max. moment from ground level (ft)	9	10	11	7	5.30	6.4
Maximum shear force (kips)	17	25	33	25	36	47
Depth of max. shear from ground level (ft)	14	15	17	7.4	9.3	10.5

<sup>1</sup>From L-Pile Type 3 Analysis

<sup>2</sup>Neglects pile interaction factors for conservatism

**Results and Discussion**

The expected lateral capacities of the pile groups are given in Table 3 for all three potential pile sizes. Based on these analyses, the 8.625-inch diameter pipe piles at Site 3 were chosen to be used in the field tests. A Shore-Western hydraulic actuator having a capacity of 235 kips in compression and 175 kips in tension will be used, along with a reaction frame and piling constructed using steel HP 10x42 piles. The observations from field tests will be analyzed and used for developing computational models for dynamic soil-pile group interaction, which is the crux of the research project.

**References**

Federal Highway Administration (FHWA). 2002. Tools and Techniques for Measuring Soil and Rock Parameters. *Geotechnical Engineering Circular No. 5*: 26 – 107. U.S. DOT: Washington, D.C.

Kulhawy, F.H., & Chen J.R. 2007. Discussion of “Drilled Shaft Side Friction in Gravelly Soils” by Kyle M. Rollins, Robert J. Clayton, Rodney C. Mikesell, and Bradford C. Blaise. *Journal of Geotechnical and Geoenvironmental Engineering* 131(8):987-1003.

Kulhawy, F.H., & Mayne, P.W. 1990. Strength. *Manual on Estimating Soil Properties for Foundation Design*: 4-48 – 4-53. Electric Power Research Institute: Palo Alta.

**Acknowledgements**

This material is based upon work supported by the National Science Foundation under Grant No. 1351828. This support is gratefully acknowledged. Any opinions, findings, and conclusions or recommendations expressed in this material are those of the authors and do not necessarily reflect the views of the National Science Foundation.

## Performance of a reinforced highway embankment to Canada's North



E. M. B. De Guzman  
University of Manitoba, Winnipeg, MB  
[deguzmem@myumanitoba.ca](mailto:deguzmem@myumanitoba.ca)

### Introduction

The completion of the Inuvik to Tuktoyaktuk Highway (ITH) has been a long standing goal of the Town of Inuvik, the Hamlet of Tuktoyaktuk, and the residents of the Inuvialuit Settlement Region (EIRB 2011). The construction of the ITH will help address the goals of Northern economic development, enabling future natural resource exploration, development, and production, and reinforcing Canadian sovereignty objectives (EIRB 2011). The ITH, which extends the Dempster Highway past the community of Inuvik to the Arctic Coast, will be an all-weather transportation link and will complete Canada's road network from the Pacific, to Atlantic, and to Arctic coasts.

The warming trend in air temperatures due to climate change in the Northwest Territories (IPCC 2014) has and will continue to pose challenges for the transportation system (TAC 2010). Highway embankments in the Arctic are usually constructed during winter conditions to preserve the permafrost foundation and minimize environmental impacts. However, there is

limited understanding on the mechanical behaviour of embankments that are initially compacted with frozen fill and experienced natural thawing and settlements during the spring and summer season following winter construction. The fill material of such embankments is dominated by soils with significant fine content that include ground ice. Fills are very difficult to compact at sub-zero temperatures when ice is present. They are relatively strong while they remain frozen but they become soft and compressible after thawing. Side-slope sloughing and fill cracking are caused by localized thaw-settlements under the shoulders and side-slopes of the embankment created by the rising of the permafrost table into the embankment fill in combination with the depression of the permafrost table at the toe of the embankment.

### Embankment Construction and Performance

Two sections along the newly constructed ITH have been instrumented to monitor temperatures, deformations, pore water pressures, and soil suctions. The reinforced test section has layers of wicking geotextiles on its side slopes to provide reinforcement and drainage path for the water during the thawing season (Figure 1). The geotextile has an overhang of 0.5 m to allow water flow out of the embankment faster and to dissipate the potential build-up of pore water pressure during thawing. The length of the geotextile installed was conceptualized to intercept the failure surface when the embankment thaws and if sloughing occurs.

The reinforced test section is instrumented with thermistors for temperature readings in the embankment fill and foundation soil, ShapeAccelArrays (SAAs) for the vertical and lateral displacements, vibrating wire piezometers for pore water pressures, and thermal conductivity sensors for suctions. Strain gauges were also installed at different locations along the length of the geotextile at different layers of the reinforced embankment. A control (unreinforced) test section with the same instrumentation was also constructed beside the reinforced test section to evaluate its performance.

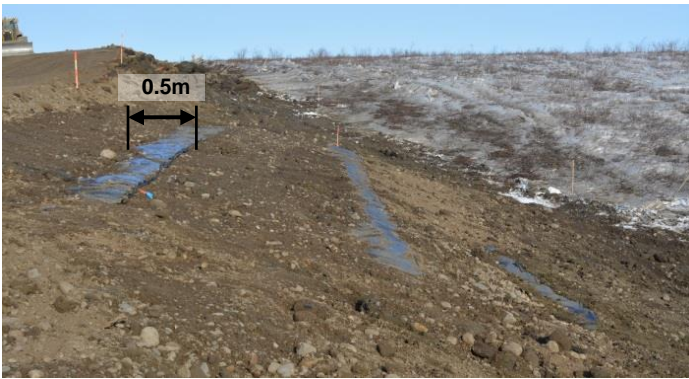


**Figure 1. Geotextiles exposed on the side slopes of the embankment**

Recorded readings indicate that the thermistors closest to the ground surface are responding quickly to the warming air temperatures. The vertical SAAs are recording lateral movements closest to the ground surface, while the horizontal SAAs are showing maximum settlements near the centerline of the embankment. The lateral displacements recorded in the reinforced section (Figure 2b) are less than that of the control section (Figure 2a). Maximum lateral deformation of the control section at point near the slope surface is approximately 40 mm greater than the geotextile-reinforced section. Figure 3 shows the two test sections along the highway, with cracks noticeable in the unreinforced sections.

**Summary**

Instrumentation were installed along the ITH embankment to monitor its performance. These are the first test sections constructed to study the effects of winter construction on highway embankment performance in Arctic Regions. Preliminary results indicate that there are less lateral movements when reinforcements are installed. The test sections are continuously being monitored to evaluate their performance. Laboratory testing will be carried out on the soil samples obtained from the site to determine its mechanical, hydraulic, and thermal properties. Pullout and tensile capacity of the geotextile will also be tested at different temperatures and environmental conditions. These properties will ultimately be used in numerical modelling to assess the behaviour of embankments constructed in Arctic Regions and develop mitigation strategies.

**References**

Environmental Impact Review Board (EIRB). 2011. EIS for Construction of the Inuvik to Tuktoyaktuk Highway, NWT. EIRB File No.: 02/10-05.

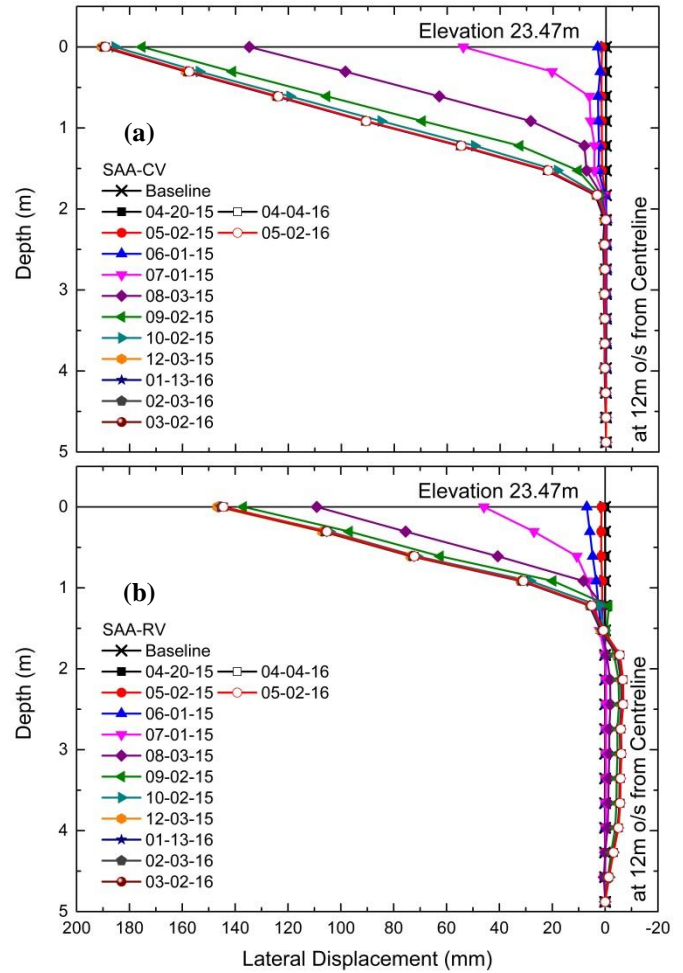


**Figure 2. Horizontal deformations at 12m o/s from centerline in (a) control and (b) reinforced sections**

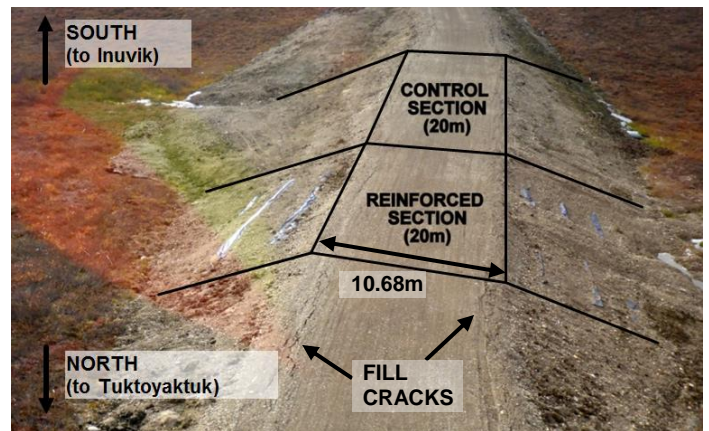


**Figure 3. Reinforced and control sections along the ITH**

IPCC, 2014. Climate Change 2014: Impacts, Adaptation, and Vulnerability. Part B: Regional Aspects. Cambridge University Press, Cambridge, United Kingdom and New York, NY, USA, pp. 688.

Transportation Association of Canada (TAC). 2010. Guidelines for Development and Management of Transportation Infrastructure in Permafrost Regions. Ottawa, Canada.

## Behaviour of helical pile groups under axial compressive loading



S.A. Lanyi  
University of Alberta, Edmonton  
[slanyi@ualberta.ca](mailto:slanyi@ualberta.ca)

### Introduction

A helical (screw) pile consists of a hollow steel shaft with one or more helices welded to it. Helical piles are versatile because they resist large loads, are reusable, and are quick to install. This pile type is becoming increasingly popular in the piling industry. Research driven design standards must catch up to this relatively new trend. The goal of this research project is to investigate the performance of helical pile groups under axial compressive loading by performing field tests on full-scale instrumented piles.

Helical piles are commonly installed in groups, which are comprised of closely spaced piles connected at the tops by a pile cap. As pile spacing within a

group decreases, the interaction between the piles increases. With increased pile-to-pile interaction, the efficiency of the group decreases, which results in the collective capacity of the pile group being less than the sum of the capacities of the individual piles. Design standards for conventional piles suggest a minimum pile spacing ratio required to avoid a grouping effect; however, there is currently no design standard specific to helical pile groups. This leads to inconsistencies within the industry and the possibility for over design or unsafe design. Helical piles have a unique load transfer mechanism, which creates the need for a unique design approach distinct from conventional piles.

### Background Theory

The decrease in group efficiency of closely spaced piles is the result of overlapping zones of influence. As pile spacing decreases, the stresses in the soil between the piles becomes compounded. Another factor that affects group interaction is the pore pressure response due to pile installation. During pile installation in fine grained soils, cavity expansion and soil deformation cause large excess pore pressure generation (Weech 2002). The pore pressure generation between a single pile and a pile group are not equivalent, resulting in a longer dissipation period for pile groups.

The group interaction of helical piles could differ from that of conventional piles. This is due to the unique load transfer mechanism of helical piles. The inter-helix spacing ratio influences the failure mechanism, and therefore the degree of interaction between piles in a group.

### Test Site

Testing will occur at the University of Alberta Farm in Edmonton, Alberta. The soil at the U of A farm consists of uniform lacustrine sediments deposited by Glacial Lake Edmonton (Bayrock and Hughes 1962). To determine the soil properties at this site a detailed site investigation, including CPT testing and Shelby tube sampling, was completed.

## **Test Piles and Instrumentation**

Test piles will have a length of 20', a shaft diameter of 2.875", and a helix diameter of 12". All test piles will have two helices.

Test piles will be instrumented with strain gauges to determine the stress distribution along the pile and the failure mechanism during testing. Drive point vibrating wire piezometers will be installed near the helices and at the center of the pile groups prior to pile installation. The piezometers will measure the amount of excess pore pressure generation caused by pile installation, and the rate of dissipation.

## **Field Test Program**

The proposed field test program will be investigating how several variables affect the group efficiency of helical piles under axial compressive loading. The variables that will be manipulated include the group spacing ratio, inter-helix spacing ratio, batter angle, and excess pore pressure at time of testing.

## **Objectives**

Based on the results of the test program, pile group design recommendations will be made regarding the group spacing ratio, inter-helix spacing, and batter angle. The testing will also provide insight on the amount of excess pore pressure generation caused by pile installation and the rate of dissipation in fine grained soils. This information can be to determine an adequate wait period between pile installation and loading.

Ultimately, the goal of this research project is to gain better understanding of the soil-pile group interaction. Industry could utilize the findings from this research to produce pile designs that more accurately reflect this interaction, resulting in more reliable and economic designs.

## **Acknowledgements**

Roterra Piling is providing financial and technical support for this research. They will be providing helical test piles, data acquisition instrumentation, and load testing equipment and assistance.

## **References**

Bayrock, L.A. & Hughes, G.M. 1962. Surficial Geology of the Edmonton District. *Alberta Research Council of Alberta, Preliminary Report 62-6.*

Weech, C. 2002. Installation and Load Testing of Helical Piles in a Sensitive Fine-Grained Soil. M.Sc. thesis. University of British Columbia.

# Use of moisture wicking geotextile for subgrade improvement in pavement design



L. G. McLaren  
E2K Engineering Ltd., Calgary  
[leanne@e2keng.com](mailto:leanne@e2keng.com)

## Introduction

Pavement design has evolved through the centuries, starting with brick and cobblestone paths through to the widely accepted AASHTO 1993 design guidelines, and continuing to new techniques today. Our understanding of how site geology affects road designs has also improved. Many road failure types have been categorized over years of studies to identify causes including asphalt thicknesses, climatic conditions, and poor subgrade soils.

In the recent past, the most widely accepted mitigation for poor subgrade soils, for example soft organic clays, was to spend the additional time and cost for thicker base layers, thicker asphalt layers, or to remove, replace, or strengthen the subgrade material. Research has shown that the use of moisture

wicking geotextiles is cost effective, as well as design effective in distributing/transferring bearing pressures that would have caused failure in a similar structure without geotextile.

## Method

### *Pavement Design Example, Cochrane, Alberta*

In the fall of 2015, a pavement design was completed for a two lane collector road in Cochrane, Alberta. During site investigations a thick layer of high plastic soft to firm clay with high organic content was discovered that could potentially cause significant structural issues for the proposed roadway. Through research and communications with geotextile companies, a decision was made to recommend the use of a moisture wicking geotextile fabric.

### *Literature Review*

Since construction for the Cochrane design project has not yet commenced, information on installation, and other uses for moisture wicking geotextile fabrics have been gathered from other sources. Figure 1 depicts a section of installed wicking geotextile for the Pioneer Mountain Scenic Byway in Montana. After attempts to repair longitudinal cracks caused by frost heave, a design with a layer of wicking geotextile and a layer of geogrid was proposed to prevent further damage and repair costs (Sikkema 2016).



**Figure 1: Installed wicking geosynthetic (Sikkema 2016)**

Another example of the use of moisture wicking geotextile in pavement design is the Dalton Highway in Alaska. Due to the character of the subgrade soils, the presence of groundwater, and freezing temperatures, significant frost boils were developing every spring leading to unsafe driving conditions. In this example, moisture wicking geotextile was used to improve the pavement conditions on the Dalton highway by wicking moisture from within the pavement structure and draining it out toward the ditches (Zhang 2012).

## Results

When pavement construction is to take place, the California Bearing Ratio (CBR) of the subgrade soils is an integral parameter in determining the thickness of base, subbase, and asphalt in the pavement structure. Clay subgrades with 3% CBR or lower would result in high structural numbers (SNs) requiring thick and costly pavement thicknesses (Christopher 2006).

The geotextile reduces the required thickness by supporting some of the road loads through its tensile strength. There are many geotextile products that can improve bearing capacity of the subgrade soils. What sets the moisture wicking fabric apart is the effect on drainage in the pavement structure.

Weaved wicking filaments use capillary action to pull moisture from within the pavement system and to draw it towards the pavement edges and out of the system (Han 2016). Figure 2 shows a microscopic view of the wicking filaments woven into the geotextile. In the Cochrane design project, where the organic subgrade clays are moisture sensitive, addition of water to the system would result in a shorter functional life of the road. In this case, the use of a wicking geotextile would significantly limit the moisture within the subgrade thereby extending the life of the road structure.

In the Cochrane design project, the client decided to move forward with a combination of subgrade replacement, and geotextile subgrade improvement.

Although research is available showing the successes attributed to this type of geotextile, it is prudent to note that the technology is still rather new and there is no long term data beyond five or six years post-construction. Currently, the moisture wicking geotextile is recommended as an effective method of improving soft organic clays, frost susceptible areas,

and other moisture sensitive subgrades in pavement design.

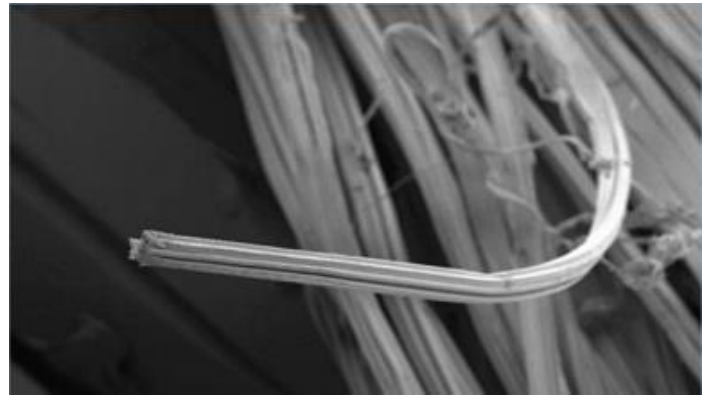


**Figure 2: Microscopic view of wicking yarns (Koninklijke 2013)**

## References

- Christopher, B.R. et al. 2006. Geotechnical Aspects of Pavements. *Federal Highway Administration Report FHWA NHI-05-037*. Washington D.C.: USA.
- Han, J. et al. 2016. Laboratory Evaluation of Wickability of Wicking Fabrics Under Controlled Temperature and Relative Humidity. In the *3<sup>rd</sup> Pan-American Conference on Geosynthetics: Page 1203-1209*. Miami Beach: USA.
- Koninklijke TenCate. 2013. Webinar: Enhanced Lateral Drainage in Pavement Systems. *Tencate Website accessed June 8, 2016 from <http://www.tencate.com/amer/geosynthetics/products/geotextiles/TenCate-Mirafi-H2Ri/default.aspx>*.
- Sikkema, M. & Carpita, J. 2016. Pioneer Scenic Byway Frost Heave Prevention and Results. In the *3<sup>rd</sup> Pan-American Conference on Geosynthetics: Page 1871-1879*. Miami Beach: USA.
- Zhang, X. 2012. Use of H2Ri Wicking Fabric to Prevent Frost Boils in the Dalton Highway Beaver Slide Area, Alaska. Fairbanks: USA.

## Design & construction of micropiles for Vale's Copper Cliff smelter



M. Redden  
Geo-Foundations Contractors Inc., Acton, Ontario  
[mredde@geo-foundations.com](mailto:mredde@geo-foundations.com)

### Introduction

The Vale Clean AER Project is a \$1 billion retrofit of the existing smelter building aimed at reducing sulfur dioxide emissions by 85% (below 0.25 ppm) through the complete retrofit of the converter aisle and the construction of a new acid plant and a wet gas cleaning plant. As part of the converter #10 retrofit, micropiles were specified to support the new construction as well as to underpin around existing column footings in restricted access.

Specialty geotechnical contractor Geo-Foundations performed the design and installation of 122 rock-socketed micropiles throughout the active smelter plant, in varying headroom conditions while facing difficult subsurface challenges and dealing with the harsh winter weather of Sudbury, Ontario. Changes to both drilling and grouting techniques were also

executed throughout the project as varying subsurface conditions were encountered.

### Geological Setting

The site is located at the Vale Copper Cliff smelter complex on the outskirts of Sudbury, Ontario. The smelter has been in operation since the early 20<sup>th</sup> century and was originally built on a 2-3m layer of slag (by-product of the smelting process). Below the slag layer is loose sandy silt and sandy clay, moisture contents ranging from 25% to 50%. This wet layer extends down to a highly variable bedrock depth ranging from 6 m to 17 m within the work area. This bedrock (quartz diorite, norite) also exhibits large amounts of perched water and Unconfined Compressive Strength (UCS) values upwards of 140 MPa.

### Design Overview

Micropiles were designed to handle individual service loads up to 1899 kN in compression, 427 kN in tension and 71 kN in lateral load. The weak overburden soils and lateral loads facilitated the use of permanent casing to bedrock, 324 mm diameter x 12.7 mm wall thickness. Compression and tension loads were taken through a rock socketed bond zone featuring a 76 mm or 64 mm central reinforcing threadbar (517 MPa) extending up into the cased section. Grouting of the micropiles was performed using a neat cement grout (0.45 water/cement ratio), grout was tremie pumped from the bottom of the hole until filled, a pressure cap was then installed and grout injected under pressure to seal around the casing tip annulus (USFHWA Type B). Micropiles were designed in accordance with the US Department of Transportation and US Federal Highway Administration, Micropile Design and Construction Guidelines, June 2000, using the service load design (SLD) method.

### Installation Methodology

Micropiles were drilled inside the active smelter plant with tight access and in headroom conditions between 3 m and 10 m (Figure 1). Drilling was completed using rotary percussive concentric duplex with air and water flush. J-teeth were welded to the permanent casing to

allow seating into the hard sloping bedrock. This method would seal off the above wet overburden layer and allow for the construction of a clean rock socket using a down the hole hammer. All drill cuttings were captured at the collar of the hole and diverted to a specially designed containment bin for removal in order to eliminate any impact to smelter operations. Quality control throughout the project consisted of full time inspection of all drilling, bar insertion and grouting tasks. A record for each pile was established accompanied by a 23-point inspection and testing protocol (ITP).



**Figure 1: Drilling micropile casing in 3.3 m of headroom**

### **Installation Challenges and Remedial Actions**

Challenges with micropile installation were faced throughout the project at different stages. The weak and wet overburden layer below the initial slag crust led to issues with silt plugging the drill bit and rods, as well as excessive ground disturbance as air flush was increased to reduce plugging. A change in the drilling methodology was introduced to minimize the potential for these issues. A head of synthetic polymer drilling mud was pumped through the drill rods during the addition of casing segments. This helped to stabilize the hole and prevent basal heave of the silt into drill rods that would plug off the air and water flush. Ground disturbance was reduced by keeping the drill bit a minimum 1 m inside the casing during overburden drilling to maintain a soil plug and eliminate any air flush from extending beyond the casing diameter. Upon reaching the rock elevation, the drill bit would extend out of the casing in order to help

seat the casing into rock and continue on to drill the rock socket.

In certain areas of the work, excessive ground water in the bedrock caused collapsing of the rock socket and washing out of grout during tremie pumping. Pre-treatment of the rock mass was achieved using downstage grouting to seal off the perched water. A thixotropic grout additive was used to ensure stability of the grout and prevent wash out under flowing water conditions. Pre-treatment of the rock allowed for the rock socket to be drilled without collapse and tremie grouting to be completed using traditional means and methods.

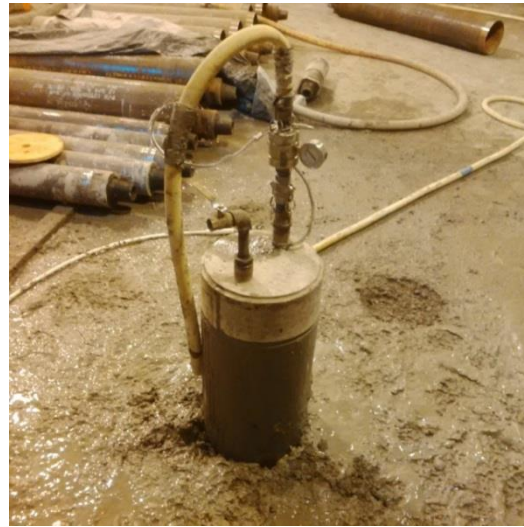


**Figure 2: Pressure grouting through micropile casing**

### **Conclusion**

Successful micropile construction is closely linked to the workmanship and high level of quality control performed. The difficult nature of this project's constructability and geotechnical conditions required quick modification to drilling and grouting techniques throughout. Maintaining a high level of quality control during the course of these changes was a top priority. The successful design, construction and remedial actions performed allowed all subsequent work to proceed without any modifications.

### **References**

SNC Lavalin Inc. 2014. Foundation Design Recommendations Report for Converter #10 Upgrades, Report No.507763-061-1414-4GER-0013, dated January 16, 2014.

# Technical Session 5

# Numerical Modelling

# Large-strain consolidation of thawing soils



S. Dumais  
 Université Laval, Québec (QC)  
[simon.dumais.2@ulaval.ca](mailto:simon.dumais.2@ulaval.ca)

J.-M. Konrad  
 Université Laval, Québec (QC)

## Introduction

Thawing of frozen ground can lead to generation of pore water pressure and to thaw settlement. This process referred to as thaw consolidation is particularly problematic when drainage is impeded in less permeable fine-grained saturated soils and for ice-rich soils. The assessment of thaw consolidation related instabilities is paramount for the safe design of infrastructure built on permafrost especially in the context of climate change. A large-strain thaw consolidation model developed by coupling large-strain consolidation and heat transfer equations into a moving boundary scheme is presented here.

## Thaw consolidation modelling

One-dimensional thaw consolidation is represented in Fig. 1. Lagrangian coordinates  $a$ , which move along with the soil deformations are used for the proposed model. As a result, boundary conditions can

seamlessly be implemented without knowing the exact location of the boundaries prior to the analysis.

The ground is at an initial temperature lower than the freezing point of the soil  $T_f$  and thawing of the ground is initiated by a step increase in surface temperature  $T_s$ . The frozen region is considered impermeable and incompressible. Thus, the thawed region undergoing consolidation is delimited by a pervious boundary at the surface and an impervious boundary at the thaw front  $Z(t)$ .

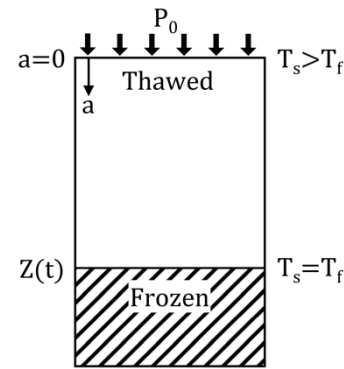


**Figure 1: One-dimensional thaw consolidation**

## Large-strain consolidation

Consolidation of thawing soils is best modelled using large-strain consolidation theory because it accounts for the variation of the soil properties as consolidation proceeds. Furthermore, allowing finite strains ensures that boundary conditions at the surface moves with the surface settlement. Conventional thaw consolidation theories with a small strain limitation may underestimate of the excess pore water pressure and the rate of thaw penetration which may lead to unsafe design.

Gibson et al. (1981) proposed the following governing equation for large-strain consolidation:

$$[1] \frac{d[k_v(e)]}{de} \frac{G_s - 1}{1+e} \frac{\partial e}{\partial a} + \frac{\partial}{\partial a} \left[ - \frac{k_v(e)(1+e_0)}{\gamma_w} \frac{d[\sigma'_v(e)]}{de} \frac{1}{1+e} \frac{\partial e}{\partial a} \right] = \frac{1}{1+e_0} \frac{\partial e}{\partial t}$$

where  $e$  is the void ratio,  $e_0$  is the initial void ratio,  $G_s$  is the specific gravity of the solid particles,  $\gamma_w$  is the unit weight of water, and  $\sigma'_v(e)$  and  $k_v(e)$  are void ratio dependent functions for the effective stress and hydraulic conductivity.

Eq. 1 is easily implemented in a moving boundary scheme in Lagrangian coordinates because it is derived in terms of void ratio. Functions  $\sigma'_v(e)$  and  $k_v(e)$  are usually characterized by linear relationships in a semi-logarithmic plot as illustrated in Fig. 2.

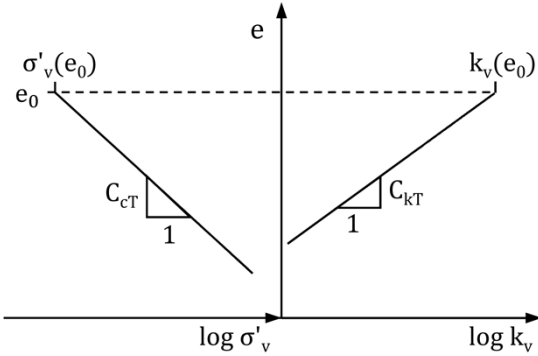


**Figure 2: Constitutive relationships  $\sigma'_v(e)$  and  $k_v(e)$  for large-strain consolidation**

### Heat transfer

In thaw consolidation modelling, a thermal component is used to define the position of the interface between the thawed and frozen regions. The following equation used to model conductive and advective heat transfer is used in the model:

$$[2] \left( C - L_w \rho_i \frac{\partial \theta_i}{\partial T} \right) \frac{\partial T}{\partial t} + c_w \rho_w v_a \frac{1+e_0}{1+e} \frac{\partial T}{\partial a} = \frac{\partial}{\partial a} \left[ \lambda \frac{(1+e_0)^2}{(1+e)^2} \frac{\partial T}{\partial a} \right]$$

where  $C$  is the volumetric heat capacity of the soil,  $L_w$  is the latent heat of water,  $\rho_i$  and  $\rho_w$  are the density of ice and water,  $\theta_i$  is the volumetric ice content,  $T$  is the temperature,  $c_w$  is the heat capacity of water,  $v_a$  is the water flow velocity and  $\lambda$  is the soil thermal conductivity.

The consolidation component is used as a mass transfer equation in combination with Eq. 2. Consequently, the water flow velocity and the soil's thermal properties modelled as a function of the void ratio are calculated using Eq. 1.

### Coupling

Eq. 1 and 2 are coupled into a moving boundary scheme in Lagrangian coordinates as illustrated in Fig. 1. Any Dirichlet or Neumann boundary conditions can be specified for the thermal component. However, thaw penetration must be unidirectional from top to bottom with no freeze back allowed at the surface.

Boundary conditions for the consolidation component are expressed in terms of void ratio. The impervious condition at the thaw front is formulated in terms of the movement of the boundary and of the

volume change due to phase change from ice to water.

### Typical results

Typical results for the simulation of a laboratory thaw consolidation test are presented in Fig. 3 from the implementation of the model in the software *COMSOL Multiphysics*. Fig 3a presents temperature profiles as a function of depth at different time steps and Fig. 3b presents void ratio profiles.

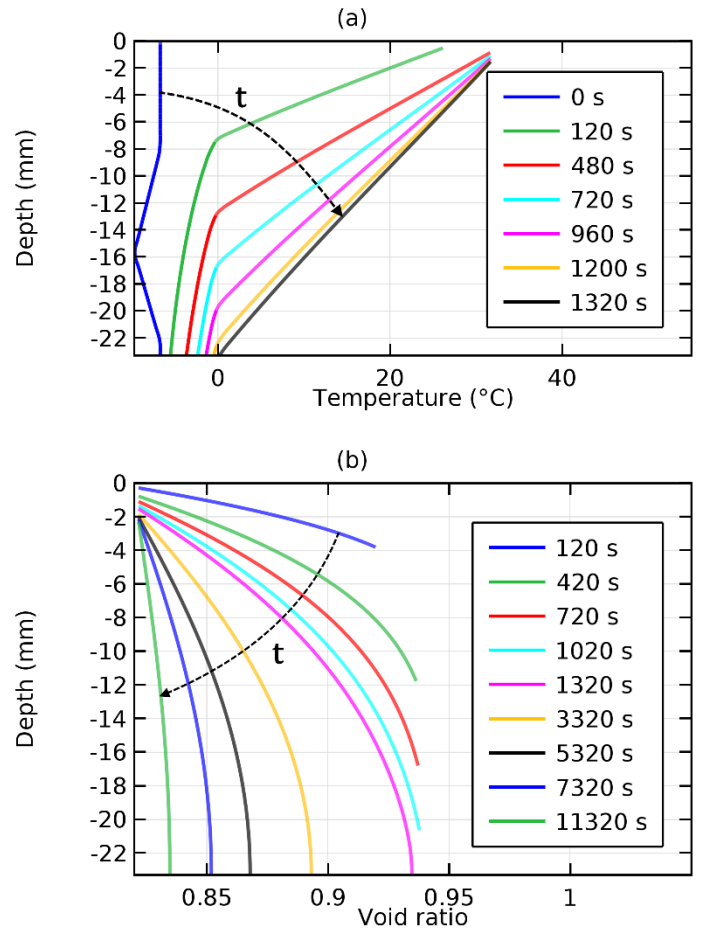


**Figure 3: Typical simulation results, (a) heat transfer component, (b) consolidation component**

### Conclusion

A large-strain thaw consolidation model is proposed. The model outputs are temperature and void ratio as a function of depth and time.

### References

Gibson, R.E., Schiffman, R.L. & Cargill, K.W. 1981. The theory of one-dimensional consolidation of saturated clays. II. Finite nonlinear consolidation of thick homogeneous layers. *Canadian Geotechnical Journal* 18(2): 280–293.

## Thermal-hydraulic modelling a Canadian deep geological repository



P. Abootalebi  
GeoEngineering Centre at Queen's-RMC, Kingston  
[pedram.abootalebi@queensu.ca](mailto:pedram.abootalebi@queensu.ca)

### Introduction

Due to continual demand for more energy along with need for carbon-reduced energy sources to limit climate change effects, nuclear power has become one of the reliable energy sources. Beside the benefits of nuclear power, it brings ethical and environmental responsibility to safely take care for waste products. Canada like every other jurisdiction around the world who has come to the decision, has decided a deep geological repository as a long term solution.

A deep geological repository consists of a network of tunnels at a depth of at least 500 m in a stable rock formation where the used fuel bundles will be located within containers and surrounded by an engineered barrier system. The engineered barrier system is composed of bentonite-based materials due to bentonite's desirable material properties such as low permeability, high swelling potential. Since the waste

inside the container generates heat over time, high thermal conductivity for engineering barriers is required to dissipate smoothly the thermal energy from the container to bounded bedrock without applying excessive heat to the container (not more than 100°C after Maak 2006.). Thus, thermal conductivity is an important characteristic in terms of size and efficiency of the repository.

The environment would likely include competing gradients of groundwater pressure driving moisture into the repository and thermal gradients driving moisture away from the used fuel container. Therefore, engineered barriers might experience varied saturation degrees and temperatures over the design lifetime. Hence, for comprehensive modeling, it is necessary to determine thermal properties of engineered barriers over a wide range of moisture contents (degree of saturations) and variable temperatures (25°C and 80°C). In this presentation, methods for measuring the thermal properties along with selected results are explained. Preliminary modeling of the Canadian concept for the deep geological repository is also presented.

### Materials and Methods

The engineered barriers that surround the used fuel containers within the Canadian concept include; highly compacted bentonite, dense backfill and gapfill. The container is surrounded by highly compacted bentonite block with minimum dry density of 1.7 g/cm<sup>3</sup> and called buffer box. Between adjacent buffer boxes a block of dense backfill will be placed as spacer block. This material is composed of a mixture of crushed granite, illite clay and bentonite with minimum dry density dry density of 2.1 g/cm<sup>3</sup>. The gap between bedrock and buffer box will be filled with gap fill material which is 100 % bentonite made out of pellet size grains along with powder bentonite in the matrix with minimum dry density of 1.41 g/cm<sup>3</sup>.

Due to diverse dry densities proposed for sealing materials, two test procedures were followed for measuring thermal properties at low density and high density materials (Abootalebi et al. 2014).

## Experimental Result

Selected thermal conductivity result is plotted in Figure 1 for highly compacted bentonite made out of National Standard (Na.St) bentonite. The blue circles are room temperature data and the red diamonds are the thermal conductivity results for tests performed at 80°C. Room temperature tests were performed at 11 degree of saturations in triplicate. The 80°C tests were performed at 4 degree of saturations again in triplicate. The test results show thermal conductivity increases with increasing saturation. Comparing the Sr=0% and Sr=100% results shows indicates a 2-3-fold increase in thermal conductivity from dry to saturated with  $R^2=0.98$  for linear relationship. The effect of temperature is undetectable in the highly compacted bentonite.

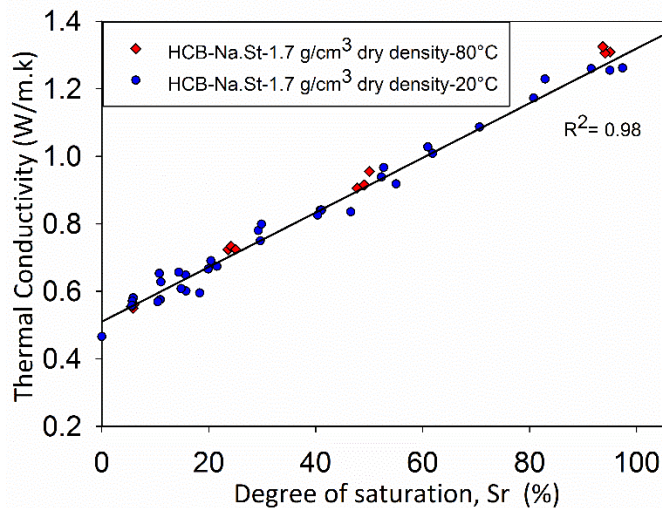


**Figure 1. Thermal conductivity measurements of highly compacted bentonite as a function of degree of saturation at 20°C and 80°C**

## Thermal-Hydraulic Model

This is the first time numerical simulations of the current Canadian concept for deep geological repository have considered the effects of moisture on the thermal response. The critical design consideration is surface temperature of the container. These models with constant thermal properties were used to bound the maximum and minimum temperature of the container at critical times of its use. The geometry and boundary condition has been taken from a report by NWMO (Gue 2015) and experimental data were used to gain maximum and minimum container surface temperature due to changing degree of saturation of highly compacted bentonite. The results are plotted in Figure 2 illustrating the increase in container

temperature associated with decreasing the degree of saturation of the highly compacted bentonite.

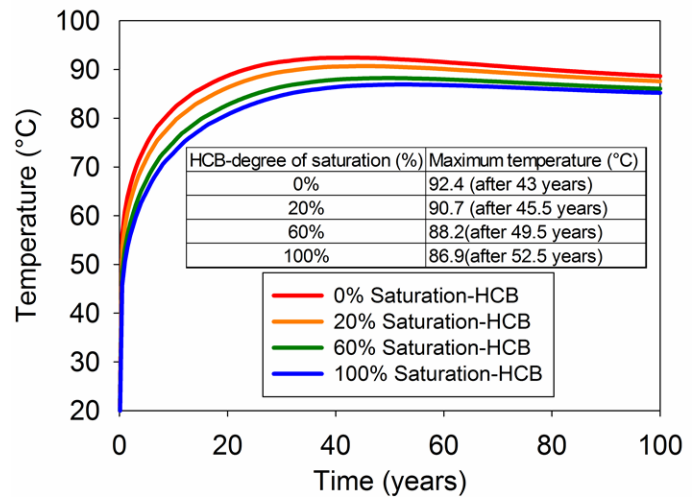


**Figure 2. Container Surface Temperature over 100 years- deep geological repository model**

## Summary

The current concept for Canada's inventory of spent nuclear fuel is a deep geological repository. During the transient phase of the deep geological repository evolution, a number of thermal, hydraulic, chemical and mechanical aspects of the engineered barriers must be considered. Amongst other design aspects, the characterization of the thermal properties of the engineered barriers as a function of moisture content and temperature is a key component of the analysis. In this presentation, thermal properties of engineered barriers are reported and then used in thermal model of the Canadian concept of the deep geological repository.

## References

- Abotalebi, P. Siemens, G. 2015. Thermal property testing of an engineered barrier for use in a deep geological repository, in 68th Canadian Geotechnical Conference, GeoQuebec 2015, Sep 20 2015. Quebec, Canada: Canadian Geotechnical Society
- Guo, R. 2015. Thermal Modelling of a Mark II container, Nuclear Waste Management Organization technical Report NWMO-TR-2015-06.
- NWMO. 2015. Progress Through Collaboration – Annual Report. 173 pp.
- Maak, P. 2006. Used fuel container requirements. Ontario Power Generation Preliminary Design Requirements. 06819-PDR-01110-10000 R02.

# Geostatistical modeling of hydraulic conductivity within a compacted dam core



É. Hébert  
Université Laval, Québec  
[etienne.hebert.3@ulaval.ca](mailto:etienne.hebert.3@ulaval.ca)

J. Côté  
Université Laval, Québec  
[jean.cote@gci.ulaval.ca](mailto:jean.cote@gci.ulaval.ca)

M. Smith  
Hydro-Québec, Montréal  
[smith.marc@hydro.qc.ca](mailto:smith.marc@hydro.qc.ca)

## Introduction

The hydraulic barrier performance of compacted till cores of embankment dams is highly dependent on compaction conditions during construction, which alongside basic geotechnical properties may significantly vary spatially. The recent development of new tools and a better understanding of the variability of soil properties enable the integration of such variability in design and behavior analysis using geostatistics as a modeling tool.

This study focuses on the assessment of the hydraulic conductivity of the compacted till core of an embankment dam from north-eastern Québec using construction control data. The study also aims to improve the geostatistical analysis method developed

in previous studies (Venkovic et al. 2013, Smith & Konrad 2011, Soulié et al. 1983) in order to obtain a more accurate representation of the actual field conditions.

## Field data

The field data set for the studied dam was collected during its construction in the form of construction control tests, which were performed using nucleodensimeters and various laboratory tests. The available measured parameters are: the clay-size fraction (% passing 2  $\mu\text{m}$ ), the in situ and optimum water content and the in situ and maximum dry density, from which the in situ and optimum saturation degrees can be calculated. The core was built using till from five different borrow pits located around the construction site, one of which showed a significantly higher clay-size fraction.

## Empirical hydraulic conductivity estimation

Hydraulic conductivity is strongly influenced by compaction conditions. If a till is compacted on the wet side of the optimum compaction curve ( $S_r \geq S_{r_{opt}}$ ), its pores sizes will be homogeneously distributed and will have a low hydraulic conductivity, whereas if the same till is compacted on the dry side of the compaction curve ( $S_r < S_{r_{opt}}$ ), its pores sizes will be associated to macro pores formed between aggregated clay particles and therefore have a higher hydraulic conductivity.

In order to estimate the hydraulic conductivity in a more representative way that takes into account the influence of compaction conditions, a model based on the works of Leroueil et al. (2002), which allows the estimation of the hydraulic conductivity as a function of the fabric and clay-size fraction, was developed for this study.

## Quasi 3D interpolation grid

Dams present a new challenge in regards to the assessment of the spatial continuity of geotechnical parameters as they are built by laying lifts of materials on top of each other. Because of the time period between the placement of two lifts, factors such as weather conditions and changes in the origins

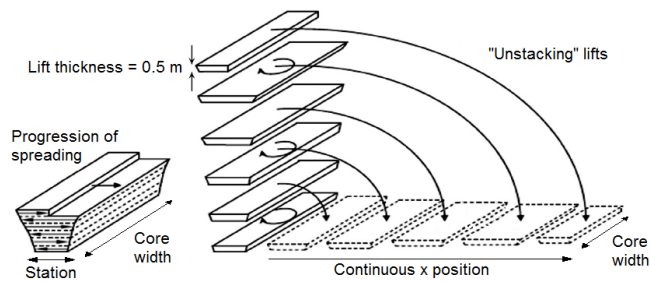


**Figure 1. Deconstruction of the core structure (from Smith & Konrad 2011)**

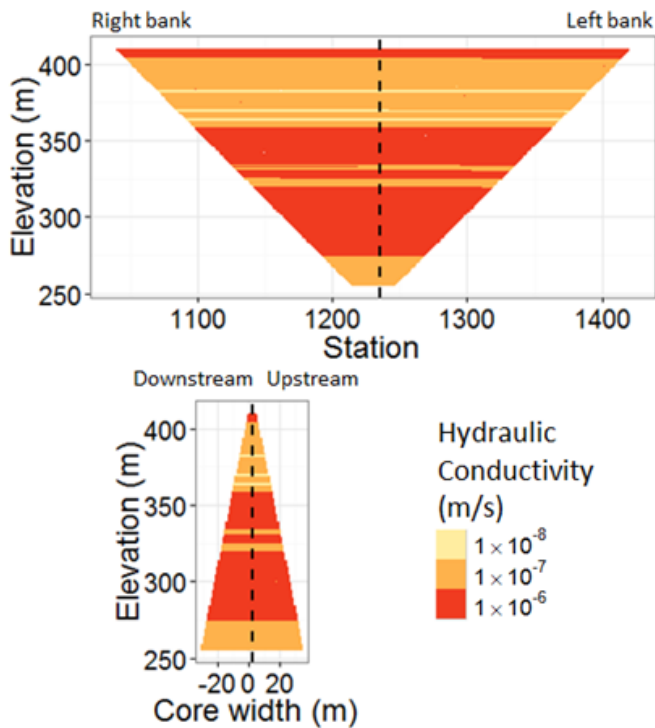


**Figure 2. Hydraulic conductivity estimation results for the central cross sections of the core**

of the materials can cause significant variations in the geotechnical properties of each lifts. Due to the construction sequence, a dam spatial continuity only exists in the direction of the progression of spreading and its parameters should not be assessed using a 3D interpolation structure (Venkovic et al. 2013).

As each lift can be considered a 2D spatial structure, it is possible to deconstruct the core according to each lift and place them next to each other horizontally (Figure 1). The resulting quasi 3D interpolation grid allows the 2D modeling of the studied parameters at every coordinates of the core while maintaining the 3D nature of the structure.

## Results

The geostatistical analysis results are showed on Figure 2, where the estimated hydraulic conductivities are presented for the two central cross sections of the core. The results show that the core hydraulic conductivity is mostly in the order of  $10^{-6}$  to  $10^{-7}$  m/s and that smaller areas located between elevations of 350 to 400 m show values in the order of  $10^{-8}$  m/s. The lower hydraulic conductivity areas are linked to the use of a higher clay-size fraction till during the construction.

These results highlight the stratified structure of the core, a characteristic that was already observed for other dams in past studies which showed that the hydraulic conductivity of compacted till cores mainly vary according to the elevation. The use of a 3D approach allows to detect fluctuations of the hydraulic conductivity within single lifts, a feature that wasn't observed previously and show that variations of the hydraulic conductivity within the core not only occurs according to the elevation.

The next steps of the study will aim to further improve the geostatistical approach used to model embankment dams, which will in turn allow the study of more complex dam mechanics such as filter criteria, internal erosion and piping.

## References

- Leroueil, S., Le Bihan, J.-P., Sebaihi, S., Aliescu, V. 2002. Hydraulic conductivity of compacted tills from northern Quebec. *Canadian Geotechnical Journal* 39: 1039-1049.
- Smith, M. & Konrad, J.-M. 2011. Assessing hydraulic conductivities of a compacted dam core using geostatistical analysis of construction control data. *Canadian Geotechnical Journal* 58: 1246-1268.
- Soulié, M., Favre, M., Konrad, J.-M. 1983. Analyse géostatistique d'un noyau de barrage tel que construit. *Canadian Geotechnical Journal* 20: 453-467.
- Venkovic, N., Lebeau, M., Konrad, J.-M. 2013. Geostatistical assessment of the hydraulic conductivity of an embankment dam. *Proceedings of the 66<sup>th</sup> Canadian Geotechnical Conference, Montréal, September 29 to October 3.*

# Modelling of supercritical carbon dioxide sorption on various geological media



J.W. Winfield  
 Faculty of Engineering, University of Wollongong,  
 Wollongong, Australia  
[jw778@uowmail.edu.au](mailto:jw778@uowmail.edu.au)

## Introduction

Since the Industrial Revolution, anthropogenic CO<sub>2</sub> has been released into the atmosphere in gradually more significant quantities due to the burning of fossil fuels and other industrial processes. The ramifications of this rapid increase in CO<sub>2</sub> and other greenhouse gases is manifest in notable negative changes to climate systems. Therefore, it is critical to develop technologies to mitigate this problem. One very promising approach to reducing greenhouse gas emissions is CO<sub>2</sub> capture, transport, and sequestration in deep subsurface geological layers. The present research improves upon the current storage capacity equations by extending them to cover a wider range of materials and in situ conditions. It is the intention that the results obtained, equations built and the method of analysis described in the present research are used to assist in solving the carbon emissions dilemma.

## Dubinin-Radushkevich mathematical model

Dubinin and Radushkevich (1947) proposed an equation for describing the physical adsorption of gases on microporous solids. Their original idea was later refined and became more fashionable due to the additional work of Dubinin (1967) and Dubinin (1975). The Dubinin-Radushkevich (D-R) equation is currently one of the most widely used isotherm equations in adsorption theory and has successfully modelled experimental data from gas adsorption tests on microporous carbons (Gil and Grange 1996).

The mathematical basis for the D-R equation stems from the concept of Polanyi's potential. The isotherm equations have a semi-empirical origin and were derived for adsorption on heterogeneous microporous solids by solving Stoeckli's integral equation. The original D-R isotherm model, shown in Figure 1, is a relationship between excess sorption and equilibrium pressure.

$$Q_{excess} = Q_0 \left( 1 - \frac{\rho_{free}}{\rho_{ads}} \right) e^{-D \left( \ln \left( \frac{P_s}{P} \right) \right)^2}$$

Where:

$$Q_{excess} = \text{free phase sorption of CO}_2 \left( \frac{\text{m}^3 \text{ of CO}_2 \text{ at NTP}}{\text{tonne of Sample}} \right)$$

$$Q_0 = \text{surface adsorption capacity free parameter} \left( \frac{\text{m}^3 \text{ of CO}_2 \text{ at NTP}}{\text{tonne of Sample}} \right)$$

$$\rho_{free} = \text{interpolated free phase CO}_2 \text{ density at } P \text{ (kg/m}^3\text{)}$$

$$\rho_{ads} = \text{density of the adsorbed CO}_2 \text{ phase (kg/m}^3\text{)}$$

$$D = \text{free parameter (unitless)}$$

$$P_s = \text{saturation pressure (MPa)}$$

$$P = \text{equilibrium pressure (MPa)}$$

## Figure 1: D-R Equation

The free parameters are Q<sub>0</sub> and D; their numeric value is typically chosen based on "best fit" criteria. However, embryonic connections are beginning to form between these free parameters and characteristics of the sorbate and sorbent. Q<sub>0</sub> is perhaps related to the microporous structure of the sorbent, and D is thought to be related to the heat of adsorption and affinity of the gas to the sorbent (Day et al. 2008).

### Modified D-R isotherm equation

The original D-R equation was modified by Sakurovs et al. (2007) to attempt to cover a wider range of experimental conditions. Part of the modification involved an indirect change of independent variable from gas pressure to gas density. The modification also brought about the addition of an extra term. The extra term attempts to account for possibilities such as Henry's law dissolution, differences in the accessibility to the sorbent between helium and CO<sub>2</sub>, and errors in bomb volume, sample density and porosity (Sakurovs et al. 2007). By using this modification to the D-R equation Sakurovs et al. (2007) successfully demonstrated that the range of the experimental environment can be extended to include supercritical conditions. This notion is reinforced by the work done by Day et al. (2008) who showed that the modified D-R equation fits well to experimental data from supercritical sorption tests.

### Extended modified D-R isotherm equation

A limitation of the modified D-R equation is that it only considers the CO<sub>2</sub> in the adsorbed phase or CO<sub>2</sub> that has integrated into the solid matter of the sorbent. It does not include contributions of free phase CO<sub>2</sub> that fill the pore spaces of a material and, as a consequence, does not reflect the total amount of CO<sub>2</sub> within the sample. It also limits the types of material that can be modelled by the D-R isotherm equation.

The modified D-R equation was extended to include contributions to sorption by the volumetric filling of pore spaces with CO<sub>2</sub> in its free state. The extended D-R (eD-R) equation now has the capability to model and predict the total amount of CO<sub>2</sub> that can be stored for a much wider range of materials. This extension now allows material whose main form of storage is via the filling of pore space (such as a sandstone layer under a suitable cap rock) to be accurately represented by the D-R isotherm equation. The eD-R isotherm model, shown in Figure 2, is a relationship between total sorption and free phase CO<sub>2</sub> density.

In this form it is applicable to many different materials and describes the total amount of CO<sub>2</sub> that can be potentially stored in any suitable sequestration target. In this study CO<sub>2</sub> sorption experiments up to 10 MPa at 40°C were performed on two dry coal and three dry sandstone samples using a gravimetric apparatus. The eD-R model provided an excellent fit to the experimental sorption data over the entire pressure

range and under all experimental conditions (refer to Figure 3).

$$Q_{total} = Q_0 \left(1 - \frac{\rho_{free}}{\rho_{ads}}\right) e^{-D \left(\ln\left(\frac{\rho_{ads}}{\rho_{free}}\right)\right)^2} + k \cdot \rho_{free} + \frac{\rho_{free} \cdot V_s \cdot \phi}{m_s \cdot \rho_{free, NTP}}$$

Where:

$$\frac{\rho_{free} \cdot V_s \cdot \phi}{m_s \cdot \rho_{free, NTP}}$$

= contribution to total sorption from CO<sub>2</sub> in its free state  $\left(\frac{\text{m}^3 \text{ of CO}_2 \text{ at NTP}}{\text{tonne of Sample}}\right)$

$k$  = free parameter ( $\text{m}^6 \cdot \text{kg}^{-1} \cdot \text{t}^{-1}$ )

**Figure 2: eD-R Equation**

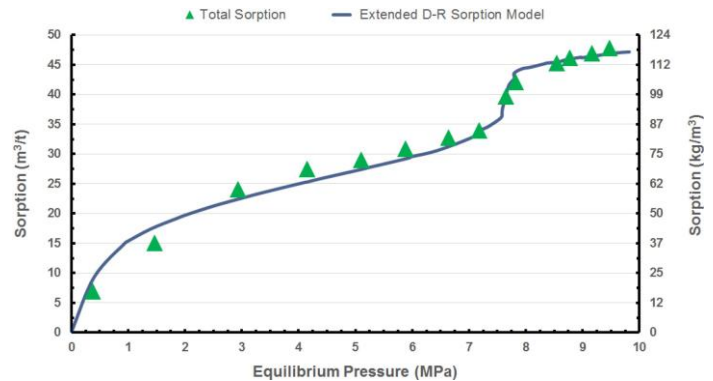


**Figure 3: eD-R Isotherm Model (Coal A)**

### References

- Day, S. Sakurovs, R. and Weir, S. 2008. Supercritical gas sorption on moist coals. *International Journal of Coal Geology*, 74, 213-214.
- Dubinin, M. 1967. Adsorption in micropores. *Journal of Colloid and Interface Science*, 23, 487-499.
- Dubinin, M. 1975. Physical adsorption of gases and vapors in micropores. *Progress in surface and membrane science*, 9, 1-70.
- Dubinin, M. and Radushkevich, L. 1947. Equation of the characteristic curve of activated charcoal. *Chem Zentr*, 1, 875.
- Gil, A. and Grange, P. 1996. Application of the Dubinin-Radushkevich and Dubinin-Astakhov equations in the characterization of microporous solids. *Colloids and Surfaces: Physicochemical and Engineering Aspects*, 113, 39-50.
- Sakurovs, R. Day, S. Weir, S. and Duffy, G. 2007. Application of a modified Dubinin-Radushkevich equation to adsorption of gases by coals under supercritical conditions. *Energy and Fuels*, 21, 992-997.

# Verification of geotechnical centrifuge physical modelling using slope stability and bearing capacity models



J.S. Kingswood  
 Royal Military College of Canada, Kingston  
[John.Kingswood@rmc.ca](mailto:John.Kingswood@rmc.ca)

## Introduction

The Royal Military College of Canada (RMCC) has acquired a geotechnical centrifuge to be used for teaching and research. To confirm and have confidence in this equipment, verification tests needed to be conducted. Two well understood geotechnical mechanisms, slope stability and shallow foundation bearing capacity, were tested to confirm the scaling relationships as well as the ability to accurately model prototype behaviour.

## Calibration Physical Model Methods

### Theory

Prototypes can be converted proportionally with the number of times the force of gravity (N) being applied by the rotational motion of the centrifuge. RMCC's centrifuge can apply up to 300 times the force of gravity to a model. The maximum dimensions of a

model are 180x300x100mm (height, y, width, x, depth, y) which corresponds to a prototype with dimensions of up to 54x30x90m, a volume of 145,800 m<sup>3</sup>, and a weight of approximately 250 tonnes of soil.

### Modelling of Models and Analytical Solutions

Pairs of models of each prototype structure with a factor of safety (FoS) of 1.0 were constructed at two different scales. Kaolin clay, with varied water content to adjust shear strength, was used as the soil for each pair of structures.

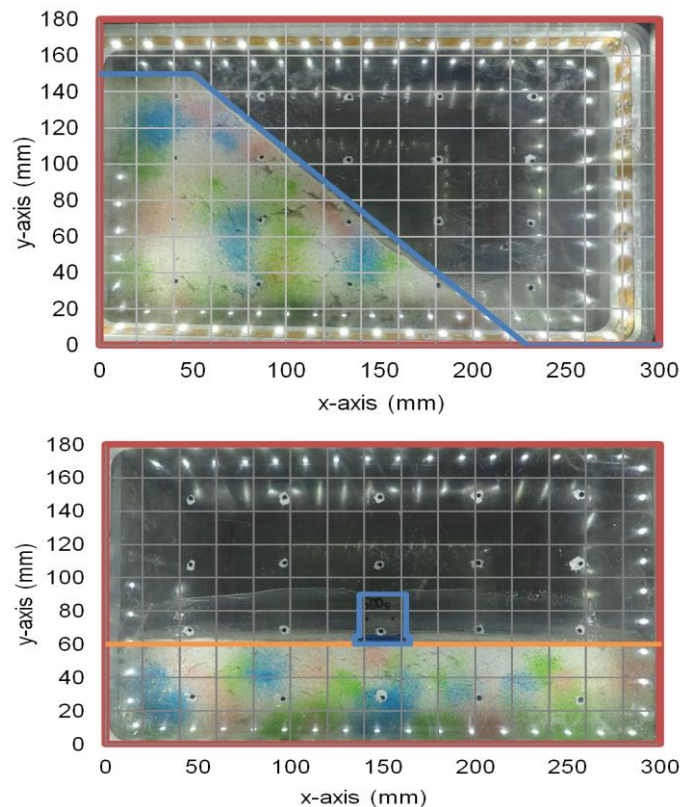


**Figure 1: Geometry of 150mm slope (upper) and 30mm shallow foundation (lower) in centrifuge cradle**

The models were then placed in the centrifuge (Figure 1) and subjected to the appropriate scaling forces (Table 1). For example, a 100mm slope with a 29 kPa shear strength was subjected to 108g, corresponding to a 10.8m slope prototype with a FoS of 1.0. The forces applied at each failure were then evaluated to confirm the proportionality with the other relative scale model for each pair. This was done for both the slope and the shallow foundation, varying shear strength for each

pair of models. A total of 6 models (3 pairs) were constructed and tested for each prototype structure.

**Table 1 Models Tested**

Slope Stability			Bearing Capacity		
H <sub>model</sub> (mm)	N <sub>failure</sub>	H <sub>prototype</sub> (m)	B <sub>model</sub> (mm)	N <sub>failure</sub>	B <sub>prototype</sub> (m)
150	69	10.4	60	79	4.74
100	108	10.8	30	144	4.32
150	82	12.3	60	89	5.34
100	119	11.9	30	172	5.16
150	97	14.6	60	74	4.44
100	149	14.9	30	148	4.44

Using Taylor’s charts (Taylor, 1948) and Terzaghi’s bearing capacity equation (Terzaghi, 1967), models of the prototypes designed for a FoS of 1.0 were observed, noting the scaling forces at failure. They were then evaluated to determine how closely the scaled prototype dimensions at failure corresponded to the analytically predicted values.

## Analysis and Results

### Analysis

In order to accurately identify the time of failure (and corresponding scaling forces) particle image velocimetry (Stanier, et al., 2015), was used.

By tracking individual particle movements, the relative difference in movement within the soil mass indicating failure along a shear plane could be determined accurately and identified before simple observation could detect it.

The pairs of scaled models of each structure successfully demonstrated the ability of the methodology to obtain proportional results. The prediction of the models’ behaviour by Taylor’s slope stability charts and Terzaghi’s bearing capacity equation was also shown to be accurate.

Both the internal consistency between models and the external correspondence with analytical predictions confirm RMCC’s ability to be able to both teach and conduct research as well as to confirm that the methodology used can be applied to further use of the equipment.

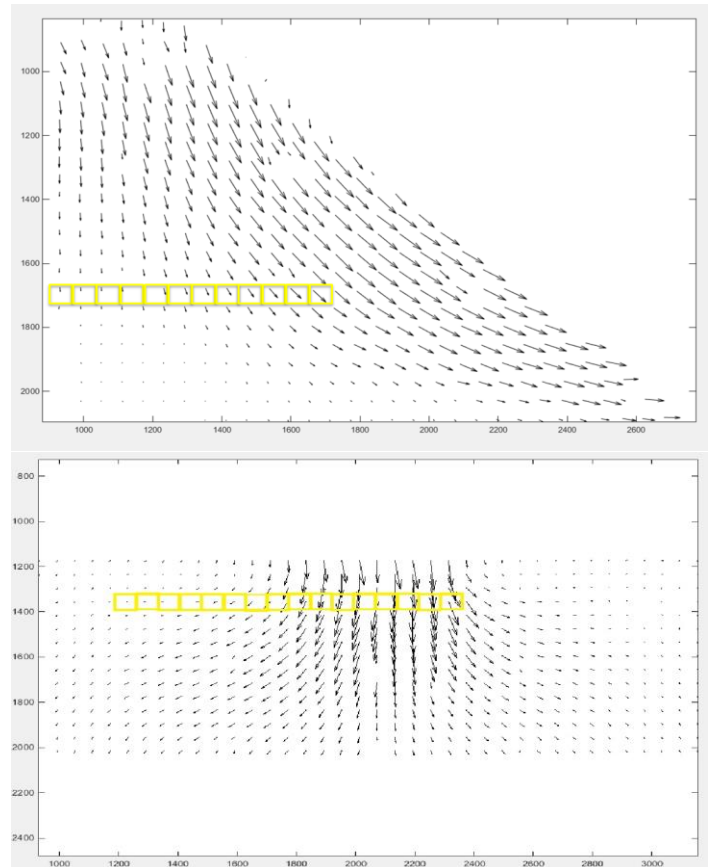


**Figure 2: PIV analysis of slope failure (upper) and shallow foundation failure (lower)**

## References

- Madabhushi, G. 2015. *Centrifuge Modelling for Civil Engineers*, CRC Press, Boca, Raton, FL, USA.
- Stanier, S.A., Blaber, J., Take, W.A., and White, D.J. 2015. Improved image-based deformation measurement for geotechnical applications. *Canadian Geotechnical Journal*, 53(5): 727-739.
- Taylor, D.W. 1948. *Fundamentals of Soil Mechanics*, John Wiley & Sons, New York, NY, USA.
- Terzaghi, K. and Peck, R.B. 1967. *Soil Mechanics in Engineering Practice*, 2nd ed., John Wiley & Sons, New York, NY, USA.

# Direct numerical integrations of geotechnical laboratory tests: Useful tools to better understand soil behaviour



V. Castonguay  
 Université Laval, Québec (QC)  
[vincent.castonguay.2@ulaval.ca](mailto:vincent.castonguay.2@ulaval.ca)

## Introduction

Constitutive soil models are mathematical representations of the stress-strain behaviour of soils. They are a key component of any numerical modelling and are also very useful to better understand fundamentals of soil behaviour on a day-to-day basis. Direct numerical integration of geotechnical tests using such models are invaluable tools to gain a deeper understanding of many soil behaviour characteristics.

The concept of direct numerical integration is briefly presented in this abstract, focusing on a simple yet very functional constitutive soil model: NorSand.

## Direct numerical integration of geotechnical tests

The direct numerical integration of a geotechnical test consists of a stepped modelling procedure where a constitutive soil model is solved to evaluate stresses for certain applied strains. At each modelling step, a

small plastic shear strain increment is applied and the corresponding stresses are calculated, taking into account the boundary conditions and/or stress paths implied by the modelled test. Such numerical procedure is easily implemented in calculation software such as MatLab (which was used to prepare this abstract), Excel's VBA and Python. Detailed procedure for direct numerical integrations are presented by Jefferies & Been (2015).

## Simple geotechnical tests modelling using NorSand

NorSand is a critical state based constitutive soil model (Jefferies, 1993). It can be viewed as a generalization of the CamClay soil model (Roscoe & Schofield, 1963), retaining its simplicity while addressing its known deficiencies (in particular for sands). It uses the state parameter  $\psi$  (Been & Jefferies, 1985) as its main input parameter to model different densities. An excellent description of the soil model, its calibration and use is available in Jefferies & Been (2015).

The NorSand soil model can easily be used to predict the behaviour of sands for a variety of geotechnical tests, including the triaxial test, using a direct numerical integration procedure. Such simulations are presented in Figure 1 and 2 for two different densities of Reid Bedford sand – a loose sample ( $\psi = 0.05$ ) and a dense sample ( $\psi = -0.01$ ).

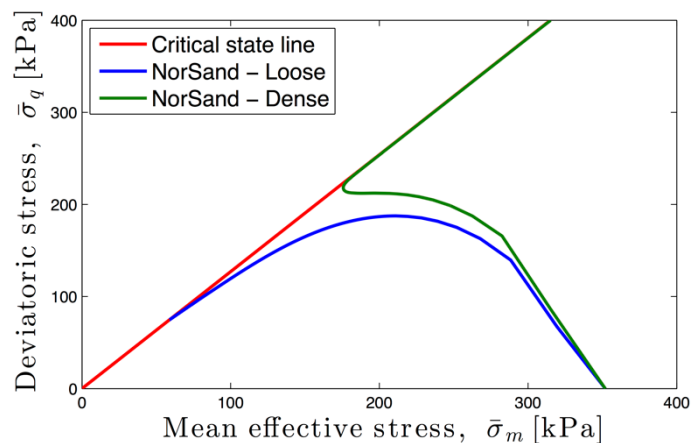


**Figure 1. Undrained triaxial simulations for loose and dense states – Stress path**

The direct numerical integration of a triaxial test allows the visualization of the influence of initial state on the response of the sand. In Figure 1 two different behaviours are evident: while the dense sample shows important dilatancy, the loose sample exhibits a very contractive behaviour. The implications of these behaviour differences are well represented in Figure 2 where the associated stress-strain curves are shown. The dilation exhibited by the dense sample is associated with an important increase in stress to further deformations. Conversely the contractive behaviour of the loose sample implies an important drop in resistance, characterized by an important drop in deviatoric stress for a small strain increase.

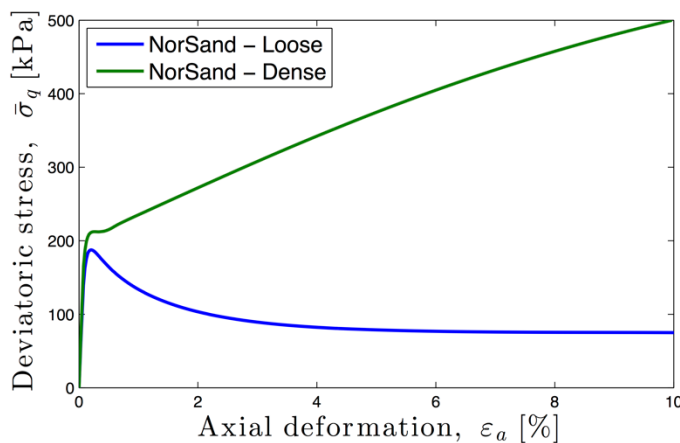


**Figure 2. Undrained triaxial simulations for loose and dense states – Stress-strain curves**

The direct numerical integration of triaxial tests gives access to easy simulations of a wide array of test conditions, for example: drained *vs* undrained conditions, loose *vs* dense initial state, isotropic *vs* anisotropic consolidation, etc.

More complex geotechnical tests such as the cyclic simple shear test can also be implemented using the direct numerical integration approach. Such test simulations are presented in Figure 3 and 4, again for Reid Bedford sand. The stress path followed by the sample in Figure 3 is typical of cyclic simple shear tests on sands: as the shear stress is cyclically applied, pore pressure generates, shifting the stress state closer to its critical state. The stress-strain response is shown in Figure 4 where a degradation in stiffness as the cycles accumulate is apparent. As pore water pressure rises during shearing the effective stress reduces. This effective stress reduction in turns leads to greater deformation caused by a softer sand response.

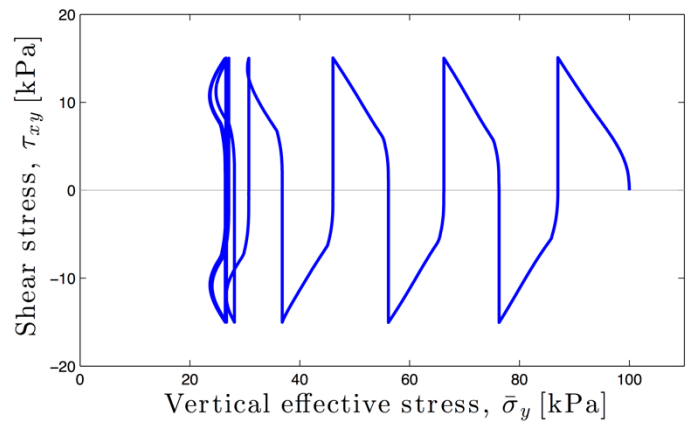


**Figure 3. Cyclic simple shear simulations – Stress path**

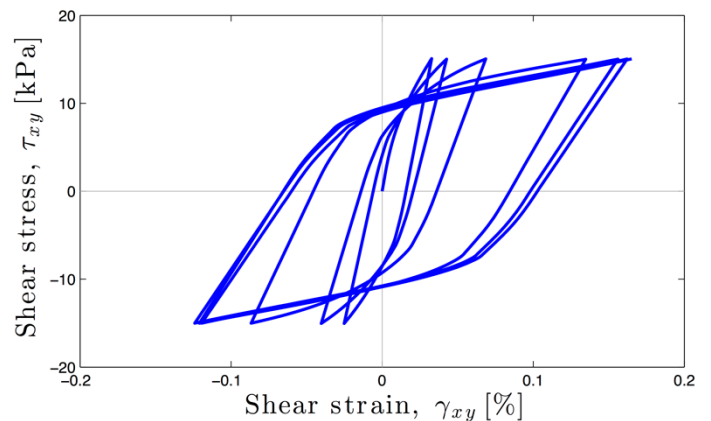


**Figure 4. Cyclic simple shear simulations – Stress-strain curve**

## Conclusion

Simple constitutive soil models can easily be implemented in programming software by using the direct numerical integration approach, hence avoiding the use of complicated numerical modelling software. The few examples presented in this abstract demonstrate the pedagogical potential of using this simple programming method (in depth description of such procedure is available in Jefferies & Been, 2015).

## References

- Been, K. & Jefferies, M. G. 1985. A state parameter for sands. *Géotechnique*, 35(2): 99-112.
- Jefferies, M. & Been, K. 2015. *Soil liquefaction: A critical state approach*, 2nd ed., Taylor & Francis Group, New York, NY, USA.
- Jefferies, M. G. 1993. Nor-Sand: A simple critical state model for sand. *Géotechnique*, 43(1): 91-103.
- Roscoe, K. H. & Schofield, A. N. (1963). *Mechanical behaviour of an idealized 'wet' clay*. Paper presented at the European Conference on Soil Mechanics and Foundation Engineering, Wiesbaden (Germany).

# Technical Session 6

# Site Characterization

# Characterization of hazards affecting hillslopes damaged by the 2015 earthquakes in Nepal



L. C. Hockin  
 Simon Fraser University (SFU), Burnaby  
[lhockin@sfu.ca](mailto:lhockin@sfu.ca)

N.J. Rosser, Durham University, UK  
[n.j.rosser@durham.ac.uk](mailto:n.j.rosser@durham.ac.uk)

D. Stead, SFU  
[dstead@sfu.ca](mailto:dstead@sfu.ca)

## Introduction

Nepal is a mountainous, developing country which straddles the boundary between the Indian and Eurasian tectonic plates. The convergence of the plates leads to the development of the Himalayan mountain range and with it, the potential for large earthquakes that release strain on locked faults (Avouac et al. 2015). In April 2015, the moment magnitude (M<sub>w</sub>) 7.8 Gorkha earthquake occurred on a locked portion of the Main Himalayan Thrust Fault (MHT) initiating a sequence of hundreds of aftershocks and triggering extensive landsliding throughout Central Nepal (Kargel et al. 2016).

## Landslides in Nepal

### Pre-Earthquakes

In Nepal, landslides represent a major constraint on development causing significant economic loss and fatalities (Petley et al. 2007). A database of fatal landslides in Nepal for the period of 1978-2005 indicates an average of 78 fatalities per year wherein fatal landslides are coincident with the monsoon cycle of South Asia from June to September.

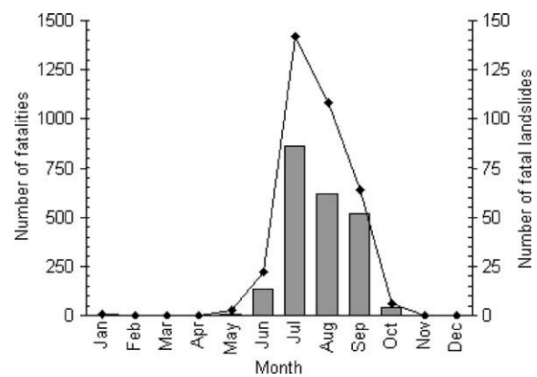


**Figure 1.** Landslide fatalities (bar graph) and the number of fatal landslides (line graph) by month for the period 1978-2005 in Nepal (Petley et al. 2007).

### Post-Earthquakes Coseismic and Postseismic

Following the earthquakes, multiple international teams carried out landslide mapping efforts. The resultant work identified thousands of coseismic and postseismic landslides prior to the 2015 monsoon.

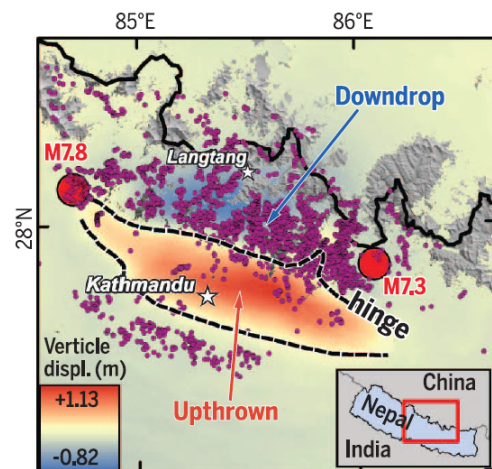


**Figure 2.** Landslide distribution (purple dots) with surface deformation and main epicenters (Kargel et al. 2016).

### Hillslope Damage

Hillslope damage, in the form of pervasive ground cracking (Figure 3), has been widely reported.



**Figure 3. Ridgetop cracking outside of Listi, Central Nepal. Photo taken May 12, 2016.**

Existing research indicates that landslide occurrence is a function of structural geology and damage accumulation in brittle hillslope materials through a process of progressive slope failure (Agliardi et al. 2013, Gischig et al. 2015, Parker et al. 2015, Stead and Wolter 2015). However, the development of progressive slope failures and the inter-relationships between damage, kinematics and geological structure/tectonics remain poorly understood (Agliardi et al. 2013, Stead and Wolter 2015)

### Proposed Research

The proposed research is an investigation of the mechanical evolution of hazards affecting hillslopes damaged by the 2015 earthquakes in Nepal. The area of focus will be the Upper Bhote Koshi (UBK) valley in Sindhupalchowk District approximately 100 km north of Kathmandu. Figure 4 shows a typical damaged settlement on the Arniko Highway in Sindhupalchowk.

This research will enable better prediction of future slope behaviour to identify hazard zones which may influence the response and relief efforts following major earthquakes, both in Nepal and beyond.

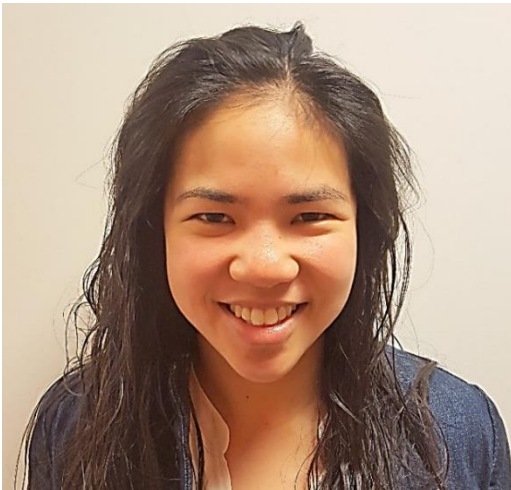


**Figure 4. Rockfall damage (foreground) and landslide deposit (left background) in Sindhupalchowk. Photo taken May 11, 2016.**

### References

- Agliardi, F., Crosta, G.B., Meloni, F., Valle, C., and Rivolta, C. 2013. Structurally-controlled instability, damage and slope failure in a porphyry rock mass. *Tectonophysics* 605:34–47.
- Avouac, J. P., Meng, L., Wei, S., Wang, T., & Ampuero, J. P. (2015). Lower edge of locked Main Himalayan Thrust unzipped by the 2015 Gorkha earthquake. *Nature Geoscience*: 1-6.
- Gischig, V.S., Eberhardt, E., Moore, J.R., and Hungr, O. 2015. On the seismic response of deep-seated rock slope instabilities – Insights from numerical modelling. *Engineering Geology*, 193: 1-18.
- Kargel, J. S., Leonard, G. J., Shugar, D. H., Haritashya, U. K., Bevington, A., Fielding, E. J., ... Young, N. (2016). Geomorphic and geologic controls of geohazards induced by Nepal's 2015 Gorkha earthquake. *Geomorphology* 351(6269), aac8353.
- Parker, R.N., Hancox, G.T., Petley, D.N., Massey, C.I., Densmore, A.L., and Rosser, N.J. 2015. Spatial distributions of earthquake-induced landslides and hillslope preconditioning in northwest South Island, New Zealand. *Earth Surface Dynamics Discussions*, 3(1):1-52.
- Petley, D.N., Hearn, G.J., Hart, A., Rosser, N.J., Dunning, S.A., Over, K., and Mitchell, W.A. 2007. Trends in landslide occurrence in Nepal. *Natural Hazards* 43(1): 23-44.
- Stead, D., and Wolter, A. 2015. A critical review of rock slope failure mechanisms: The importance of structural geology. *J Struct Geol*, 74:1–23.

# Applications of terrain analysis in geotechnical engineering



H. K. Wong  
 Golder Associates Ltd., Vancouver  
[Hazel.Wong@golder.com](mailto:Hazel.Wong@golder.com)

## Introduction

Attaining quality information on the terrain conditions of a project can greatly enhance the planning and investigation process, and significantly decrease overall project costs. The information can form a baseline from which sound decisions can be made throughout the lifetime of a project. This presentation introduces a general background on terrain mapping and provides geotechnical project examples of its applications.

## Definition

Terrain analysis involves interpreting, mapping, and displaying the terrain conditions of a selected area. It involves delineation of a study area into relatively homogenous terrain units, or polygons, based on surficial material texture, deposit type, surficial expression, slope, depth to bedrock, and geomorphological process. Other parameters may also be defined, such as drainage, surface erosion potential, and terrain stability.

## Guidelines

Terrain classification is generally based on the Howes and Kenk (1997) Terrain Classification System for British Columbia. In British Columbia, terrain analyses are generally carried out for Terrestrial Ecosystem Inventory (TEI), bioterrain, and terrain stability mapping projects under guidelines from the B.C. Ministry of Environment (BCMOE 2010).

## Polygon labels

Polygon labels can be as complex or as simple as the project requires. A terrain polygon label may look like Figure 1, below. Mapping with labeled terrain polygons may look like Figure 2.

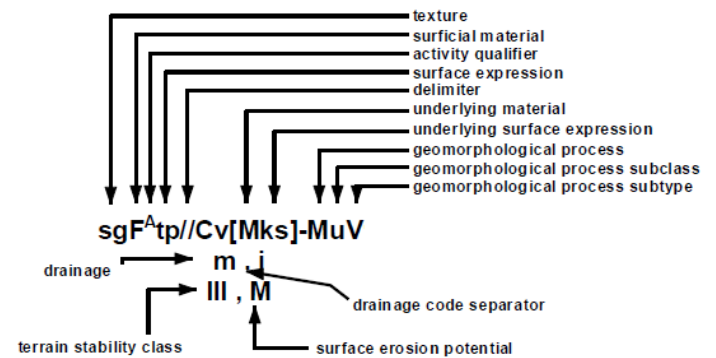


**Figure 1: Example of terrain polygon label, including Howes and Kenk (1997) parameters, as well as drainage, surface erosion potential, and terrain stability**

## Approach

The general approach of a terrain mapping study includes the following:

- 1) Project planning and selection of study area;
- 2) Review of existing information;
- 3) Preliminary interpretation of imagery and desktop mapping;
- 4) Fieldwork to confirm or “ground-truth” preliminary mapping;
- 5) Revision of desktop mapping with results of fieldwork and other supporting data;
- 6) Final deliverable and reporting; and,
- 7) Review for quality assurance and control by experienced and qualified terrain specialists.

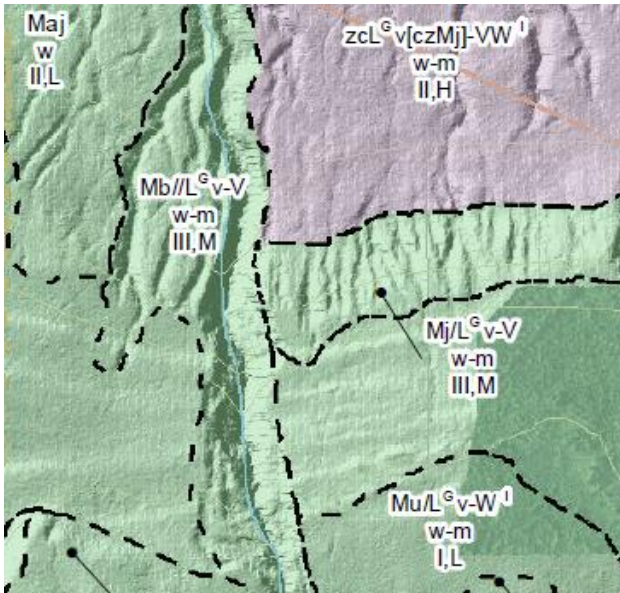


**Figure 2: Example of terrain polygons and labels.**

### **Applications for Geotechnical Engineering**

Terrain mapping can be applied in numerous ways to geotechnical engineering projects.

#### *Project siting*

Project planning can be greatly enhanced by using terrain analysis to determine the most suitable location for placing an alignment and facilities, where a crossing can be safely built, where organic deposits may be encountered, or where geological hazards impacting the development may be present or have the potential to occur. Project examples of this application include hazard mapping along major highway corridors for highway expansion and realignment. It has also been applied in the siting of extensive pipeline projects in Northern BC and Alberta, particularly in alignment studies and crossing designs.

#### *Strategic planning for field investigations*

A field investigation may be planned and carried out more efficiently if the project team understands the present terrain conditions. This includes access planning and choosing test-hole locations in order to target or identify certain material types. It also helps to select the proper equipment for the investigation by determining the expected material types, thickness of overburden, and depth to bedrock. Project examples include assisting in access planning by locating suitable helicopter landing areas close to areas of anticipated shallow bedrock in Northern BC. It also aided in planning of test hole drilling techniques and required materials by mapping anticipated material

types and discussing the information with contractors for a more accurate estimation of budget and timeline.

#### *Resource mapping*

The terrain of a study area can be selectively mapped as to highlight source areas for particular resources. For example, a granular source study may produce a map which only delineates the extent of aggregate resources such as by tracing out terraces or eskers, and of riprap sources such as locating suitable exposed bedrock. Project examples include mapping potential sources of borrow material along or proximal to highways, railways, and pipeline corridors in BC and Yukon.

#### *Thematic mapping*

In many cases, it may be more relevant to a client to map or provide only a selective parameter such as deposit type, slope stability, or geological hazards. All other data is stored in a database compiled from one or multiple projects. Examples include geological hazard assessments along railway and highway development projects to produce an inventory of geological hazards for ongoing monitoring and remediation.

#### *International Projects*

The terrain classification system was developed for British Columbia but can be adapted to include unique deposit types, geomorphological features, or processes of other provinces and territories in Canada, as well as other countries. Project examples include mapping of well sites in Alberta and for mining and infrastructure projects in South America and Africa.

### **Conclusion**

Terrain mapping has a variety of proven applications toward the enhancement of a geotechnical engineering project throughout its lifetime, and the information is a valuable resource for both present and future purposes.

### **References**

- British Columbia Ministry of Environment (BCMOE). 2010. Terrain Ecosystems Information: Guidelines for Developing a Project Plan. Version 1.0. Ecosystem Information Section, Ecosystem Branch. *For the Land Base Investment Program, Forest Investment Account.*
- Howes, D.E. & Kenk, E. 1997. Terrain classification system for British Columbia (Version 2). B.C. Ministry of Environment, Fisheries Branch, and B.C. Ministry of Crown Lands, Surveys and Resource Mapping Branch.

# The use of specific energy for open pit rock mass characterization



J. Danielson  
Simon Fraser University, Burnaby, British Columbia  
[John.danielson@sfu.ca](mailto:John.danielson@sfu.ca)

## Introduction

Specific energy in rock drilling is the energy required to excavate a unit volume of rock. It is calculated using the equation:

$$SE = \left(\frac{F}{A}\right) + \left(\frac{2\pi}{A}\right)\left(\frac{NT}{u}\right)$$

Where  $F$  is thrust,  $A$  is area,  $N$  is rotation speed,  $T$  is torque, and  $u$  is penetration rate.

Although specific energy was described as a function of rock strength when first introduced (Teale, 1965), it is rarely used for characterizing rock mass strength in geotechnical design.

Specific energy data is widely used in open pit blast planning, and can be measured wherever blast holes have been drilled, providing full areal coverage of an open pit. If shown to be correlated to the rock strength parameters commonly used in open pit slope design, specific energy datasets may have great potential for use in open pit rock mass characterization. Preliminary investigation of the relationship between RMR'76 (Bieniawski, 1979) and specific energy has already

been undertaken in the field of tunnel boring (Exadaktylos et al., 2008).

This presentation will use a specific energy dataset of over 100,000 blast holes from a mine in central British Columbia to show that specific energy reasonably correlates with rock quality and may be useful in identifying and characterizing fault zones.

## Correlating Specific Energy with Rock Mass Rating (RMR)

The mine area is composed almost entirely of tonalite that has undergone various degrees of shearing and alteration. The most altered zones are foliated and schistose, with typically 'Poor' ( $21 < \text{RMR} < 40$ ) rock mass ratings. Unaltered zones are typically 'Fair' to 'Good' quality ( $41 < \text{RMR} < 80$ ).

The specific energy dataset (shown in part on Figure 1) was compared with RMR from ten geotechnical holes that were drilled in the pit. RMR data plotted against nearby specific energy data, where distances between data points are less than 7.6 m (25 ft), show a good albeit scattered correlation (Figure 2). A linear fit through the origin results in the following relationship with an  $R^2$  value of 0.9:

$$\text{RMR}'76 = 1.2 \times SE$$

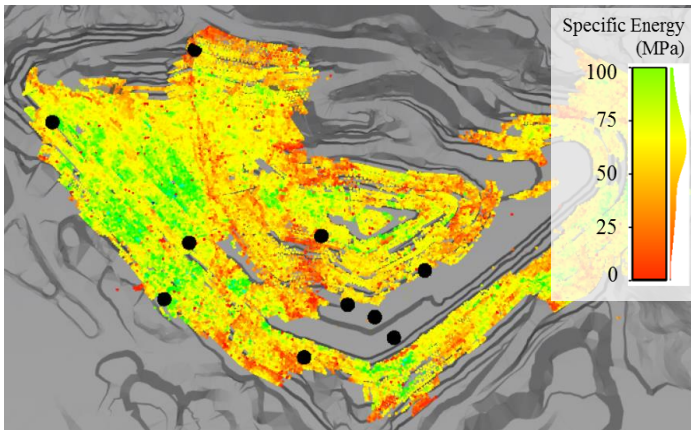
The correlation between RMR and specific energy is sensitive to the distance between compared data points. Larger distance cutoffs are more likely to compare RMR and specific energy from dissimilar rock masses, resulting in weaker correlations, while smaller cutoffs reduce the number of points available for comparison. The 7.6 m distance limit was chosen as a compromise between these two factors.

## Identification of Fault Zones

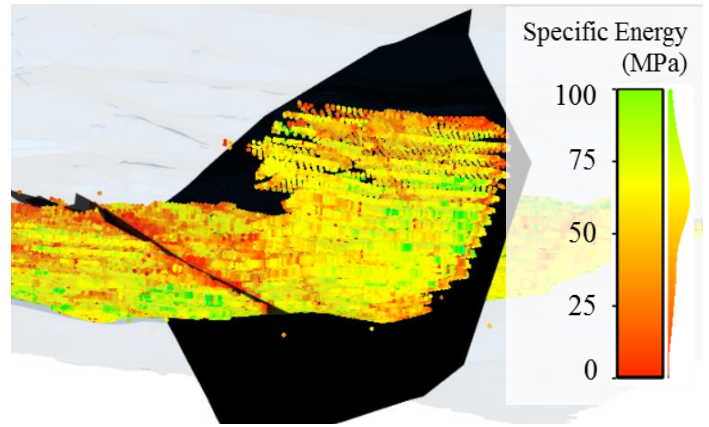
Mostaghimi and Kennedy (2015) describe the major geological structure groups at the mine as (1) large, sub-horizontal to shallowly dipping, ductile, and compressive high-strain zones, associated with foliation, (2) north-south striking oblique-slip faults, and (3) large faults dipping moderately to the west.

Figure 1 shows roughly planar concentrations of low specific energy data points. Some low specific energy concentrations appear to directly match major

mine-scale faults provided by the mine as 3D surfaces (Figure 3). Other planar concentrations may represent examples of the structure groups summarized above – this will be investigated further after the concentrations are mapped.



**Figure 1. Specific energy near the current pit topography. Geotechnical drill hole collars are shown in black.**



**Figure 3. Specific energy compared with two fault surfaces provided by the mine, shown in black.**

### Future Work

The author intends to expand on the preliminary results shown above to demonstrate the potential applications of specific energy in open pit rock mass characterization.

### References

- Bieniawski, Z. T. 1979. The geomechanics classification in rock engineering applications. *Proceedings of the 4th International Congress on Rock Mechanics*, 41–48.
- Exadaktylos, G., Stavropoulou, M., Xiroudakis, G., de Broissia, M., & Schwarz, H. 2008. A spatial estimation model for continuous rock mass characterization from the specific energy of a TBM. *Rock Mechanics and Rock Engineering*, 41(6), 797–834.
- Mostaghimi, N., & Kennedy, L. 2015. Structural geology of the Granite Lake Pit, Gibraltar copper-molybdenum Mine, south-central British Columbia (NTS 093B/08,/09): preliminary observations. *Geoscience BC Summary of Activities 2014* (Report 2015-1), 129-140.
- Teale, R. 1965. The concept of specific energy in rock drilling. *International Journal of Rock Mechanics and Mining Sciences & Geomechanics Abstracts*, 2(1), 57–73.

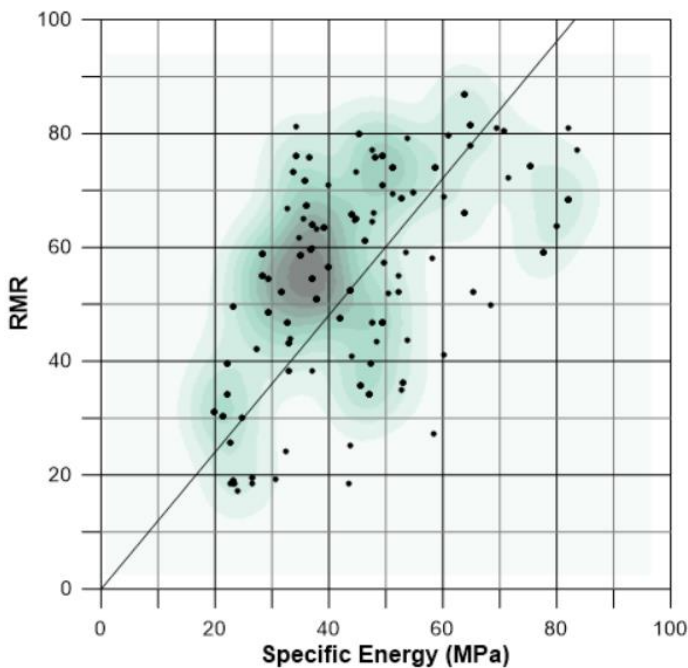


**Figure 2. RMR vs. specific energy**

## Spatial variability of particle size distribution in waste rock



D. R. Barsi  
University of Alberta, Edmonton  
[dbarsi@ualberta.ca](mailto:dbarsi@ualberta.ca)

### Introduction

Recent studies and reviews have demonstrated a need to characterize waste rock at any given mine site. Cash (2014) reviewed waste rock characterization studies from seven mine sites. She concluded that these investigations provided information on conceptual behavior, but did not improve the understanding of the relationships between physical properties, hydrology, and geochemistry. Amos et al. (2015) reviewed several field-scale investigations of waste rock characterization. These investigations included studies into the coupling of hydrogeology, geochemistry, thermal regime, and gas transport. This review highlighted the importance of site-specific waste rock characterization.

A research program at Diavik Diamond Mines was carried out in order to study the spatial variability in waste rock properties. The study included researchers from the University of Alberta, University of British

Columbia, Carleton University, and University of Waterloo.

### Research Program

#### *Field Research*

During the summer of 2014, a small scale (45,000 m<sup>3</sup>; 50 m by 70 m and 13 m high) waste rock pile was deconstructed at Diavik Diamond Mines. Diavik is located on Lac de Gras in the Northwest Territories, Canada. The site exists in a region of continuous permafrost, and has a mean annual air temperature of -12°C (Yip and Thompson 2015). This small scale “test pile” had been constructed and instrumented to monitor the physical, geochemical, hydrological, and thermal performance to guide the cover design of a full scale waste rock pile. A total of three test piles were built, using traditional push-dump and end-dump methods, in order to observe how natural freezing could limit the production of acid rock drainage (ARD). After nearly a decade of operation one test pile was deconstructed in order to sample in situ materials, and compare physical data to instrumentation records (water quality, moisture content, temperature, and gas composition). As part of this study hundreds of samples were collected to study in-situ physical, geochemical, microbiological, and hydrological properties. Approximately 250 locations within the pile were sampled for the characterization of the particle size distribution (PSD). The PSD samples were collected as 70 kg bulk samples. Figure 1 provides an aerial view of the test piles research site.

#### *Laboratory Testing*

Upon completion of the deconstruction, PSD samples were shipped to the University of Alberta for laboratory characterization. A testing procedure, based on ASTM standards and past research efforts, was used to process the bulk samples and determine the PSD of the waste rock. This data was then used to study the spatial variability of the material properties within the test pile.

## Data Analysis

The large number of sample locations enabled an evaluation of the spatial variability of the PSD within the pile. Ten profiles were prepared from the south end of the pile to the northern edge at 5 m spacing's. Twelve east-west profiles were also prepared at 3 m spacing. The intersection of each profile was also sampled vertically at an approximate spacing of 3 m. This sample arrangement allows for the creation of a 3D mesh, with material properties at each node. The three dimensional variability in the PSD throughout the pile was then assessed (separate studies investigated the spatial variability in pore water quality, microbiology, moisture content, and ice growth). Using these data, researchers can compare the in-situ material properties (water quality, moisture content, ice location, and PSD) to those recorded with instrumentation, and data collected during the pile construction. This will allow previous models of the test pile's performance to be confirmed or updated.

## Results

At the time of this abstract, initial analysis of the data set has been completed. Approximately two thirds of the collected PSD samples were processed, and used to produce particle size distribution curves. The data set was then examined based on the benches, profiles, and sections from which they were sampled. The most interesting result of this examination was the evidence of segregation with depth in the test pile. Figure 2 shows the frequency of each particle size, on each of the benches (Bench 1 is at the top, followed by Benches 2, 3, and 4). It can be seen that the upper benches have a higher proportion of finer material, while lower benches have a greater proportion of coarse material. Further study of these data will explore the relationship between the spatial variability of the PSD and volumetric moisture content, and hydraulic conductivity. This type of data will be helpful in determining where and how water and air will move through the material. These are important components in understanding heat transfer within the pile. It may also provide deeper insight into how the material will weather, and the potential impacts on the environment.



**Figure 1. Test Piles Research site. Type I pile on the left during deconstruction. Type III pile in bottom right, and covered pile in top right.**

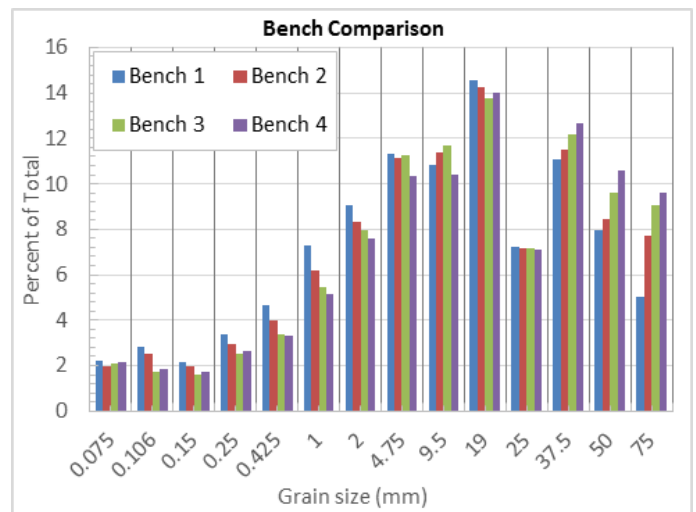


**Figure 2. PSD frequency in each bench.**

## References

- Amos, Richard T., David W. Blowes, Brenda L. Bailey, David C. Sego, Leslie Smith, and A. Ian M. Ritchie. 2015. "Waste-Rock Hydrogeology and Geochemistry." *Applied Geochemistry* 57: 140-156.
- Cash, A. E. 2014. "Structural and Hydrologic Characterization of Two Historic Waste Rock Piles." Masters, University of Alberta.
- Yip, C. G. and K. S. Thompson. 2015. *Diavik Diamond Mine NI 43-101 Technical Report*.

## Resource development on karst terrain, Vancouver Island B.C.



M. Dinsdale, GIT, A. Ag.  
Environmental Geoscientist, Island Geosciences Inc.  
Courtenay, BC  
[mdinsdalegeotech@gmail.com](mailto:mdinsdalegeotech@gmail.com)

### Introduction

The dissolution of upper Triassic limestone bedrock on Vancouver Island has resulted in the formation of Karst topography. Numerous karst features occur on Vancouver Island with the most notable being the Horne Lake, Upana and Little Hustan caves.

Karst topography forms as a result of the production of carbonic acid within the soil profile ( $\text{H}_2\text{O} + \text{CO}_2 \rightarrow \text{H}_2\text{CO}_3$ ). This dissolves calcium carbonate rich bedrock ( $\text{CaCO}_3 + \text{H}_2\text{CO}_3 \rightarrow \text{Ca}^{2+} + 2 \text{HCO}_3^-$ ), producing a variety of unique landforms.

In 1999, reconnaissance-level karst inventory work was completed for the entire province of British Columbia (KISVAP, 2001). Karst vulnerability potential maps were produced largely based on geological mapping. High vulnerability potential was assigned to areas underlain by limestone, and calcareous silts and shaly limestones were assigned a moderate vulnerability potential (Stokes, 1999).

### Karst Landforms

Factors such as geology, climate, topography, hydrology, biology, and time can influence the resultant Karst topography. Limestone outcrops are found throughout British Columbia and the presence of soluble carbonate-rich bedrock combined with steep surface slopes and subsurface hydraulic gradients, with high levels of rainfall on coastal British Columbia terrain allows for a heightened potential for Karst development on Vancouver Island (KMH, 2003). Impurities in the bedrock, low pH/acid generation, and hydrologic gradients can alter the solubility potential.

Many Karst systems are known to have specific climates and unique flora and fauna. Larger systems provide recreational value for spelunking and even diving as some features may have connectivity to the subsurface or underground system, or to other Karst features nearby.



**Figure 1: Significant sinkhole (>2m in diameter) located in high vulnerability terrain, northern Vancouver Island.**

The Karst Inventory Standards and Vulnerability Assessment Procedures for British Columbia (KISVAP, 2001) categorizes Karst landforms into surface or epikarst features, based on their dimensional characteristics. Epikarst features lie within the soil/vegetation horizon and allow for diffuse water flow into the subsurface system. Should the site be disturbed, site degradation may lead to soil

loss and the potential transfer of sediment and fine organic matter into openings (KISVAP, 2001). Surface karst features are larger features and are more likely to have connectivity to the subsurface environment. They are further classified into linear features, negative/positive relief intersection features, insurgent, or exsurgent features. Examples of these include but are not limited to sinkholes (Figure 1), springs, swallets, losing streams, and caves.

### Resource development and the KFA

Karst landforms have a distinctive topography and are considered a unique, non-renewable resource with significant biological, hydrological, mineralogical, scientific, cultural, recreational, and economic values (KMH, 2003).

As much of the limestone on Vancouver Island is forested, resource development (e.g. timber extraction and resource road construction) on Karst prone terrain is likely to occur. Harvesting on Karst features can impact the subsurface environment by increasing sediment delivery (thus increasing erosion), diverting water (increasing dissolution processes), or by impacting the biological environment. Areas with known karst features or a high karst vulnerability potential require a Karst Field Assessment (KFA) before resource development can occur. The purpose of the KFA is to “obtain detailed information on karst resources within and adjacent to an area of proposed development, and to assess the vulnerability of the karst unit” (KISVAP, 2001) at the site level.

### Karst Vulnerability and Significance

The site level Karst vulnerability is determined by; 1) the physical characteristics, potential, and density of surface karst and epikarst development; 2) surficial deposits (type, thickness), and bedrock types; 3) slope class, drainage, geomorphic indicators; and 4) biological (flora/fauna) indicators (KISVAP, 2001). In order to determine the final karst vulnerability rating, the significance of a qualifying Karst feature must be determined. The following ten criteria are assigned a low, moderate, or high significance potential rating: the dimensional characteristics, connectivity to the subsurface, hydrology, geological, educational, archaeological, cultural and recreational values, rarity/abundance, and visual qualities (Figure 2). This information can be further applied to documents such as the Karst Management Handbook for British Columbia (KMH, 2003) to identify the best management practices.

As significance criteria is varied, it may require a number of experts to determine the significance of a particular karst feature. This process requires a high level of professional judgement, and complex surface karst features may require additional inspections by qualified personnel working within the required scope of practice (i.e. biologist, archaeologist, cavers). Knowledge of nearby features located outside of the study area is crucial to rating the significance criteria, which may impact resource management decision making.

### References

- Stokes, T. 1999. Reconnaissance Karst Potential Mapping and Inventory for British Columbia: Testing of the KISP Methodology. *Prepared for B.C. Ministry of Forests, Research Branch.*
- Province of British Columbia 2003. Karst Management Handbook for British Columbia (KMH), B.C. Ministry of Forests, Victoria, B.C.
- Resources Inventory Committee 2003. Karst Inventory Standards and Vulnerability Assessment Procedures for British Columbia (KISVAP), Version 2.0. *Resources Information Standards Committee, Victoria, B.C*

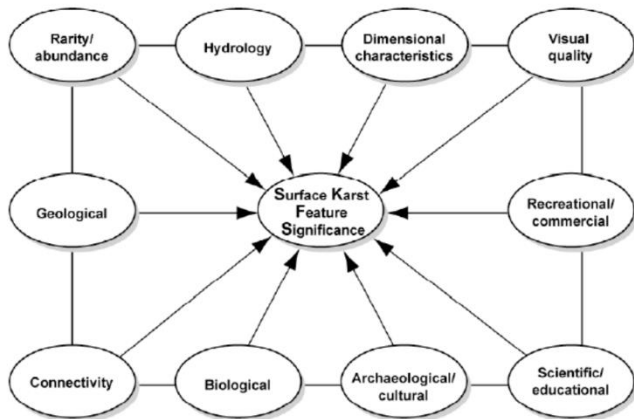


Figure 2: Characteristics and values contributing to surface karst feature significance (KISVAP, 2001).

## Evaluating water and chemical release from oil sands fluid fine tailings using multiple tracers



K. Dompierre  
University of Saskatchewan, Saskatoon, Canada  
GEO-SLOPE International, Calgary, Canada  
[kathryn.dompierre@geoslope.com](mailto:kathryn.dompierre@geoslope.com)

L. Barbour  
University of Saskatchewan, Saskatoon, Canada  
[lee.barbour@usask.ca](mailto:lee.barbour@usask.ca)

### Introduction

Oil sands mining in Northern Alberta faces a number of environmental challenges, many of which are associated with the long-term containment of waste materials produced by the oil sands extraction process (Gosselin et al. 2010). Fluid fine tailings (FFT), one of the waste materials, are a mixture of fine-grained minerals, oil sands process affected water, and residual bitumen from the extraction process. These soft tailings have low shear strengths due to their high water content (and low solids content), which persists for many years (Kasperski & Mikula 2011). The FFT pore water contains high concentrations of dissolved constituents, naphthenic acids, and petroleum hydrocarbons (Allen 2008; Dompierre et al. 2016;

Kavanagh et al. 2011). Thus, inclusion of FFT in typical reclamation landscapes is often difficult.

One proposed method of disposing of FFT is to place the soft tailings within depleted mine pits below a water cap in an 'end pit lake' (EPL). Thirty EPLs have been proposed in the Athabasca oil sands region; half of which will incorporate unprocessed FFT below a freshwater cap (Prakash et al. 2011). Mass and thermal energy transfer from the FFT into the overlying water cap may affect the chemical regime and biological functions within the water cap. Chemical constituents of concern may move from the FFT into the overlying water cap via two key processes: (1) advective-diffusive mass transport with upward pore water flow caused by settling of the FFT; and (2) mixing created by wind events or unstable density profiles through the lake water and upper portion of the FFT.

Multiple tracers (stable isotopes of water, chloride, and heat) were used to trace pore water movement and assess mass transport through the FFT in the first EPL, Base Mine Lake, developed at Syncrude Canada Ltd.'s Mildred Lake mine. Field measurements were compared with numerical models to determine the main mechanisms contributing to mass transport. Assessing the physical movement of constituents across the FFT-lake interface is central to determining the ability of an EPL to sequester FFT, and for defining the chemistry of the overlying lake water.

### Methodology

Sampling of the water cap and FFT was conducted between May 2013 and October 2015 to catalogue stable isotopes of water signatures and chloride concentrations at Base Mine Lake. Tailings samples were obtained every 0.1 m from the FFT-water interface to an FFT depth of approximately 3 m. Isotope samples were analyzed at the University of Saskatchewan according to methods outlined by Wassenaar et al. (2008) and chloride samples were processed at a commercial laboratory.

A temperature measurement station was installed from a platform with 30 thermistors ( $\pm 0.1^\circ\text{C}$ ) attached to a Kevlar cable at 1 to 2 m intervals throughout the entire FFT deposit. Temperatures were measured once

a day, from September 2013 to March 2014, to observe seasonal temperature variations through the FFT and lake water.

Commercial finite element software (GeoStudio©) was used to develop one-dimensional mass (advection, dispersion, diffusion) and heat (convection, conduction) transport models. Several transport scenarios were simulated (e.g., diffusion/ conduction alone or with a range of advection/ convection rates), some of which also included shallow mixing of the upper FFT with lake water to represent the effect of FFT disturbance due to instability in the overlying water cap. The simulated results were compared to the field measurements (as illustrated in Figure 1) in order to determine which modelled mechanism(s) most likely contributed to the movement of mass (or heat) in the system.

## Results

The results from the chloride models suggested that a diffusion-only mass transport regime could have generated the measured chloride profile. However, the stable isotopes of water and heat transport models both indicated that the dominant mass transport regime was advection ( $0.004 \text{ m}^3/\text{d}/\text{m}^2$ ) with a fall disturbance event in which the upper 1 m of FFT was mixed with lake water. When a similar disturbance was added to the chloride models, inclusion of advective mass flux ( $0.002 \text{ m}^3/\text{d}/\text{m}^2$ ) provided the best overall fit. A comparison of the results from the three separate tracers provided a more comprehensive picture of the mass exchange between FFT and the water cap in the first EPL. Together they indicated the dominant mass transport regime during 'normal' conditions in Base Mine Lake (advection due to FFT settlement), the presence of rapid disturbance events (most likely associated with lake overturning in the fall), and the potential depth of FFT implicated by this disturbance.

This investigation provides valuable insight for assessing the geochemical evolution of the lake water and performance of EPLs as an oil sands reclamation strategy. Findings from this study will assist in the development of monitoring and management plans for future EPLs.

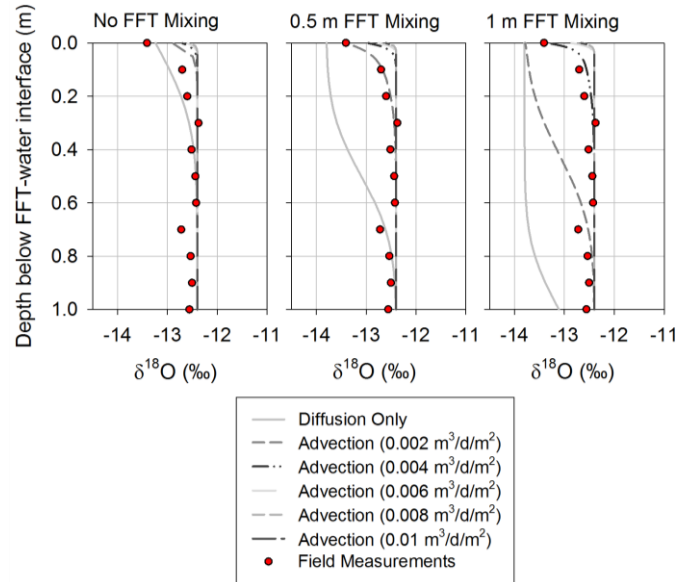


**Figure 1. Isotope mass transport model results compared to field measurements**

## References

- Allen, E.W. 2008. Process water treatment in Canada's oil sands industry: I. Target pollutants and treatment objectives. *Journal of Environmental Engineering Science* 7(2): 123-138.
- Dompierre, K.A., Lindsay, M.B.J., Cruz-Hernández, P. & Halferdahl, G.M. 2016. Initial geochemical characteristics of fluid fine tailings in an oil sands end pit lake. *Science of the Total Environment* 156: 196-206.
- Gosselin, P., Hrudehy, S.E., Naeth, M.A., Plourde, A., Therrien, R., Van Der Kraak, G. & Xu, Z. 2010. Environmental and Health Impacts of Canada's Oils Sands Industry. The Royal Society of Canada, Ottawa, ON, Canada.
- Kasperski, K.L. & Mikula, R.J. 2011. Waste streams of mined oil sands: Characteristics and remediation. *Elements* 7(6): 387-392.
- Kavanagh, R.J., Frank, R.A., Oakes, K.D., Servos, M.R., Young, R.F., Fedorak, P.M., MacKinnon, M.D., Solomon, K.R., Dixon, D.G. & Van Der Kraak, G. 2011. Fathead minnow (*Pimephales promelas*) reproduction is impaired in aged oil sands process-affected waters. *Aquatic Toxicology* 101(1): 214-220.
- Prakash, S., Vendenberg, J.A. & Buchak, E. 2011. The oil sands pit lake model – sediment diagenesis module. In F. Chan, D. Marinova, & R.S. Anderssen (eds), *19th International Congress on Modelling and Simulation*. Modelling and Simulation Society of Australia and New Zealand, Perth, Australia, 3761–3767.
- Wassenaar, L.I., Hendry, M.J., Chostner, V.I. & Lis, G.P. 2008. High resolution pore water  $\delta^2\text{H}$  and  $\delta^{18}\text{O}$  measurements by  $\text{H}_2\text{O}(\text{liquid})\text{-H}_2\text{O}(\text{vapor})$  equilibration laser spectroscopy. *Environmental Science & Technology* 42: 9262-9267.

# Poster Session 1

# Liner System Design: An Outside Look at the State of the Practice



B. Olsen, M. Eng., P.Eng.  
 Western Tank and Lining, Richmond BC  
[ben@wtl.ca](mailto:ben@wtl.ca)

## Introduction

Use of geosynthetics in Canada has increased dramatically over the past 30 years. We have seen geotextiles used as separation layers, filtration layers, and geomembrane protection layers; geocomposites used as drainage layers and leachate collection layers; geomembranes used as low permeability layers; and all three types of materials used in liner systems for a number of applications.

State of the practice for liner system design is to assess a number of critical criteria (Koerner, 2012), including, but not limited to: interface friction; anchoring; leachate drainage; overburden pressure; differential settlements; gas collection; and iner bedding and/or protective mineral or geotextile layers.

Once these design criteria are assessed and understood, specific thicknesses, type of liner and peripheral layers are chosen to meet demands of the

site. Site demands are highly variable depending on location and application.

The following sections will assess standard of practice for liner systems in applications such as municipal solid waste, waste water and mine waste. Following will be a brief look at the path forward for use of geosynthetics and an assessment of what is required for proper installation.

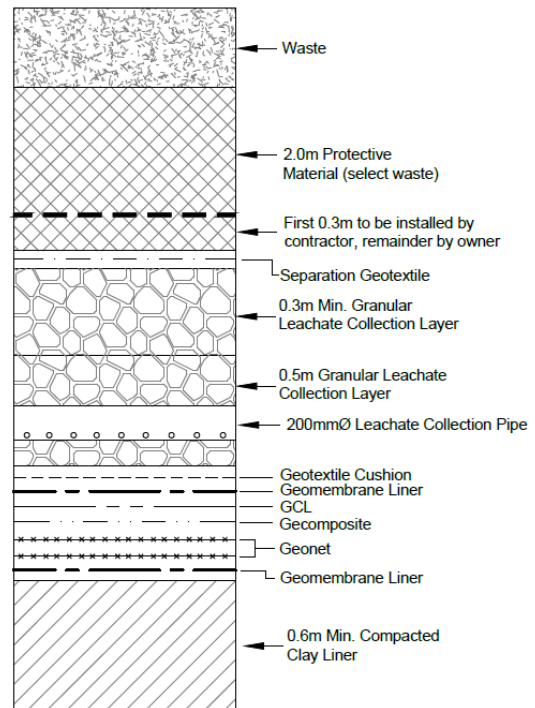


**Figure 1. Municipal solid waste liner system as taken from private tender, job location: Alberta.**

## Municipal Solid Waste

Municipal solid waste applications typically include 60 mil (1.5 mm) thickness high density polyethylene (HDPE) with varying asperity height to account for increase in required interface friction; geotextile cushion layers of varying thicknesses; and geocomposite drainage layers for leachate collection. Geosynthetic clay liners (GCL) are used as leak isolation layers in lieu of substantial insitu clay seepage barriers at the base of the landfill.

At times, although not common, municipal solid waste applications can include both primary and secondary liners, as shown in Figure 1. Design can be highly variable. More robust applications include 2

layers of 60 mil HDPE with a drainage geonet in between. At the base of the system is a leak isolation layer such as compacted clay, till or GCL layer (Muller, 2007).

### Waste Water

Liner systems in use as a low permeability barrier in waste water applications are prevalent in most municipalities. These are typically smooth 60 mil HDPE with a geotextile cushion layer, as shown in Figure 2. Thinner liners, such as 40 mil HDPE and linear low density polyethylene (LLDPE) are not common, as ice formation and variable water levels have been found to cause substantial damage.

Secondary liners are not common in this application, however GCLs, especially those with scrim reinforcement, have been used as leak isolation layers.

While the use of GCLs as a base layer for ponds greater than 3 m has been shown to cause dispersion of bentonite and ultimately failure of the GCL, recent findings from Rowe and Orsini (2002) show scrim reinforced GCLs can accommodate over 60 m of constant hydraulic head.

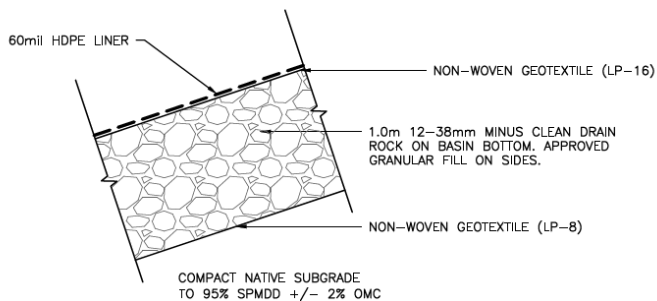


**Figure 2. Typical liner system detail as obtained from public tender of sewage treatment plant in Golden, BC.**

### Mine Waste

Liner systems for storage of mine waste in Canada are not as common as that of municipal solid waste or waste water. This is possibly due to corporate incentive, environmental regulations, and proximity to cities and towns. As such, liner systems for these applications are highly variable. Typically 40 mil to 60 mil in thickness, nearly always LLDPE, and mostly textured.

Specifying LLDPE liners in Canada is more common than in the US or Europe. This is likely due to potential for differential settlements and the fact that LLDPE has higher elongation properties than HDPE. However, this is somewhat perplexing given recent

findings from Peggs et al (2004) on maximum allowable multiaxial strains.

GCL for use in mining applications is not common in Canada. Ion exchange can be a concern with mine waste, although use of enhanced polymers can mitigate this. As always, site-specific testing should be completed prior to use.

### Conclusion

Liner system design has been briefly addressed in this paper followed by a summary of state of the practice in Canada for three different applications: municipal solid waste, waste water, and mine waste.

With increasing popularity of liners in Canada – especially as public knowledge of environmental protection measures grows – design engineers will be required to incorporate the use of liner systems more.

Geotechnical engineers in the mining field especially will be pushed to provide stable tailings facilities that limit the potential for seepage. Even where not required, the assurance of a liner system will help to allay public concern of mine waste seepage.

What is and will always be important is the requirement for proper liner specification, detailed and site specific understanding of interface friction, strong and regimented third party construction quality assurance, and a careful, experienced, IAGI certified installer.

### References

- Koerner, R. 2012. *Designing with Geosynthetics*. 6h Ed. Xilbris Corp, New York, USA.
- Muller, M. 2007. *HDPE Geomembranes in Geotechnics*. Springer Berlin Heidelberg. New York, USA.
- Peggs, I., Schmucker, B., Carey, P. 2004. *Assessment of Maximum Allowable Strains In Polyethylene and Polypropylene Geomembranes*.
- Rowe, K., Orsini, C. 2002. *Internal Erosion of GCLs Placed Directly Over Fine Gravel*.

## Measurement of dissolved gas pressures during unloading of loose gassy sands



A. Khurana  
Schulich School of Engineering, University of Calgary  
[aditi.khurana@ucalgary.ca](mailto:aditi.khurana@ucalgary.ca)

J. L.H. Grozic  
University of Calgary, Calgary  
[jgrozic@ucalgary.ca](mailto:jgrozic@ucalgary.ca)

C. Ryan  
University of Calgary, Calgary  
[cryan@ucalgary.ca](mailto:cryan@ucalgary.ca)

B. Ladd  
University of Calgary, Calgary  
[bladd@ucalgary.ca](mailto:bladd@ucalgary.ca)

### Introduction

Soils with relatively large quantity of dissolved gas within the pore fluid are known to have the potential to commence and propagate liquefaction of the soil. Gassy sands commonly occur in offshore and coastal regions and submarine and offshore slope failures are often inevitable in such soils. Gas in most cases, is present as occluded bubbles within the soil matrix and changes the soil properties. The shear strength and the volume change behavior are affected the most. The ratio of the pore water pressure and the total dissolved gas pressure ( $P_{TDG}$ ) controls if and when free gas is likely to form during unloading, which affects the compressibility of the pore fluid and the integrity of

the overall soil matrix. Previously,  $P_{TDG}$  has not been measured, but rather has been estimated based on differences between the pore water and capillary pressures, which may result in inaccuracies and incorrect model predictions.

The purpose of this paper is to quantify both total dissolved gas pressure and pore water pressure in gassy sand to investigate the response to unloading. An experimental investigation was carried out on gassy sand using a rigid wall sand pack instrumented with pore pressure and dissolved gas measurements. The dissolved gas pressure was measured using a prototype probe recently developed at the University of Calgary. The  $P_{TDG}$  (Total dissolved gas pressure) probe consists of a pressure transducer connected to a diffusion head. The diffusion head consists of a transducer connection fitting and a 2 m length of small diameter (0.64 mm), thin walled (0.17mm) silicone tubing coiled around a shaft. The silicone tubing is permeable to gases, but not water. Dissolved gases are exchanged between the water and the probe's void volume via diffusion through the wall of the silicone tubing. The pressure transducer then reads the pressure of these dissolved gases (A.H. Manning et al. 2003). The figure 1 below displays the total dissolved gas pressure probe used in the set-up. The total dissolved gas pressure probe has been successfully applied to groundwater dissolved gas measurements.

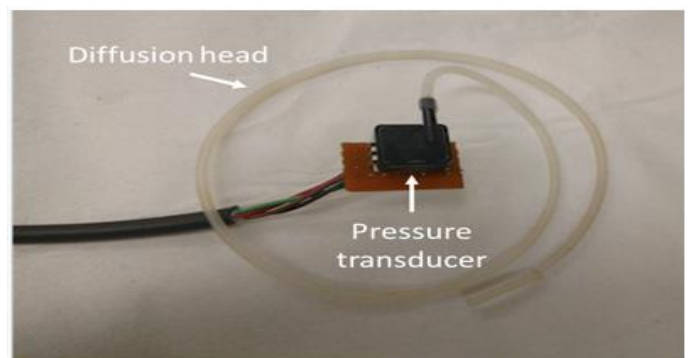


**Figure 1: Total dissolved gas pressure probe used in the set-up**

### Experimental Set-up

Ottawa sand (50/70) was selected for testing due to its ease of preparation and past success in triaxial tests. Gassy soils were prepared using a circulation system.

This circulation system was used to prepare CO<sub>2</sub> dissolved water and to percolate it through the specimen. The water pressure in the pore space was measured using gauge pressure transducers of capacity 1350kPa. The two pressure transducers were connected to the specimen's top and bottom drainage port.

### Preliminary Experiments

A laboratory program was carried out to study the undrained unloading behavior of gassy soils as opposed to that of saturated soils. Specimen fully saturated with deaired distilled water was tested in undrained unloading conditions and then the same procedure was followed for a gassy soil specimen (fully saturated with CO<sub>2</sub> saturated water).

### Results

#### Saturated (Non gassy) soils

Since there was no gas in the specimen, the pore pressure did not increase upon reduction of the total stress. Due to absence of gas in the specimen, the P<sub>TDG</sub> remained almost zero throughout the test. This test simply confirmed that the testing apparatus was responding as anticipated. Figure 2 below illustrates this result.

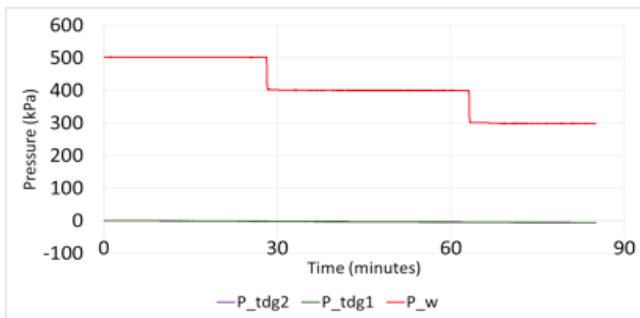


**Figure 2: P<sub>TDG</sub> and pore pressure response of saturated soil specimen**

#### Gassy soils

The behavior of the gassy specimen was observed to be dominated by gas exsolution process. When the cell pressure was lowered, the pore pressure initially dropped and then increased towards an asymptotic value. This happened because gas exsolution process was initiated when the pore-pressure dropped below the liquid/gas saturation pressure. As the gas began to exsolve, bubbles formed, and the pore pressure increased under undrained conditions. With time, the pore pressure stabilized to a value close to the total

dissolved gas pressure. This is depicted in the Figure 3 below.

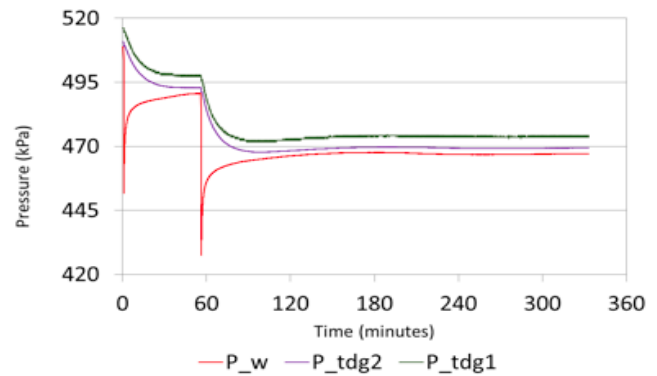


**Figure 3: P<sub>TDG</sub> and pore pressure response of gassy soil specimen**

### Conclusions

The following conclusions were drawn from the experimental and theoretical research:

- Accurate measurement of PTDG using probe is a great tool to enhance our understanding of gassy soil behavior
- During unloading of a gassy soil, gas exsolution and bubble formation occurs (which is captured by PTDG probes) causing pore pressures to increase.

### References

- Amaratunga A. and Grozic J.L.H. 2009. On the undrained unloading behavior of gassy sands. *Canadian Geotechnical Journal*, 46(11): 1267-1276
- Sills, G.C., Wheeler, S.J., Thomas, S.D., and Gardner, T.N. 1991. Behaviour of offshore soils containing gas bubbles. *Geotechnique*, 41(2): 227-241.
- Sobkowicz, J.C. and Morgenstern, N.R. 1984. The undrained equilibrium behavior of gassy sediments. *Canadian Geotechnical Journal*, 21, 439-448.
- Roy, J.W. and Ryan, M.C. 2010. In-well degassing issues for measurements of dissolved gases in groundwater. *Ground Water*, 48(6): 869-877.
- Roy, J.W. and Ryan, M.C. 2013. Effects of unconventional gas development on groundwater: A call for total dissolved gas pressure field measurements. *Groundwater*, 51(4): 480-482.
- Manning A.H., Solomon D. Kip and Sheldon Amy L. 2003. Applications of a total dissolved gas pressure probe in groundwater studies. *Groundwater*, 41(4): 440-448.
- Dusseault, M.B. 1979. Undrained volume and stress change behavior of unsaturated very dense sands. *Canadian Geotechnical Journal*, 16(4): 627-640

# Design of an Instrumentation System for a Tailings Dam



Maraika De Groot  
 BGC Engineering, Vancouver  
[mdegroot@bgcengineering.ca](mailto:mdegroot@bgcengineering.ca)

Andrew Critchley  
 BGC Engineering, Kamloops  
[acritchley@bgcengineering.ca](mailto:acritchley@bgcengineering.ca)

## Introduction

The Pueblo Viejo mine, principally owned by Barrick Gold and located in central Dominican Republic, began production of gold in August 2012. BGC Engineering Inc. is the designer of the tailings dams and provides Engineer of Record services for the El Llagal Tailings Storage Facility (TSF), which is the waste storage area for this mine. The primary containment dam is Lower Llagal (LL) Dam which is planned to be constructed to a maximum height of 150 m.

The TSF site is in an area of high seismicity, and frequent and intense lightning storms during the rainy season. Intense short duration precipitation events are common.

An instrumentation system was designed for the LL Dam for two purposes: first, to confirm that field performance is as intended and second, to provide a warning system that can be used to advise the owners

of actions that should be taken as outlined in the Operations, Monitoring, and Surveillances manual.

The instrumentation system design was guided by the principals outlined in Dunnycliff (1993). The discussion herein focuses on the selection of instrumentation types, the installation locations in the LL Dam, and installation techniques.

## Dam Design and Construction

The LL Dam is a rockfill dam with an inclined low permeability fill core built in incremental raises using the downstream construction method. A graded filter zone is located downstream of the core and blanket filters are placed along critical foundation areas. The dam is founded on saprolitic soils and weathered rock. As of July 2016, the LL Dam was constructed to a maximum height of approximately 100 m. Figure 1 shows a simplified cross-section of the LL Dam.

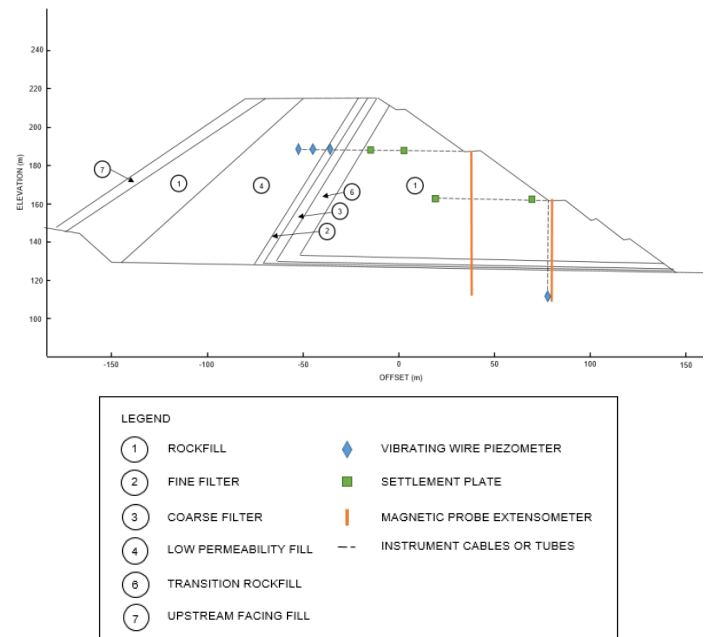


**Figure 1 Simplified cross-section of the LL Dam with instrumentation.**

## Instrumentation System Design

### Monitor Pore Pressure

Pore pressures are a fundamental component of predicting strength for fine grained materials, and are used in multiple aspects of dam design, for example slope stability modelling. If pore pressures exceed

those used in design, further investigation is required. Vibrating wire piezometers (VWPs) were installed in the LL Dam to monitor pore pressure generation and are located in the following locations:

- LPF core: to monitor accumulation and dissipation of construction induced pore pressures and the influence of rising tailings pond levels. VWPs were installed in the downstream portion of the LPF core.
- Fine Filter: to verify that the filters are free draining
- Foundation soils and rock: to evaluate potential construction induced pore pressure responses and assess phreatic surface levels.

#### *Monitor Dam Deformation*

Static settlement is expected during staged construction. Additionally, earthquakes can result in abrupt deformations of the dam. Three different instrument types were installed both internally and externally on the dam to monitor the magnitude and location of rockfill deformations. The instruments installed to monitor dam deformations include:

- Magnetic Probe Extensometers (MPEs) installed in the downstream rockfill shell
- Settlement Plates installed in the downstream rockfill shell
- Survey Prisms installed on the surface of the upstream and downstream shell, and along the crest.

An MPE consists of telescopic inclinometer casing with magnetic targets and measures both vertical and lateral movements. Vertical movements are measured by using a reed switch probe to locate the magnetic targets and lateral movements are measured by using an inclinometer probe.

Modelling of dam deformations was undertaken and results were used to identify the optimum locations for the MPEs and settlement plates to target areas with the highest expected deformations. Survey prisms were installed in order to compare surface deformations to deformations measured by the MPEs and settlement plates.

#### **Installation Techniques**

VWPs and settlement plates have cables and hydraulic tubes that are extended as dam construction progresses. Instrument cables and tubes were routed downstream to the dam face, through the downstream rockfill shell, to instrument houses on designated

instrumentation benches. To protect the cables and tubes from damage and excess strain, cables and tubes were run through a protective conduit of HDPE pipe. The conduit was installed in a trench and surrounded with bedding material to protect the pipe from stress concentrations, punctures, or damage. To protect the VWP electrical cables and readout locations from damage by lightning, a lightning protection system was installed.

MPEs were installed into competent rock foundations and are surrounded by bedding material to protect the casing from damage as they were raised through the downstream rockfill shell. An installation sequence was designed for the MPEs in order to raise the MPE casing in a timely manner as surrounding rockfill was placed in lifts.

#### **Current Instrumentation**

As of July 2016, 50 VWPs, 6 MPEs, and 7 settlement plates are installed in the LL Dam or dam foundation. These instruments in conjunction with survey prisms are monitored on a regular basis. Additional instruments will be installed as the dam is raised.

#### **References**

Dunncliff, J. 1993. Geotechnical Instrumentation For Monitoring Field Performance. John Wiley & Sons, Inc., New York, N.Y.

# Estimation of hydraulic conductivity of coarse soil using pedotransfer functions



N. Singh  
 University of Manitoba, Winnipeg  
[Singhn38@myumanitoba.ca](mailto:Singhn38@myumanitoba.ca)

H. M. Holländer  
 University of Manitoba, Winnipeg  
[hartmut.hollaender@umanitoba.ca](mailto:hartmut.hollaender@umanitoba.ca)

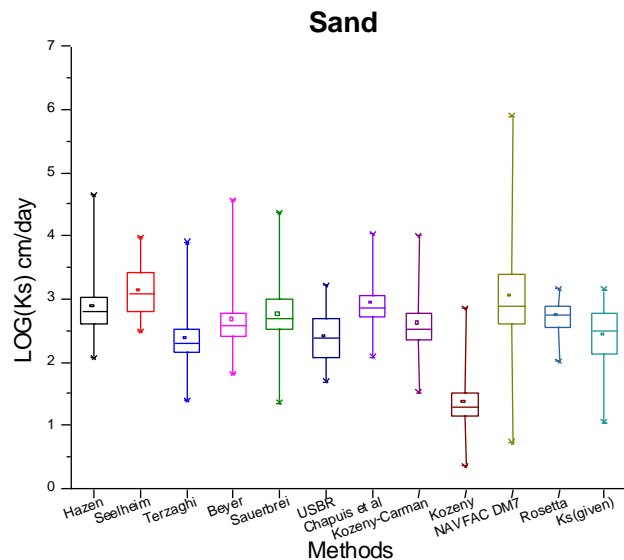
## Abstract

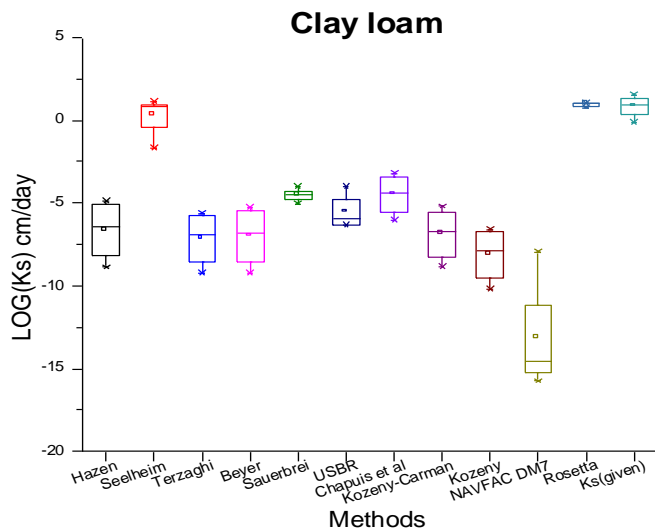
Hydraulic conductivity is a key parameter for the prediction of water flow through the soil (Hollander et al. 2016). A cost efficient method to determine the hydraulic conductivity is the application of pedotransfer functions (PTFs) on the soil particle size data.

We collected sixty disturbed, and fifteen undisturbed soil samples from a pasture site in La Broquerie, Manitoba, Canada. Sieving was carried out according to ASTM C136/C136M – 14 (2006) (particle diameter  $\geq 75$   $\mu\text{m}$ ) and laser deflection (particle diameter  $< 75$   $\mu\text{m}$ ) using a Mastersizer 2000

(Malvern Industries) was carried out for determining the soil particle size from the disturbed soil samples. Along with that UNSODA soil data was taken into account for estimation of saturated hydraulic conductivity for all the different types of soils. Ten different PTFs including empirical, semi-empirical formulas (e.g. Hazen, Beyer, Zieschang) (Vienken and Dietrich 2011) and a neural network model (ROSETTA) (Schaap et al. 2001) were used for predicting the hydraulic conductivity from the particle analysis. Hydraulic conductivity of the undisturbed soil samples was measured using permeameter testing according to ASTM D2434-68 (2006). It was estimated that empirical equations (e.g., Terzaghi, Kozeny Carman) (Milan Vuković 1992) give reliable values for coarse grain soil (like sandy, loamy sand and sandy loam soil) whereas; ROSETTA estimates reliable values for both fine grain soil (like clay, silty clay loam silty loam soil) and for coarse grain soil.

## Figures





## References

- ASTM C136/C136M – 14, 2006. Sieve Analysis of Fine and Coarse Aggregates. ASTM international.
- ASTM D2434-68, 2006. Standard Test Method for Permeability of Granular Soils (Constant Head) ASTM International.
- Hollander, H. M., Z. Wang, K. A. Assefa & A. D. Woodbury, 2016. Improved Recharge Estimation from Portable, Low-Cost Weather Stations. *Ground Water* 54(2):243-54 doi:10.1111/gwat.12346.
- Milan Vuković , A. S., 1992. Determination of hydraulic conductivity of porous media from grain-size composition. Water Resources Publications.
- Schaap, M. G., F. J. Leij & M. T. van Genuchten, 2001. ROSETTA: A computer program for estimating soil hydraulic parameters with hierarchical pedotransfer functions. *Journal of Hydrology* 251(3-4):163-176 doi:10.1016/S0022-1694(01)00466-8.
- Vienken, T. & P. Dietrich, 2011. Field evaluation of methods for determining hydraulic conductivity from grain size data. *Journal of Hydrology* 400(1–2):58-71 doi:<http://dx.doi.org/10.1016/j.jhydrol.2011.01.022>.

## Static axial compression testing of HD™ helical piles: Case study of an active project in Northern Manitoba



S. Beaudry, B.Sc., EIT  
TREK Geotechnical Inc., Winnipeg, Manitoba  
[sbeaudry@trekgeotechnical.ca](mailto:sbeaudry@trekgeotechnical.ca)

### Introduction

Construction of the Keewatinohk Converter Station (KCS) in Northern Manitoba is currently underway as part of the Bipole III Transmission Reliability Project. HD™ helical piles were selected as the preferred foundation type for the building and various ancillary structures. The Design-Build Contractor elected to undertake static axial compression testing of these piles to support the use of a higher geotechnical resistance factor in the calculation of pile capacities using Limits State Design (LSD). A review of background information, installation methodology, and preliminary test results are included in this case study.

### Background

The Northern converter station, KCS, is located near Gillam, Manitoba in a region of discontinuous

permafrost. Site investigations and instrumentation monitoring revealed the presence of sporadic permafrost throughout the site. Thaw sensitive soils consisting of ice-rich interlayered clay silt and sand, and clay till, were observed up to depths of approximately 20 m below the ground surface. The presence and extent of permafrost merited careful consideration of the long-term effects of permafrost degradation with respect to the selection and design of the most practical foundation type. Site development activities involved the removal of the insulating organic ground cover (peat) and raising the site with granular fill. Based on these changes to the thermal regime, the design approach assumed that existing permafrost will thaw over the design life of the facility resulting in the development of significant drag loads on piled foundations. As such, axial compressive capacity derived from skin friction must be neglected and all capacity must come from the pile toe (end-bearing).

Open-ended helical piles with a shaft diameter of 244 mm (9.625 inches) and single 457 mm (18 inch) helix were selected and designed for the KCS building. Approximately 700 piles are required to support the building of which 2% must be static load tested to confirm LSD design capacity.

The pile installation method involves pre-boring a 305 mm diameter hole to below the depth of thaw-sensitive soil, advancing the pile to ensure that the pile tip and helix are fully embedded into the underlying hard glacial till, and backfilling the annulus with drill cuttings.

Static axial compression testing has been performed on 23 piles installed to date with additional testing scheduled as piling progresses. Testing is conducted in general accordance with ASTM standard D1143 – Standard Test Methods for Deep Foundations Under Static Axial Compressive Load - with minor exceptions to suit field conditions. The load-deformation behavior of each tested pile is evaluated and compared against the design Ultimate Limit State (ULS) and Serviceability Limit State (SLS) loading and deflection requirements.

## **References**

- ASTM International. 2007 (2009). ASTM Standard D1143, "Standard Test Methods for Deep Foundations Under Static Axial Compressive Load". ASTM International, West Conshohocken, PA, 2013, [www.astm.org](http://www.astm.org)
- Canadian Commission on Building and Fire Codes. 2010. National Building Code of Canada. Volume 1.
- Canadian Geotechnical Society. 2006. Canadian Foundation Engineering Manual. 4<sup>th</sup> Edition.
- Golder Associates Ltd. 2016. Bipole III Keewatinohk Converter Station - Geotechnical Foundation Design Report.
- Golder Associates Ltd. 2015. Bipole III Keewatinohk Converter Station, HVDC Area - DRAFT Geotechnical Investigation Data Report.

# Characterization of large rock slides using an integrated remote sensing approach



A.M. Westin  
Simon Fraser University, Burnaby, BC  
[Allison.Westin@sfu.ca](mailto:Allison.Westin@sfu.ca)

D. Donati, D. Stead, J.J. Clague  
Simon Fraser University, Burnaby, BC

T.W. Stewart, M.S. Lawrence  
BC Hydro

## Introduction

The efficient analysis and characterization of large rock slides can be extremely challenging. Inaccessibility, steep slopes, and rockfall activity may preclude the comprehensive collection of geomechanical data, resulting in inadequate characterization of the rock mass, data and model uncertainty, and potential misinterpretation of the mechanisms governing failure and deformation. Recent developments in remote sensing techniques have greatly enhanced our ability to collect data without the need for direct access to difficult terrain.

Terrestrial and Airborne LiDAR allow large point clouds of data to be obtained and automatically registered in three-dimensional space. Terrestrial Digital Photogrammetry and Structure-from-Motion techniques take advantage of photographic datasets for constructing three-dimensional models of rock faces. In this study, data derived using these remote sensing techniques are combined and integrated in an innovative study of a large rock slide in British Columbia. Our principal objective is to show that remotely acquired structural and geomechanical data can be effectively used to characterize rock masses.



**Figure 1: Location of the Downie Slide in southeastern British Columbia, Canada.**

## Background

This presentation contains preliminary results of a multi-imagery investigation of the Downie Slide (Fig. 1) – a massive, extremely slow-moving (average 1.21 cm / yr, (Cruden and Varnes 1996)), translational rock slide located in southeastern British Columbia, approximately 80 km north of Revelstoke on the west side of the present-day Revelstoke Reservoir (Kalenchuck et al. 2013). This prehistoric landslide was first identified in 1956 by J.E. Armstrong (Brown and Psutka 1980). It is approximately  $1.5 \times 10^9 \text{ m}^3$  in volume (Brown and Psutka 1980) and extends 3200 m (Piteau *et al.* 1978) from the now-submerged toe to the headscarp, which rises steeply up to 125 m, and has a lateral extent of 2400 m parallel to Revelstoke Reservoir. The maximum thickness of the slide mass is between 245 m (Imrie *et al.* 1992) and 270 m (Brown and Psutka 1980).

## Study Methods

A three-dimensional model of portions of a drainage adit within the Downie Slide was completed using short-range photogrammetry using a Canon EOS 5D Mark II camera with a 20 mm lens and laser scanning using a FARO Focus3D x 330 (Fig. 2).

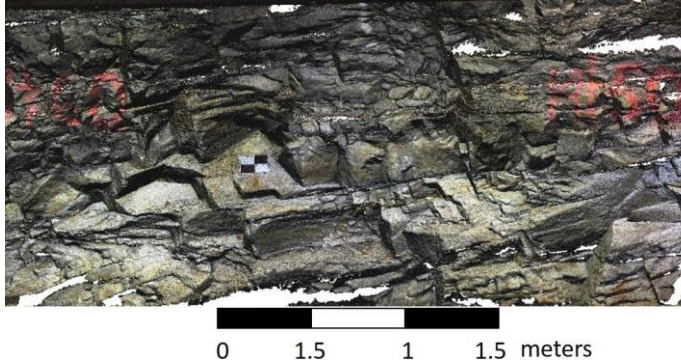


**Figure 2: Point cloud of a section of the south adit.**

The head scarp of the Downie Slide was investigated using long-range terrestrial laser scans using a Riegl VZ-4000 laser scanner. A DJI Phantom 4 unmanned aerial vehicle was employed to photograph the inaccessible cliff. A Structure-from-Motion approach was used to construct a three-dimensional model of the head scarp from the photographic images.

Discontinuity data including orientation, spacing, location and persistence were extracted from the three-dimensional models of the adit and head scarp. The remotely sensed data were compared with data collected using traditional field techniques and will be employed as input data for future 3D-distinct element and lattice spring numerical modeling.

Airborne LiDAR data were analyzed in a GIS environment. Aspect, slope, hillshade, and relative relief maps of the slide area were constructed from these data (Fig. 3). A detailed lineament analysis revealed surface evidence of variable slope damage. Displacement vectors derived from surface monitoring were superimposed on the maps, and a tentative correlation between slope deformation, and large-scale structural and damage features was made. Results from the GIS analysis were used to delineate structural sub-domains within the landslide. Multi-sensor remote sensing imagery has provided a large database of features, which will be used in future three-dimensional geomechanical models.

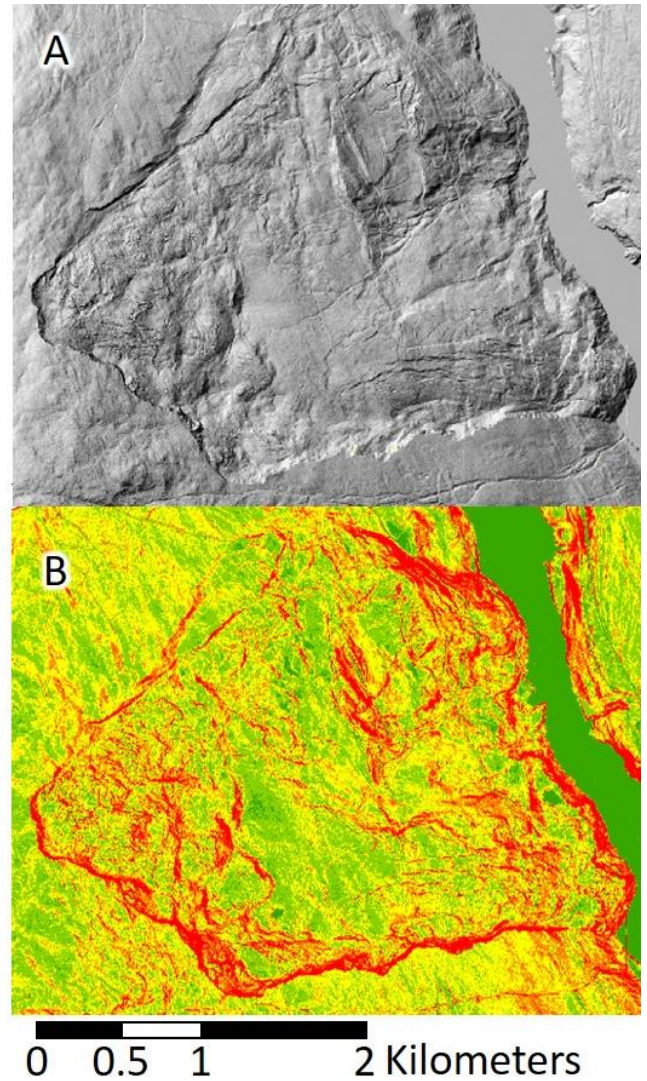


**Figure 3: Hillshade (A) and slope (B) derived from airborne LiDAR data.**

## Reference

- Brown, R. and Psutka, J. 1980. Structural and Stratigraphic setting of the Downie slide, Columbia River valley, British Columbia, *Can J Earth Sci*, 17: 698–709.
- Cruden, D.M. and Varnes, D.J. 1996. Landslide types and processes. *In* Landslides, Investigations and Mitigation. Special Report 247, Transportatino Research Board, Washington, pp. 36-75.
- Imrie, A., Moore, D. and Enegren, E. 1992. Performance and Maintenance of the Drainage System at Downie Slide, *Landslides Sixth Intern. Symp.*, Christchurch.
- Kalenchuck, K., Hutchinson, D., and Diederichs, M. 2013. Geomechanical interpretations of the Downie Slide considering field data and three-dimensional numerical modeling. *Landslides* 10: 737–756.
- Piteau, D., Mylrea, F, and Blown, I. 1978. Chapter 10: Downie Slide, Columbia River, British Columbia, Canada. *In* Rockslides and Avalanches: 365–392. New York, USA.

# Thermal design method for culverts built on permafrost



L. Périer  
 Laval University, Québec  
[loriane.perier@gci.ulaval.ca](mailto:loriane.perier@gci.ulaval.ca)

G. Doré  
 Laval University, Québec

## Introduction

In cold regions, water management is known to be a major concern due to its impact on the thermal stability of the permafrost. As a matter of fact, poor water management around the embankment exacerbates soil instabilities and similarly, water circulation through a culvert affects the thermal regime of underlying permafrost and can cause significant damage.

Understanding the impact of the water circulation in a culvert on the permafrost stability is essential for the development of design principles for drainage systems along linear infrastructures.

## Objectives

There is no known design method for culverts based on heat exchange between the culvert and the underlying soil. Therefore, the objectives of the research work summarized in this paper are 1) to

quantify the effect of flow rate and water temperature on the thermal regime; and 2) to propose a culvert design tool taking into consideration the heat flux under a culvert.

## Methods

### Instrumentation

A culvert located on the Alaska Highway was instrumented in early May 2013. The road is built on warm and discontinuous permafrost which is considered as potentially unstable because its annual temperature is higher than -2 °C.

A probe containing three thermistors was placed underneath the culvert near the inlet. The probe measured the soil's temperature at the surface, and at depths of 15 cm and 30 cm.

A thermistor was also installed upstream of the culvert inlet to measure the temperature of the water entering the culvert.

Finally, a flow meter was placed at the inlet to provide flow rate data.

### Mathematical model

The field data were used to validate a mathematical model developed based on the physical principles of heat transfer.

This model, expressed by the following equation, relates heat flux  $\delta$  with water temperature  $T_w$  and flow rate  $Q$  (Périer 2015).

$$\delta = \frac{\theta(T_w - T_{pmf})}{\frac{S_m}{Cst \cdot Q^{0.8} \cdot P_m^{0.2} \cdot r_c} + \frac{\ln(r_{ie}/r_{ii})}{k_i} + \sum \frac{\ln(r_{se}/r_{si})}{k_s}}$$

$\theta$  is the angle at which the heat flux is applied,  $T_{pmf}$  is the temperature at the top of permafrost which can be considered equal to 0 °C in this case,  $S_m$  and  $P_m$  are respectively the wet area and the wet perimeter,  $r_c$  is the inside culvert radius,  $r_{ie}$  and  $r_{ii}$  are the outside and inside insulation radius,  $r_{se}$  and  $r_{si}$  are the outside and inside soil radius,  $k_i$  and  $k_s$  are the insulation and soil thermal conductivities.

### Flow rate and water temperature quantification

The mathematical model was used to analyze the impact of the water temperature, the flow rate and the culvert diameter. Figure 1 shows the impact of the size of the pipe and of the flow rate on the heat flux.

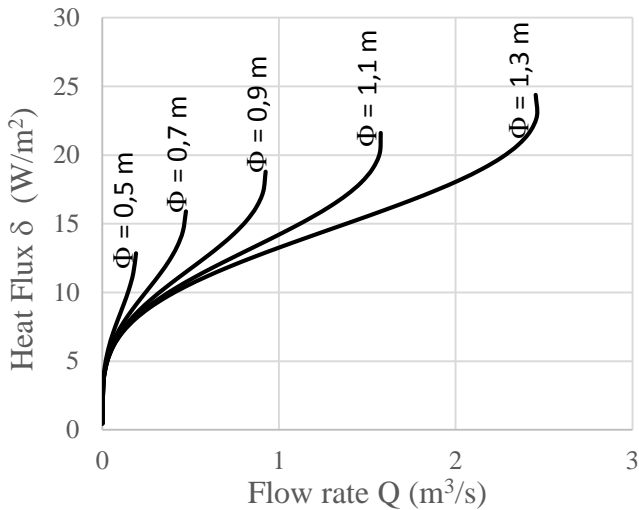


**Figure 1 : Influence of the pipe diameter and flow rate on the heat flux**

For the same flow rate, the heat flux increases with decreasing pipe diameter because the wet area is decreasing.

Figure 2 presents the impact of water temperature on the heat flux. The water temperature significantly influences the heat flux.

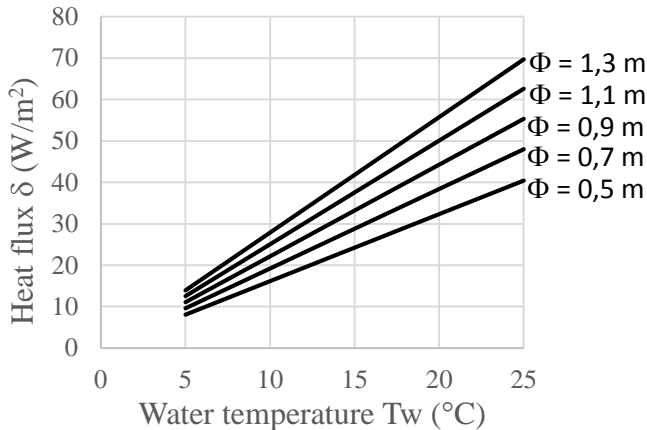


**Figure 2 : Influence of the water temperature on the heat flux**

Consequently, the water temperature has an important impact on thermal regime under the culvert. So, water temperature, which can be characterized by the water source and its provenance, should be taken into account in the design of culverts on permafrost.

### Design tool, the Beaver Creek Culvert example

The Beaver Creek Culvert has a diameter of 0.9 m. The average temperature of water is 2.5 °C and the average flow rate is 0.04 m<sup>3</sup>/s.

Considering these values, Figure 3 is used to assess the heat flux transferred from the culvert to the soil. In such a case, the heat flux is equal to 2.7 W/m<sup>2</sup>.

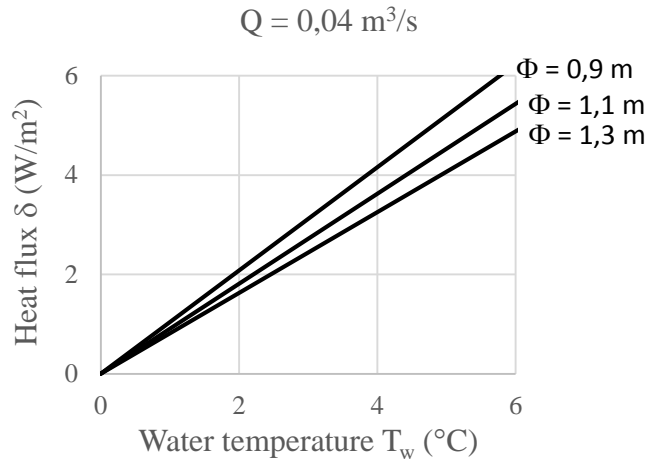


**Figure 3 : Estimation of the heat flux for a 0.04 m<sup>3</sup>/s flow rate**

### Conclusion

A mathematical model was developed to link water temperature, flow rate and heat flux. The model made it possible to quantify the effect of water temperature and flow rate in terms of the quantity of heat transmitted from the culvert to the ground.

It was observed that for the same flow rate, the heat flux is smaller for a larger pipe diameter due to its wet area. It was also noted that the impact of flow rate and water temperature on the heat flux was respectively moderate and large.

Finally, a design tool has been proposed to estimate the heat flux as a function of water temperature average, flow design and pipe diameter.

### References

- Périer, L. 2015. Étude de l'influence du débit et de la température de l'eau sur le régime thermique autour des ponceaux construits sur pergélisol. *Master thesis. Université Laval. 119p.*
- Périer, L. & Doré, G. & Burn, C. 2015. Influence of water temperature and flow on thermal regime around culverts built on permafrost. *GEOQuébec. Québec, 20-23 September 2015.*

# Estimation of optimum moisture content for Fine-grained borrow pit assessment at Flin Flon, Manitoba



R.E. Turley  
BGC Engineering, Vancouver, BC  
[rturley@bgcengineering.ca](mailto:rturley@bgcengineering.ca)

B. Russell  
BGC Engineering, Vancouver, BC  
[brussell@bgcengineering.ca](mailto:brussell@bgcengineering.ca)

## Introduction

The Hudson Bay Mining and Smelting Co. Ltd. (Hudbay) Flin Flon Tailings Impoundment System (FFTIS) in Flin Flon, MB consists of numerous water retention dams which rely on a low permeability core to reduce seepage through the dam. This low permeability fill (LPF) is often fine grained material sourced from nearby borrow pits. Identifying locations with suitable borrow material is typically done with a site investigation prior to dam construction. The relationship between plasticity and optimum moisture content (OMC) can be a useful tool in borrow pit assessment.

## Background

### *Criteria for Borrow Material*

The following criteria were established for LPF to meet the requirements for the dam core:

- Grain size > 77% passing the #200 sieve
- Plasticity Index > 15
- Moisture Content +/- 2% of OMC

Grain size and plasticity are inherent characteristics of the source material, while moisture content is dependent on the condition of the borrow pit. The moisture content of a material can be altered through drying, however, it is preferable to obtain material close to OMC.

### *Flin Flon Borrow Pits*

The landscape in the Flin Flon area consists of low-lying saturated soils bounded by exposed bedrock outcrops. The LPF is found within these low lying areas and is typically wet of OMC. Previous work found that if construction occurs during the summer months, material up to 6-10% wet of OMC can be spread out and dried sufficiently to be suitable for construction. Therefore, borrow pit assessments need to identify clay that is less than 10% wet of OMC.

## Plasticity-OMC Relationship

The relationship between plasticity and OMC is well known and various authors have published charts with empirical relationships. However, authors caution that the relationship is highly variable by location. This is attributed to different clay mineralogy and the nature of cation exchange complex in the materials (Hausmann 1990). Sridharan and Nagaraj (2005) investigated different relationships and found that the plastic limit provided a better correlation with OMC and maximum dry density than liquid limit or plasticity index.

The advantage of a plasticity-OMC relationship is that the suitability of borrow pits can be assessed with fewer tests and therefore, more economically. If a site-specific relationship is known, the plasticity characteristics can be correlated with an expected OMC for each sample. The estimated OMC can be compared to the natural moisture content of the soil to assess the borrow suitability. Plasticity tests (Atterberg

limits) require less material and are less expensive than assessing the OMC by Standard Proctor tests. However, Standard Proctor tests would still be required to confirm the material still remains within the established relationship.

#### Developing a relationship for Flin Flon

An initial Plasticity Index-OMC relationship was developed with test data from the 2006-07 construction season. This relationship was used during a large borrow assessment in 2009 consisting of 93 test pits, which identified approximately 175,000 m<sup>3</sup> of suitable LPF borrow material. An additional two Standard Proctor tests were completed during this program to verify the relationship. The results of the tests are shown in Figure 1.

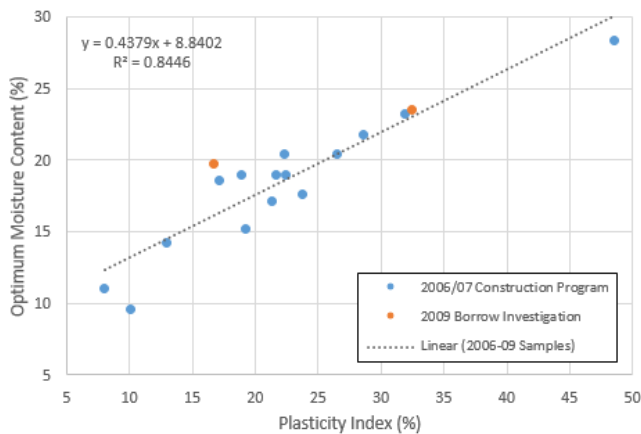


**Figure 1. Optimum Moisture Content vs. Plasticity Index Relationship for 2006-2009 Results for the FFTIS**

Since 2009, this relationship has been verified and adjusted with testing results from subsequent borrow programs in 2011, 2013 and 2015. The additional samples were added to the plot of OMC vs. PI and are shown in Figure 2.

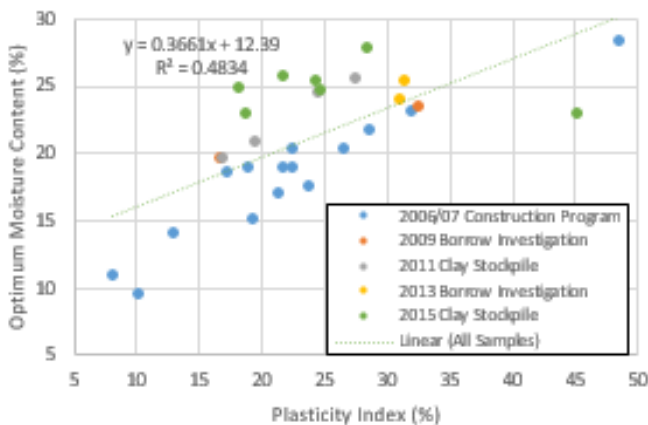


**Figure 2. Optimum Moisture Content vs. Plasticity Index Relationship for 2006-2015 Results for the FFTIS**

Figure 2 shows that the correlation between PI and OMC decreased with additional samples. The samples from 2011 and 2015 generally show a higher OMC for a given plasticity index (PI) than earlier samples. There may be a slight difference in mineralogy of the material in these borrow pits or it may be a result of different laboratories completing the tests.

The plastic limit (PL) and liquid limit (LL) were also plotted against OMC for all samples. The highest correlation resulted between liquid limit and OMC, which is different than was found by Sridharan and Naharaj (2005). The relationship between LL and OMC for all samples is presented in Figure 3.

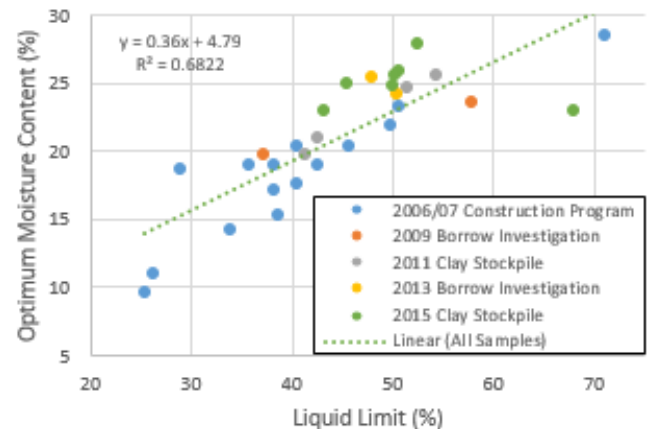


**Figure 3. Optimum Moisture Content vs. Liquid Limit Relationship for 2006-2015 Results for the FFTIS**

#### Conclusion

The relationship between plasticity and OMC has been developed for LPF at the FFTIS in Flin Flon, MB. This relationship has proven useful in identifying suitable borrow sources for low permeability fill for water retention dams by reducing sample size requirements and costs. Empirical relationships for plasticity-OMC can be useful for initial guidance and planning; however, the actual relationships can vary significantly and should always be developed and verified for specific sites for detailed engineering and construction purposes.

#### References

- BGC Engineering. 2009. 2009 Clay Borrow Investigation. Report prepared for Hudson Bay Mining and Smelting Co. Ltd. (Hudbay).
- Hausmann, Manfred R. 1990 Principles of Soil Densification *In* Engineering Principles of Ground Modification. McGraw-Hill, New York. pp. 40-42.
- Sridharan, A., and Naharaj, H. B. 2005. Plastic Limit and Compaction Characteristics of Fine-Grained Soils. Ground Improvement. 9(1):17-22.

## Cheekeye River Fan debris flow hazard



D. McClarty  
BGC Engineering, Vancouver  
[dmcclarty@bgcengineering.ca](mailto:dmcclarty@bgcengineering.ca)

### Introduction

The Cheekeye River Fan is located along Highway 99 near Brackendale, north of Squamish, British Columbia. Proposed developments on the fan have prompted an assessment of the risk posed by the debris flow hazard to existing and proposed infrastructure downstream of the Cheekeye Fan.

### Hazard Characterization

#### *Debris Flow Event History*

Multiple studies have focused heavily on characterizing previous debris flow events occurring along the Cheekeye River; these studies have combined information gained from test pit studies, dendrochronology, and historic records of past events. The results of these previous studies were combined to develop a frequency magnitude relation for debris flow events along the Cheekeye River channel. Previous events such as the Garbage Dump debris flow which occurred approximately 900 years ago

carried as much as  $2.1 \text{ M m}^3$  of material (Jakob and Friele 2010) (Figure 1).

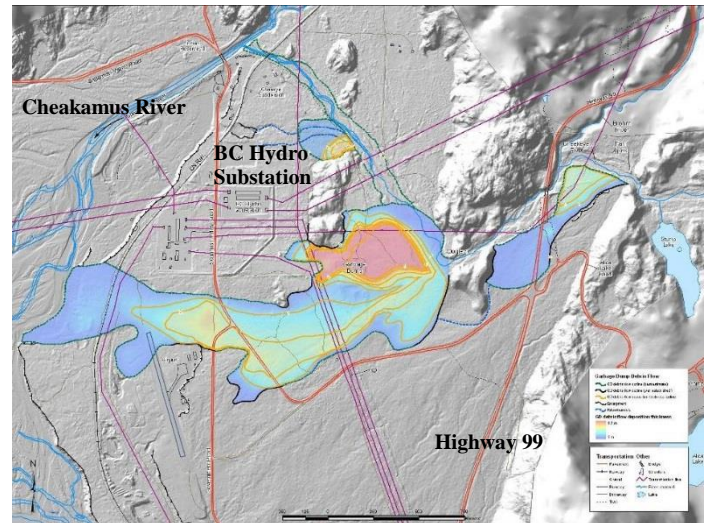


**Figure 1. Approximate extents of the Garbage Dump debris flow event.**

#### *Upper Design Limit*

The upper design limit is intended to characterize the worst case scenario by identifying the largest event which could potentially occur. Design criteria for similar debris flow events both locally and internationally were considered when selecting an upper design limit return period for the Cheekeye River Fan. Input from multiple experts in the field yielded a maximum event with a 1:10,000 year return period. Estimates for the potential size of such an event ranged in size from  $2.8 \text{ M m}^3$  to  $5.5 \text{ M m}^3$ . The worst case estimate of  $5.5 \text{ M m}^3$  was selected for use in subsequent risk assessments.

#### *Event Modelling*

Numerical modelling of a selection of debris flow events based on the frequency-magnitude relation was carried out using the program DAN3D (McDougall and Hungr 2004). The results of these model runs was used to quantify the unmitigated hazards posed by the 1:20 year, 1:100 year, 1:2500 year, and 1:10,000 year events.

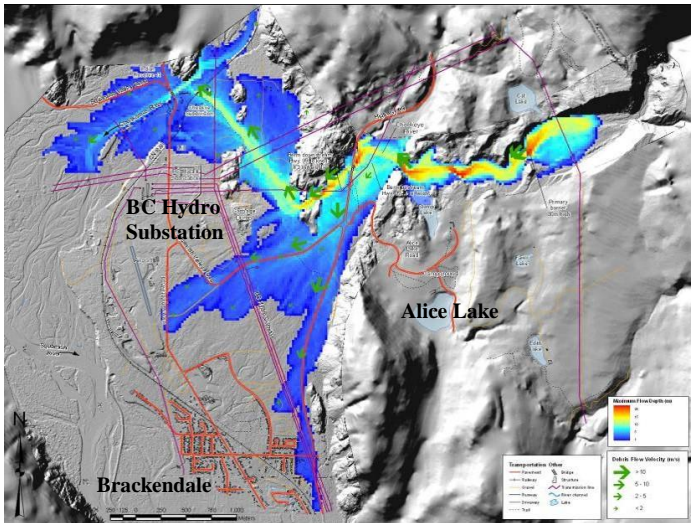


**Figure 2. 1:2,500 year return period debris flow event as modelled using DAN3D.**

### *Current Risk*

The results of the event modelling were used to quantify the debris flow hazard risk for the proposed and current developments on the fan. As no formal definitions of acceptable risk currently exist in Canada, the risk standards adopted by the District of North Vancouver were used to evaluate the risk to existing and proposed developments on the Cheekye Fan. According to these standards, the current level of debris flow hazard risk is unacceptable. Efforts to mitigate this risk are ongoing.

## **Mitigation Design**

### *Site Investigation*

In order to facilitate ongoing design work, a site investigation of the upper fan area was completed in 2014. This site investigation included multiple drill holes and test pits, as well as seismic refraction and downhole shear wave velocity surveys.

Depth to bedrock at the Upper Fan ranged from 5 m to greater than 80 m below ground surface. Overburden consisted of variable deposits of debris from past debris flow events. This material ranged in grain size from silts and sands to boulders greater than 10 m in diameter.

### *Preliminary Design Concepts*

The preliminary design concept consists of a barrier structure at the base of the Upper Fan large enough to contain a sufficient volume of the maximum design event, such that the risk to downstream developments is limited to an acceptable level. The conceptual structure includes an outlet through the barrier, which

will allow small events and portions of large events that will remain within the Cheekye River channel to flow through the barrier; thereby reducing maintenance costs to clean out the basin after a debris flow event occurs. Design of potential mitigation structures is ongoing.

## **References**

- Jakob, M., Friele, P. 2010. Frequency and magnitude of debris flows on Cheekye River, British Columbia. *Geomorphology* 114:382–395
- McGougall, S., and Hungr, O. 2004. A model for the analysis of rapid landslide motion across three-dimensional terrain. *Canadian Geotechnical Journal*, 41: 1084-1097.

## ‘Up close with virtual rock outcrops’: Geovisualization of a remotely sensed field site



M. J. Dewit  
 Simon Fraser University, Burnaby (BC)  
[mdewit@sfu.ca](mailto:mdewit@sfu.ca)

N. Hedley,  
 Simon Fraser University, Burnaby (BC)  
[hedley@sfu.ca](mailto:hedley@sfu.ca)

G. Williams-Jones  
 Simon Fraser University, Burnaby (BC)  
[glynwj@sfu.ca](mailto:glynwj@sfu.ca)

D. Stead  
 Simon Fraser University, Burnaby (BC)  
[dstead@sfu.ca](mailto:dstead@sfu.ca)

### Introduction

Geologists and engineers require access to map the lithology, geometry and structure of rock outcrops, and in many instances this may not be possible. Remote sensing methods provide a means to bridge this gap; however, the interaction between the geologist and the rock mass is in most cases severely impeded due to the observation distance. In response

to this problem, a geovisualization interface called ‘Up Close with Virtual Rock Outcrops’ was created using Unity3D, a free game engine software, to provide unrestricted access to a virtual field site at the Chasm, in central British Columbia. Building a virtual outcrop in a game-like environment using Unity3D has several benefits, including the direct interaction between the user and outcrop, the capability of having multiple datasets available in one interface, and the ability to view data from all angles.

### Field Site

The Chasm is a 7 km-long canyon approximately 20 km northeast of Clinton, BC (Figure 1) comprised of cliffs up to 200 m high of nine layered, columnar-jointed basalt lava flows, interstratified with paleosol units (Farrell et al. 2007; Andrews and Russell 2007). The Chilcotin Group basalts, to which these lavas belong, cover approximately 55,500 km<sup>2</sup> in south-central British Columbia, and range in age from Middle Oligocene (28 Ma) to Middle Pleistocene (1 Ma) (Bevier 1983; Farrell et al. 2008; Andrews and Russell 2007).

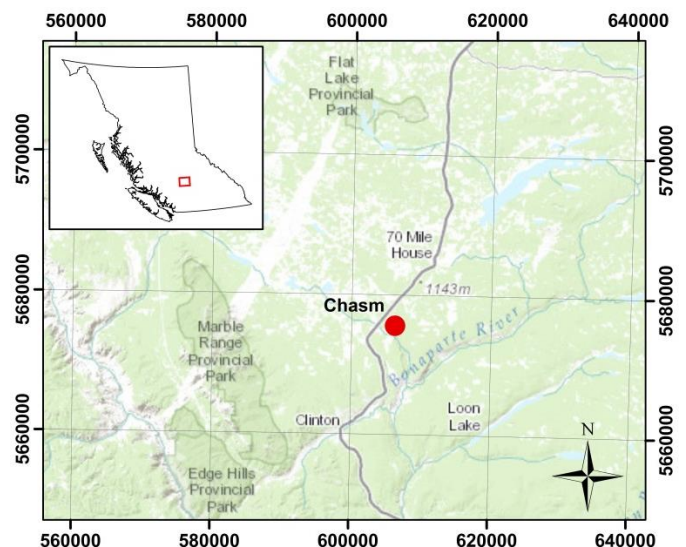


**Figure 1. Map showing the location of the Chasm in south-central British Columbia**

The abundance of exposed rock mass at the Chasm, paired with modern remote sensing methods, allows for the developed interface to include high-resolution,

multi-scale, multi-dimensional datasets acquired through field surveys in August 2015 of terrestrial LiDAR, infrared thermography, and Structures-from-Motion photogrammetry. These types of data were chosen so as to obtain three-dimensional geometry of the lava flows, upon which geotechnical and geological analyses could be made, and so properties such as composition of the rock could be determined.

### Geovisualization of a Virtual Outcrop

‘Up Close with Virtual Rock Outcrops’ is an application which allows the user to come face-to-face with the virtual rock outcrop, exploring the different datasets from all angles, investigating combinations of data through interactive menus and buttons, and examining an outcrop, in detail, which in reality is very difficult to access. Data include three-dimensional models of the outcrops in both RGB colour (Figure 2) and LiDAR reflectivity, detailed 3D high-resolution photogrammetric models of key areas of the slopes in RGB colour, LiDAR reflectivity profiles, thermal imagery, 3D mapping of geological and structural features, three-dimensional models of hand samples acquired from the field site (Figure 3), and results from thermal laboratory experiments on hand samples. The variety of datasets available not only in ‘Up Close with Virtual Rock Outcrops’, but through other remote sensing methods as well, allows the concept of a virtual outcrop to be useful to a range of Earth sciences topics including geological, volcanological, and geotechnical studies.

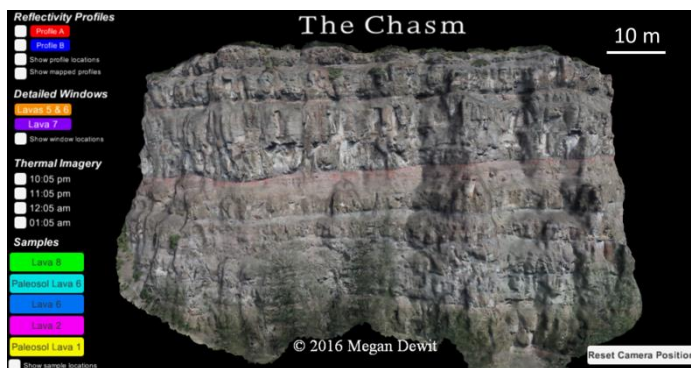


**Figure 2.** Snapshot of the geovisualization interface, showing the different available datasets for viewing. Current dataset is a three-dimensional model of a section of the east cliff face at the Chasm



**Figure 3.** Three-dimensional model of one of the hand samples of a paleosol unit at the Chasm

In a virtual field site such as that developed in ‘Up Close with Virtual Rock Outcrops’, geologists and engineers can revisit the field site whenever needed, as well as instantaneously switch between different data types in scales ranging between hand sample and full canyon outcrops, and easily analyze the relationships between these datasets. This versatility is especially important at sites like the Chasm, where accessibility is difficult, and therefore inhibiting analysis of the outcrop as well. Intended for scientists and students, ‘Up Close with Virtual Rock Outcrops’ is a means for research, analysis, and learning, and allows for direct interaction between the geologist and the outcrop in virtual space. ©

### References

- Andrews, G.D.M. and Russell, J.K., 2007. Mineral Exploration Potential Beneath the Chilcotin Group (NTS 092O, P; 093A, B, C, F, G, J, K), South-Central British Columbia: Preliminary Insights from Volcanic Facies Analysis. *Geoscience BC, Report 2007-1*, 229-238.
- Bevier, M.L., 1983. Implications of Chemical and Isotopic Composition for Petrogenesis of Chilcotin Group Basalts, British Columbia. *Journal of Petrology*, 24(2), 207-226.
- Farrell, R.E., Andrews, G.D.M., Russell, J.K., and Anderson, R.G., 2007. Chasm and Dog Creek lithofacies, Chilcotin Group basalt, Bonaparte Lake map area, British Columbia. *Geological Survey of Canada, Current Research 2007-A5*. 11p.
- Farrell, R.E., Simpson, K.A., Andrews, G.D.M., Russell, J.K., and Anderson, R.G., 2008. Preliminary interpretations of detailed mapping in the Chilcotin Group, Chasm Provincial Park, British Columbia. *Geological Survey of Canada, Current Research 2008-13*. 11p.

# Poster Session 2

## From consulting to academia and back: a different approach to data gaps



E. Stevenson  
 Thurber Engineering Ltd., Vancouver  
[estevenson@thurber.ca](mailto:estevenson@thurber.ca)

### Introduction

Differences in the approach to data gaps between consulting and academia became apparent to the author while completing a masters degree following 4 years of experience in the consulting industry.

Academia seeks to provide quantitative solutions to data gaps, whereas the consulting industry generally seeks to provide a design with adequate performance within a specified budget. In both disciplines uncertainty is accounted for with conservatism in design.

This abstract outlines the author's observations and presents two relevant case studies to illustrate some of the differences between consulting and academia. The abstract is intended to provide a rough guide for the move from academia to consulting.

### Case Study 1: Master's Paper

A colleague was researching sub-aerial landslides impacting bodies of water and causing tsunamis. The

study had made an assumption that landslide material, 3 mm diameter ceramic beads, were sufficiently large enough to not be affected by capillary forces. One purpose of the author's masters project was to test this assumption. Another purpose was to test photogrammetry as a method for measuring the landslide deposit shape.

To measure the effect of capillarity, the velocity and thickness of the landslide material at five different relative moisture conditions were measured with a high-speed camera as shown in Figure 1. The distribution of each submarine deposit was measured using photogrammetry and manual measurements.

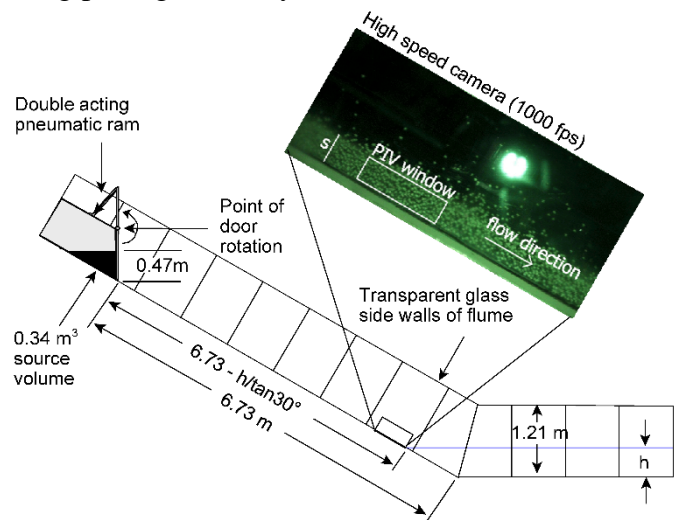


**Figure 1. High Speed Camera Measurement (Take et al. 2016)**

The high speed camera was shooting 1632 x 1200 pixel images at 1000 frames per second. The landslide front was also filmed with a go-pro camera to measure the difference of speed and position between the centre and edge of the slide.

The deposit was measured with a 22-megapixel digital camera fitted with a 50 mm fixed lens. 3-dimensional point clouds of the deposit were generated using photogrammetry software, as shown in Figure 2. The point clouds were then compared to hand measurements to confirm that they were accurate.

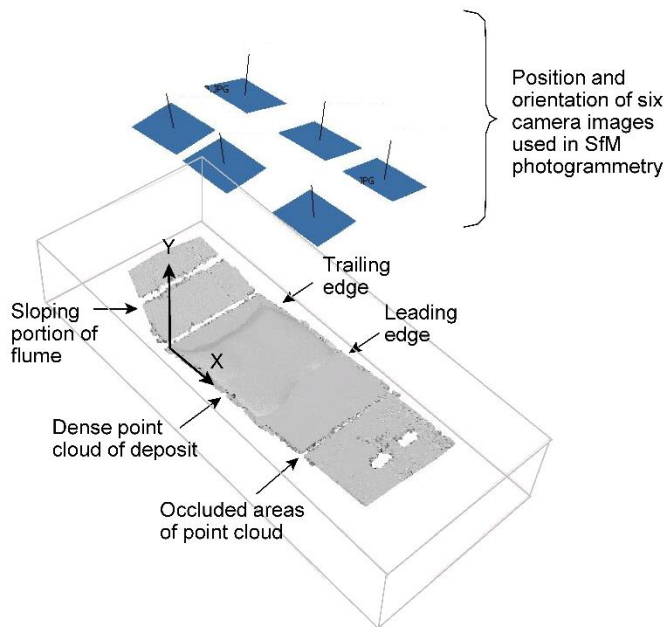


**Figure 2. Photogrammetric Measurement of Landslide Deposit (Take et al. 2016)**

During this project, the uncertainty regarding the capillary forces was studied over 5 months and about 120 to 180 hours. As there is no cost for a grad student's time it was possible to spend these resources. In consulting, this would have cost approximately \$15,000 to \$30,000 in engineering time alone.

### Case Study 2: Car Hoist Foundation

A school needed to construct a car hoist inside of an existing building and contacted a consulting company for the foundation design. There was little budget available, and construction had to be completed during spring break, which left 2 weeks for design and construction.

The car hoist had relatively low loads (12 kN) and there was an existing one already installed. Helical piles were selected for the foundation system. They could be installed using a mini excavator, induce very little vibration (so were unlikely to cause damage to surrounding structures), and the piles are relatively inexpensive.

The designer had previous experience with the interaction of foundation type and soil conditions, so the piles were designed using an in-house correlation between torque and axial capacity. Four piles were installed beneath each column to account for load eccentricities, which resulted in a factor of safety over 5 for axial resistance.

The eight piles were installed in about four hours. The number of piles could have been reduced, but cost

of the extra piles including the time to install them (less than \$8000) was less than the cost of an investigation and rigorous pile design (\$10,000–15,000). As such, the client's needs were met by improving the performance of the foundation through construction rather than engineering.

### Conclusion

As shown in the presented case studies, in academia a lot of time and effort can be spent reducing potential sources of error, since there is no unit cost to a grad student's time. As such, assumptions or other gaps in the methodology can be studied rigorously. Although consulting also experiences data gaps, they are typically investigated only when there is the potential for cost-savings over a 'safe' assumption. In some instances, there is a benefit to seek and eliminate engineering data-gaps. In others, it is more cost efficient to design using conservative assumptions.

### References

- Livneh, B. and El Naggar, M.H., 2008. Axial testing and numerical modeling of square shaft helical piles under compressive and tensile loading. *Canadian Geotechnical Journal*, 45(8), pp.1142-1155.
- Take A., Mulligan R.P., Stevenson E.P. & Miller G.S. 2016. Physical modelling of landslides into reservoirs: effect of capillarity on rheology of granular landslides at impact. *International Symposium on Landslides, Napoli 2016*.
- Tappenden, K., Sego, D. 2007. Predicting the Axial Capacity of Screw Piles installed in Canadian Soils. In *The Canadian Geotechnical Society (CGS), GeoOttawa 2007 Conference*. 2007 pp. 1608-1615.

## Proposed method of shear wave velocity measurement in a flexible wall permeameter



A. T. M. Silvester  
University of British Columbia, Vancouver  
[a.silvester@civil.ubc.ca](mailto:a.silvester@civil.ubc.ca)

R. J. Fannin  
University of British Columbia, Vancouver  
[fannin@civil.ubc.ca](mailto:fannin@civil.ubc.ca)

### Introduction

#### *Internal Erosion in Earth Dams*

Hydroelectric dams and by extension, earth dams, are a vital component of Canada's energy generation system. With many of the countries' prominent dams approaching or passing the half century mark, like other older infrastructural assets, they are beginning to show their age. One temporal mechanism that has emerged as a growing concern for earth dam safety management is seepage-induced internal erosion. By the accounts of Foster et al. (2000), internal erosion has been recognized as a contributor to nearly 50% of historic earth dam failures.

#### *Crosshole Shear Wave Tomography*

One of the emerging technologies used to manage this safety risk has been crosshole shear wave tomography

(Fannin and Garner 2008). Notably, BC Hydro employed the use of shear wave tomography to delineate the 1996 W.A.C. Bennett Dam sinkholes (Stewart and Watts 2000). Since then, shear wave tomography has been adopted as part of the ongoing performance monitoring of the dam, generating a temporal and spatial database of shear wave velocities.

Few studies have explored the relation between shear wave velocity and the micromechanics of internal erosion. As a result, the understanding of the relation is underdeveloped.

### Laboratory Study

#### *Apparatus*

Considering this research need, a lab program utilizing the existing UBC flexible wall permeameter (Slangen 2015) is proposed. Over the past year, the device has been updated and modified to allow for the inclusion of bender elements to measure shear wave velocity. A unique method for seating the bender elements within the perforated plates on either end of the specimen was devised (see Figure 1). One consequence of this modification was the reduction of the cross-sectional area for flow entering and exiting the specimen by approximately 7%.

#### *Objectives*

The overarching goal for the program of research is to develop the understanding of the relation between shear wave velocity and internal erosion to better inform the trends and analysis of crosshole seismic field data.

The immediate purpose of the author's lab study is twofold: (1) determine whether the mounting of bender elements within the UBC flexible wall permeameter adversely affects the flow regime through a reconstituted specimen, and (2) compare and contrast measured shear wave velocities with state-of-the-art bender element tests conducted in a triaxial cell (Styler 2014).

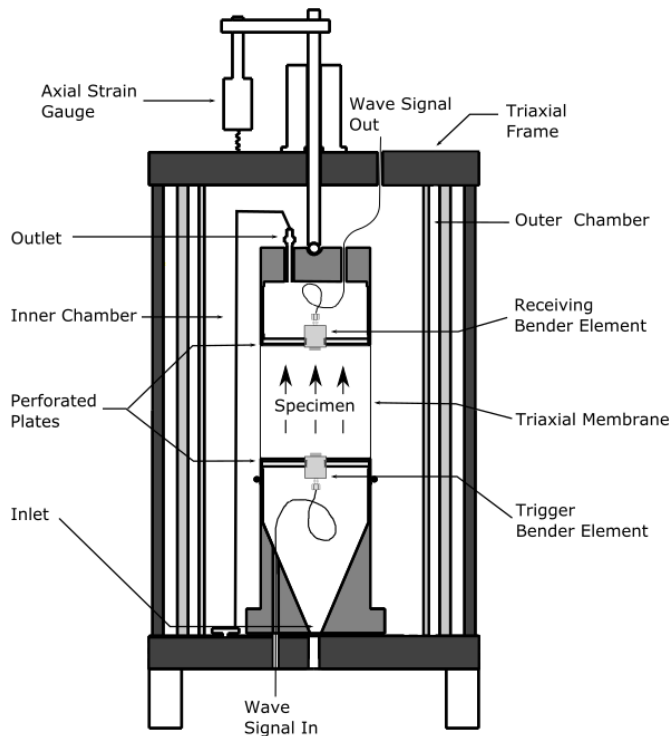


**Figure 1 - Simplified schematic of the revised flexible wall permeameter (modified from Slangen, 2015)**

### Results

Preliminary findings indicate that the presence of the bender element mounts within the flexible wall permeameter do not have an appreciable effect on the discharge through the specimen. However, tests conducted with the bender element mounts included have shown increases in the seepage-induced volumetric strain. This effect requires further evaluation before any firm conclusions can be drawn.

### References

- Fannin, R.J. & Garner, S.J. 2010. Understanding internal erosion: a decade of research following a sinkhole event. *The International Journal on Hydropower & Dams* 17(3): 93–98.
- Foster, M., Fell, R., & Spannagle, M. 2000. The statistics of embankment dam failures and accidents. *Canadian Geotechnical Journal*, 37(5):1000–1024.
- Slangen, P. 2015. On the influence of effective stress and micro-structure on suffusion and suffusion, PhD diss., University of British Columbia. Retrieved from <https://circle.ubc.ca/>.
- Stewart, R.A. & Watts, B.D. 2000. The WAC Bennett dam Sinkhole Incident. In *Proceedings of the 53<sup>rd</sup> Canadian Geotechnical Conference, Montreal, 15–18 October, 2000*. 1: 39–45
- Styler, M.A. & Howie, J.A. 2014. Continuous Monitoring of Bender Element Shear Wave Velocities During

## Geotechnical investigation and slope failure rehabilitation of an industrial process water pond



K. Burkell  
BGC Engineering, Calgary AB  
[KBurkell@bgcengineering.ca](mailto:KBurkell@bgcengineering.ca)

### Group Members:

Kristin Gray, Travis Inglis and Randall Parenteau  
Client: Adelantar Consulting

### Introduction

As part of the University of Saskatchewan College of Engineering Capstone Design Project my group was asked to provide consulting services to rehabilitate a geomembrane-lined industrial processing water pond at a plant in Northern Alberta. This pond acts as a water containment system for a large-scale production facility to draw from. This pond also serves as a drainage pond, collecting precipitation and runoff from the surrounding area. In recent years, the pond was expanded and geosynthetics were added to help with water retention, drainage, and to stabilize the soil. After the expansion of the pond, two slope failures occurred, shown in Figure 1. A smaller failure along the south side of the pond had already been fixed and therefore was not included. The failure of interest was along the north side of the pond. A bulge, 30 m wide, on the sidewall was identified close to the pond water level, and indicated a local failure of soil. Subsequent

movement occurred over a six-month period causing excessive tension in the geomembrane leading to the geomembrane being pulled out of the anchor trench surrounding the pond. This resulted in a sub-vertical back scarp in the pond slope, approximately 3 m high, ripping the geomembrane.

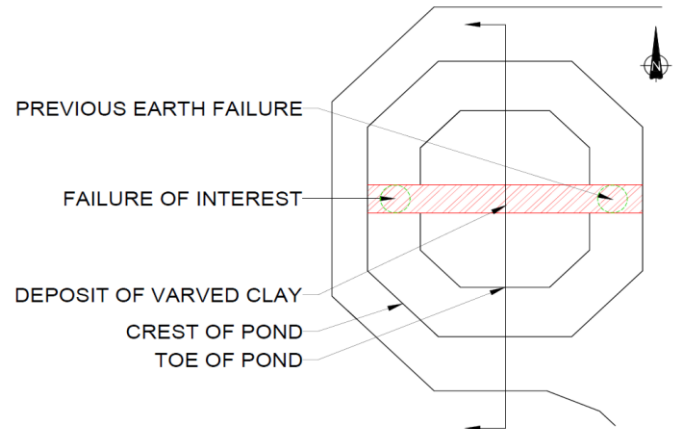


**Figure 1: Slope Failure Locations**

### The Project

#### Scope of Work

The scope of the project included an investigation to determine the key features of the site that contributed to the failure and why the failure occurred. In order to avoid another failure an in-depth investigation was a crucial part of the rehabilitation process. Once the source of the failure was understood a detailed design of a new and innovative rehabilitation solution was generated. After obtaining site history, layout and the project requirements, the main constraints of the project were linked to the operation of the facility, and the geometry of the site. The pond had to remain in operation throughout the entire rehabilitation period, which meant the pond could not be drained, and an environmentally sensitive containment structure located behind the failure posed as a space constraint.

#### The Failure

In order to determine how the failure occurred, seepage and stability analyses were conducted using GeoStudio software. Extensive modeling of in-situ conditions was conducted to determine the factor of safety of the failed slope. The specific conditions modeled consisted of:

- In-situ: 3:1 slope of material in place,
- Drains: Fully operational sub-surface drainage system in place, and
- Ineffective Drains: Geonet placed on side slope

During the detailed investigation, it was determined that the layering of the geosynthetics may have been incorrectly installed during the expansion. An additional model was used to simulate a situation where the geonet and drains were not working. This was done in order to confirm whether the layering of the geosynthetics had originally been placed in the correct order. SEEP/W was used to analyze how pore-water pressure could have contributed to the slope failure. Parameters for the SEEP/W analyses used values generated from a soil water characteristic curve. The SLOPE/W analysis was conducted using the Morgenstern-Price method, using Mohr-Coulomb parameters.

It was concluded that the construction phases during the expansion contributed to the failure. The analyses determined that the cause of the failure was, probably, a localized weak layer of soil. The weak layer of soil was located where the berm used during the staged construction had been located, see Figure 2. Another contributing factor was, probably, incorrect layering of the geosynthetics (Figure 3). The geonet was placed directly above the clay soil, which caused the geonet and drains to be ineffective, this added to the slope instability and exacerbated drainage problems. This led to a buildup of pore-water pressure behind the geomembrane, weakening the soil. A bulge was noted in the fall of 2014, with the geomembrane rupturing in the spring of 2015.

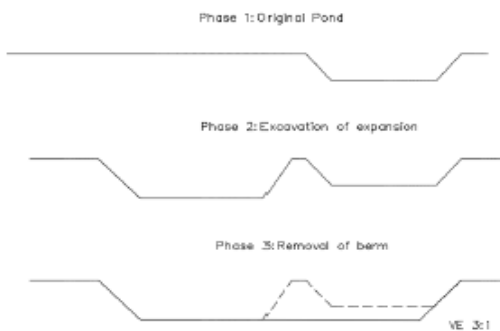


**Figure 2: Construction Phases**

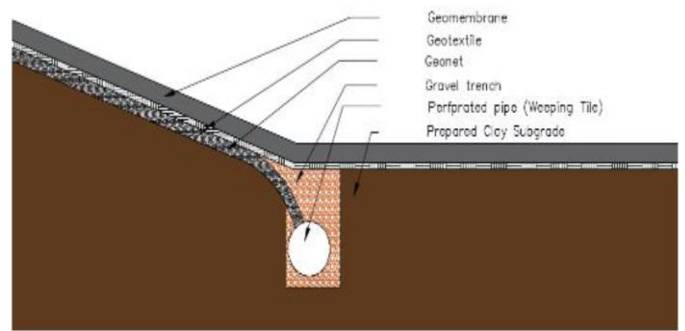


**Figure 3: In-situ Geosynthetic Placement**

### Solution

Four alternatives were considered for rehabilitation: Sheet Piles, Grout Injection Columns, Slope Rebuild with Water Filled Geomembrane Tubes, and a Gabion Mattress Buttress. The alternatives were evaluated using the following metrics: performance, cost, ease of installation, safety, and sustainability. The chosen alternative combined foam blocks, a trench drain, a new geosynthetic system, with gabion mattresses located at the toe of the slope (Figure 4). The gabion mattresses act as a buttress at the toe of the slope, increasing resisting forces, and ultimately increasing the factor of safety. Geofoam is a lightweight fill, which reduces the driving forces that would have otherwise been generated at the crest of the slope. The trench drain and correct layering of geosynthetics will dissipate pore-water pressure within the slope. The total cost of the project including construction, engineering, and site investigation tests was found to be \$788,000.

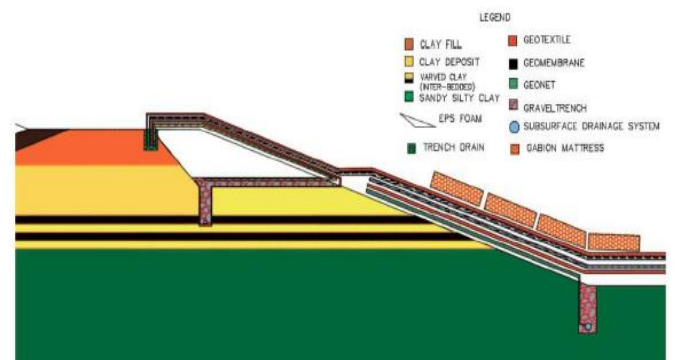


**Figure 4: Chosen Design Configuration**

# Measuring macropore characteristics and hydraulic conductivity of clay cores using computed tomography



D. Muddle  
*University of Bath, Bath, UK*  
[dm647@bath.ac.uk](mailto:dm647@bath.ac.uk)

K. Briggs  
*University of Bath, Bath, UK*

B. Dashwood  
*British Geological Survey, Loughborough, UK*

## Introduction

It is well known that flow within soils is strongly dependent on a soil's physical structure and pore space architecture and is therefore affected by the presence and interconnectivity of macropores. Macropore influence on governing flow has traditionally been hard to define within laboratory experiments. Recently however, X-ray computed tomography (CT) has developed as a means of visualising and quantifying macropore characteristics in a non-intrusive manner. Using this technique to improve our understanding of macropore influence may enable the development of current infiltration modelling.

To that end, this paper presents the results of a series of CT scans coupled with traditional physical laboratory measurements on clay samples from a railway embankment.

## Background

Over the past decade or so, CT scanning has become a more widely used experimental technique in disciplines outside of medicine, including hydrology and soil science (See Mees & London 2003; Cnudde & Boone 2013; Wildenschild & Sheppard 2013, etc.). The draw of this technique is that it allows high resolution, 3D, non-destructive imaging of soil structure and macropore networks. This imaging data can then be used to estimate many soil properties including porosity, pore connectivity and potentially permeability.

This project aims to explore the use of CT for non-destructive permeability estimation on clay samples by establishing a relationship between the pore properties of samples and permeability measurements from traditional methods.

## Method

Good quality, relatively undisturbed cores (100mm diameter, 80mm length) were scanned using a micro CT machine (Nikon X-Trek XTH225ST) at a voxel resolution of 0.057 mm<sup>3</sup>.

The scan data, reconstructed in Figure 1, was processed using a rigorous analysis procedure developed in order to filter, sharpen, segment, and skeletonise the image data of all the samples in a reliable and repeatable fashion.

The image data was used to visualise the macropores within the samples (Figure 2) and to determine sample macroporosity, pore size distributions, pore variation with depth and pore interconnectivity properties, both in partially saturated and fully saturated conditions. These scans at different moisture contents allow for a direct comparison and assessment of any changes in macropore structure as a result of wetting the sample (Figure 3). Traditional laboratory permeability tests at different scales were subsequently carried out using the samples and the results related to the CT generated image data.

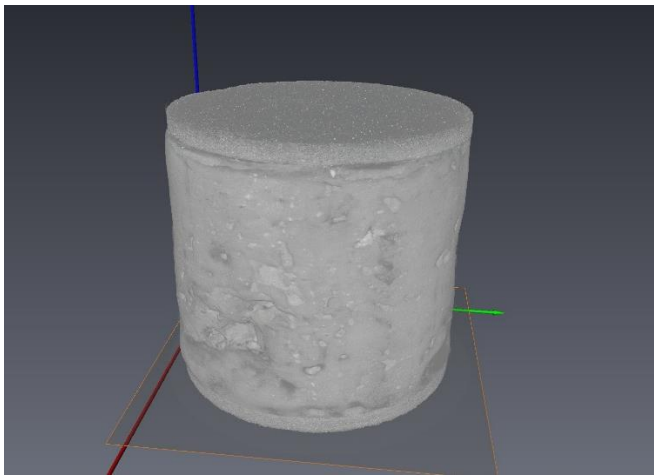


**Figure 1 - 3D Visualisation of a scanned sample**

## Results

A visualisation of the 10 largest macropores present in one scanned sample is shown in Figure 2. Estimated macroporosity varied widely between samples, although across all samples it could be considered low. No macropores extended the entire length of any of the samples. After saturation overall macroporosity, connectivity and pore network density was observed to have increased. However, as shown in Figure 3, the size of the largest pores present was significantly reduced.

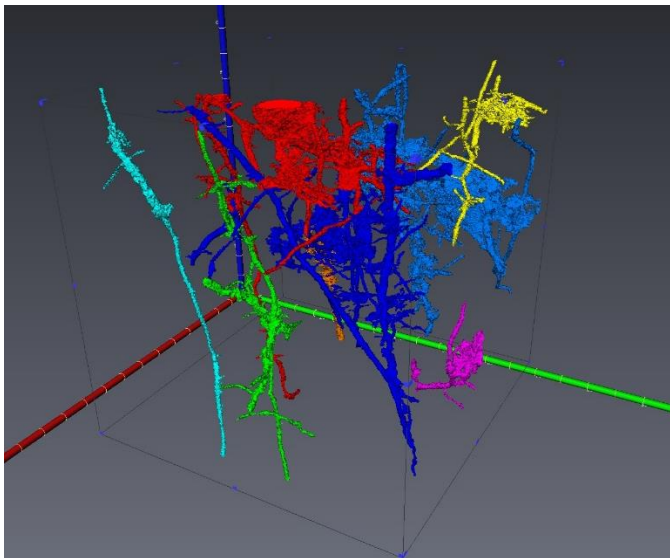


**Figure 2 - Visualisation of the 10 largest macropores in one of the samples**

Saturated permeability test results at all scales indicated that the macroporosity within the tested samples had little effect on overall permeability. This was possibly a consequence of the small number of

large macropores in even the most porous samples and the isolated nature of many of these pores.

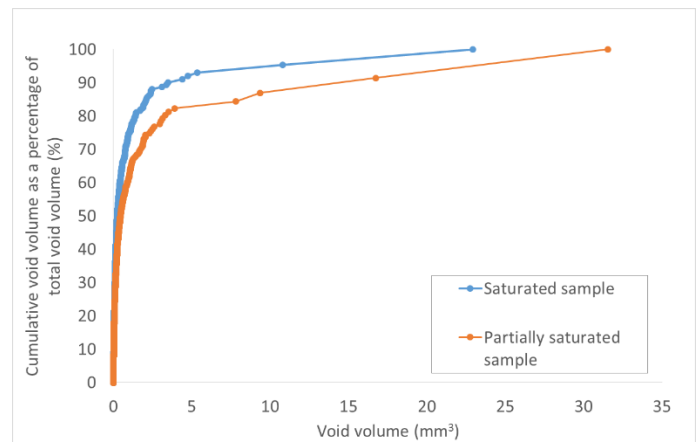


**Figure 3 - Pore size distributions derived from scanning data of a saturated and partially saturated sample**

## Conclusions

In conjunction with traditional permeability tests it is shown that the flow inside the samples appeared predominately matrix governed and that macroporosity within the tested samples had little effect on overall saturated permeability. This was supported by scanning and permeability tests of reconstituted samples with the number of large macropores further reduced.

Comparisons between saturated and partially saturated scans of the same samples showed that while overall macroporosity, connectivity and pore network density increased after saturation, the size of the largest pores present was significantly reduced.

## References

- Cnudde, V. & Boone, M.N., 2013. High-resolution X-ray computed tomography in geosciences: A review of the current technology and applications. *Earth-Science Reviews*, 123, pp.1–17.
- Mees, F. & London, G.S., 2003. *Applications of X-ray Computed Tomography in the Geosciences*, Geological Society.
- Wildenschild, D. & Sheppard, A.P., 2013. X-ray imaging and analysis techniques for quantifying pore-scale structure and processes in subsurface porous medium systems. *Advances in Water Resources*, 51, pp.217–246.

## Geomorphological mapping of the Cascade Bay Landslide using a combined airborne LiDAR and terrestrial remote sensing approach



R. W. Kremsater  
SFU, Burnaby  
[rkremsat@sfu.ca](mailto:rkremsat@sfu.ca)

D. Stead  
SFU, Burnaby  
[dstead@sfu.ca](mailto:dstead@sfu.ca)

B. C. Ward  
SFU, Burnaby  
[bcward@sfu.ca](mailto:bcward@sfu.ca)

T. H. Millard  
FLNR, Nanaimo  
[tom.millard@gov.bc.ca](mailto:tom.millard@gov.bc.ca)

### Introduction

The Cascade Bay Landslide is located on the eastern side of Harrison Lake in southwestern British Columbia. To understand the geomorphic evolution and processes currently active at the Cascade Bay

Landslide, geomorphological mapping has been undertaken based on a digital elevation model (DEM) derived from airborne LiDAR. The LiDAR-based map will be combined with outcrop discontinuity mapping from terrestrial remote sensing techniques to improve our understanding of the landslide structure and evolution, as well as provide a basis for geohazard assessment.

### Background

The highest point on the Cascade Bay Landslide is 1400 m above the surface of Harrison Lake. The landslide is approximately 2.7 km in length east to west, 1.5 km in width north to south, and has a volume of 45 million m<sup>3</sup> estimated by the dimensions of the wedge-shaped headscarp. The landslide is bisected by a NE-dipping thrust fault connected to the Harrison Lake Shear Zone (Journey and Csontos, 1989). The thrust fault separates the meta-sedimentary and meta-volcanic rocks of the Slollicum Schist from the low-grade metamorphic to non-metamorphic sedimentary and volcanic rocks of the Gambier Group (Crickmay, 1930; Monger, 1986; Lynch, 1995).

### Methods

A virtual 3-dimensional landslide model is created to allow the combined visualization of outcrop structures and surface morphology across the study area. The base layer of this digital model is a DEM derived from airborne LiDAR. The DEM has a resolution of 0.5 m and covers the landslide deposit and adjacent areas up to 600 m from the identified slide boundary.

The airborne LiDAR data is combined with terrestrial remote sensing techniques comprising terrestrial laser scanning (TLS) and structures from motion (SfM) photogrammetry. TLS has been used to create a 3-dimensional model of the headscarp with an average point resolution of 0.1 m. Portions of the headscarp inaccessible to TLS are added using the more maneuverable and versatile SfM photogrammetry. The combined approach of TLS and SfM is used to create 3-dimensional outcrop models across the study area, allowing discontinuities to be compared.

Once the 3 dimensional outcrop models are built they will be combined with the airborne LiDAR creating a model that shows the land surface morphology and outcrop structure. This model will be used to compare discontinuities observed on the outcrop to surface lineaments mapped from the airborne LiDAR DEM.

Outcrop discontinuity mapping is done in two stages. The first stage identifies large-scale discontinuities with an outcrop trace length greater than 25 meters, while the second stage maps discontinuities in windows down to the 1 m trace length. The orientations of outcrop discontinuities and surface lineaments are plotted on stereonet and rose diagrams to identify the structures controlling surface morphology across the study area.

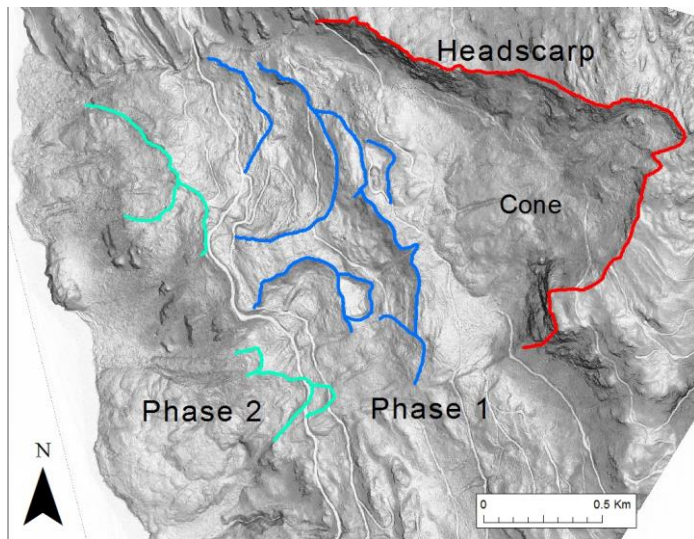


**Figure 1:** The headscarp of the initial landslide is shown in red, the slump scarps of the phase one remobilization are shown in blue, and the slump scarps of the phase two remobilization are shown in teal.

### Initial Interpretation

An initial interpretation of the geomorphologic map shows there has been at least two phases of movement after the initial failure of the Cascade Bay Landslide (Figure 1). The first phase involves the landslide deposit being remobilized by slumping in two different zones in the middle of the slide deposit. The deposits of the phase 1 remobilization are crosscut by failure zones on the lower slopes of the Cascade Bay Landslide, representing the second phase of remobilization. While the landslide deposit was being reworked during remobilization phases 1 and 2, smaller, localized failures from ongoing instabilities in

the headscarp buried the upper portion of the landslide deposit in an area known as the Cone.

Preliminary lineament mapping shows the orientations of linear outcrop sections in the headscarp are repeated in the surrounding landscape (Figure 2). This shows the landslide failed along large regional geologic discontinuities.

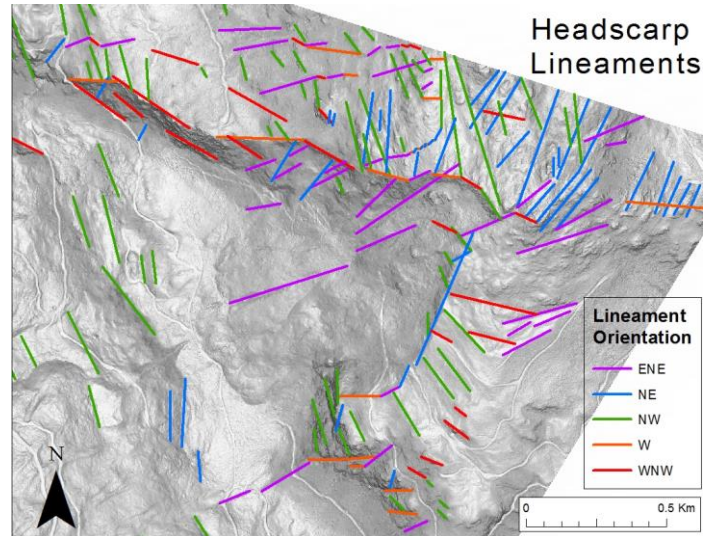


**Figure 2;** Lineament mapping of the Cascade Bay Landslide shows the orientation of each headscarp segment matches linear features in the surrounding landscape. This shows that each section of the headscarp likely failed along a large discontinuity in the rock mass.

### References

- Crickmay C.H. 1930. The structural connection between the Coast Range of British Columbia and the Cascade Range of Washington. *Geological Magazine* 67: 482-491.
- Journey J.M., and Csontos L. 1989. Preliminary report on the structural setting along the southeast flank of the coast belt, British Columbia. In *Current Research, Part E*, Geologic Survey of Canada, Paper 89-1E, 177-187.
- Lynch G. 1995. Geochemical polarity of the Early Cretaceous Gambier Group, Southern Coast Belt, British Columbia. *Canadian Journal of Earth Science* 32: 675-685.
- Monger J.W.H. 1986. Geology between Harrison Lake and Fraser River, Hope map area, southwestern British Columbia." In *Current research, part B*. Geological Survey of Canada, Paper 86-1B, 699-706.

# Large-scale testing of tie lateral resistance in two ballast materials



C. Mulhall  
 University of Alberta, Edmonton  
 Department of Civil and Environmental Engineering  
 Canadian Rail Research Laboratory  
[mulhall@ualberta.ca](mailto:mulhall@ualberta.ca)

S. Balideh, R. Macciotta, M. Hendry, D. Martin  
 University of Alberta, Edmonton

## Introduction

Blasted and crushed rock produced at Canadian National Railway's (CN Rail) McAbee Pit in British Columbia is the primary source of ballast for CN Rail in Western Canada. To reduce track maintenance costs, which are influenced by the distance from the McAbee pit to the area of track being maintained, CN Rail is evaluating the characteristics of crushed gravel, Gravel Ballast, sourced and produced in Alberta, for some of their branch lines in this province. Large-scale laboratory tests were carried out to investigate the lateral resistance provided by the two ballast types.

## Material Characterization

An extensive physical characterization of the two ballast types is currently being undertaken. The particle size distribution plots obtained from sieve

analysis are presented in Figure 1, and aggregate photographs obtained from photogrammetry analysis are shown in Figure 2. Flakiness Index and Los Angeles Abrasion testing have also been completed to determine the angularity and durability of the two ballast types. The McAbee Ballast was determined to have a flakiness index of 12% and the Gravel Ballast a flakiness index of 15%, indicating the Gravel Ballast has more flaky aggregates than the McAbee Ballast. Both had a Los Angeles Abrasion parameter of 17%, indicating they have a comparable durability.

The foremost difference between the two material types is that the McAbee Ballast consists of angular to sub-angular particles with rough faces; while the Gravel Ballast consists of particles with smooth, rounded faces (original rounded gravel) and rough angular to sub-angular faces (crushed gravel).

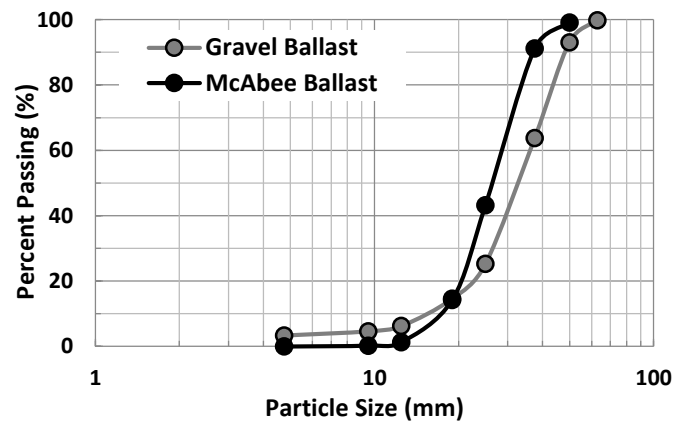


Figure 1: Ballast particle size distribution

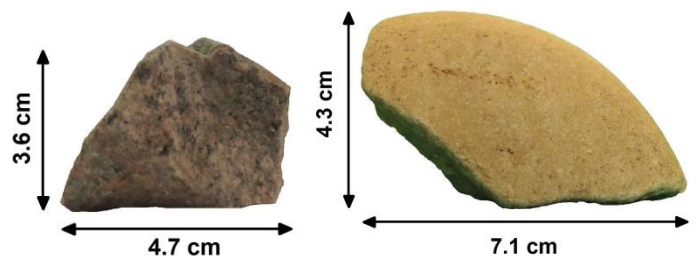


Figure 2: Photograph of McAbee Ballast (left) and Gravel Ballast (right)

## Testing Methodology

Large-scale tests, as depicted in Figures 3 and 4, were performed to evaluate the contribution of the

tie/ballast base friction (bottom of the tie sliding on ballast), crib friction (side of the tie sliding against ballast on the sides), and shoulder resistance (end of tie embedded in ballast – required modification of setting in Figure 3); to the overall tie lateral resistance. Several static normal (or vertical) loads, ranging from 5 kN to 160 kN were applied, the loads were considered to be representative of the expected range of in-service train loads transferred to an individual railway tie. The effect of a low (0.05 mm/s) and a fast (0.5 mm/s) horizontal loading rate were also evaluated. Vertical and horizontal loads and displacements were recorded; and used to determine the peak lateral resistance, at varying horizontal displacements, for each applied normal load.

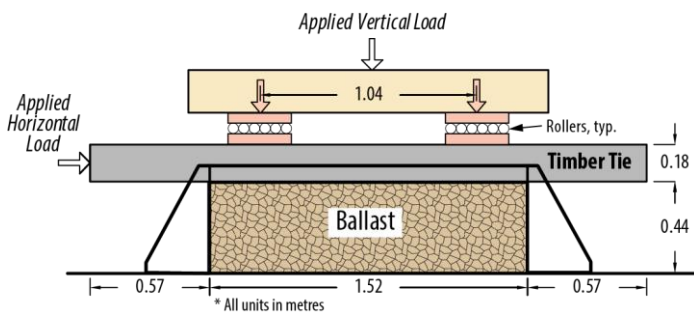


Figure 3: Ballast box loading configuration



Figure 4: Photograph of testing apparatus

### Preliminary Results

Example lateral load versus horizontal displacement curves for the McAbee and Gravel ballast are shown in Figure 5, for both the ‘base friction’ and the ‘base and crib friction’ resistance testing. These tests were completed at an applied normal load of 160 kN (~477 kPa) and a loading rate of 0.05 mm/sec. The lateral load increased with horizontal displacement until it reached a peak value at approximately 20 mm to 25 mm of horizontal displacement.

The preliminary results for the various normal loads are shown in Figure 6. The peak friction angle was calculated to be 32° and 28° for the McAbee Ballast and the Gravel Ballast, respectively. The linear strength envelopes in Figure 6 are consistent with a

frictional system, with no significant dilation. On average 10% less base resistance was developed between the railway tie and the Gravel Ballast, than the McAbee Ballast. It was also observed that the base resistance, under the applied loads, was not a function of the horizontal loading rate; and that the contribution to the peak resistance from the crib friction and shoulder friction was negligible compared to the resistance from the base friction.

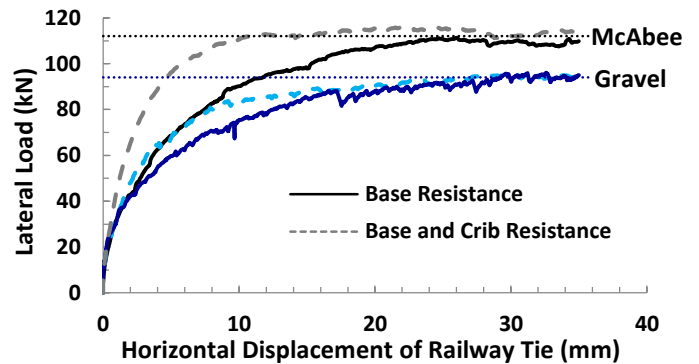


Figure 5: Example lateral load versus horizontal displacement curves for a normal load of 160 kN and a loading rate of 0.05 mm/sec

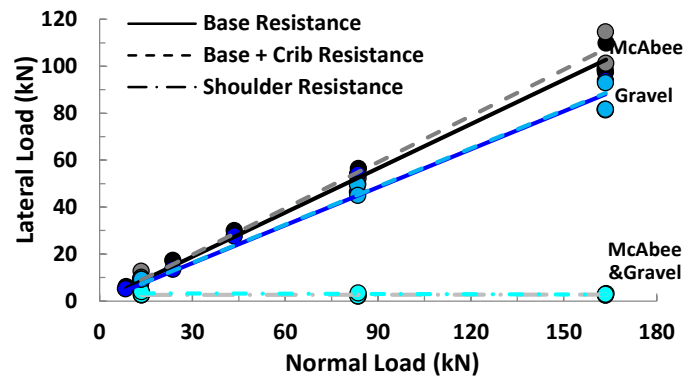


Figure 6: Comparison of the peak lateral load versus applied normal load

### Acknowledgements

This research was made possible by the Canadian Rail Research Laboratory (CaRRL) ([www.carrl.ca](http://www.carrl.ca)), which is funded by the Natural Sciences and Engineering Research Council of Canada (NSERC), Canadian Pacific Railway, Canadian National Railway, the Association of American Railways – Transportation Technology Center Inc., the National Research Council of Canada, Transport Canada and Alberta Innovates – Technology Futures.

## Studying embankment soil stability on the new Inuvik-Tuktoyaktuk Mackenzie Valley highway



D. Kennedy  
Schulich School of Engineering, University of Calgary  
[dtkenned@ucalgary.ca](mailto:dtkenned@ucalgary.ca)

### The highway

There is an important project nearing completion in the Northwest Territories. The Mackenzie Valley Highway, connecting Inuvik (population: ~3,500) to Tuktoyaktuk (population: ~950), is a 120 km long, two-lane highway that will serve as Canada's first all-weather road to the Arctic coast. Tuktoyaktuk was previously only accessible by airplane or ice-roads, which form during the winter months.

Construction on the \$300 million project began in January 2014. Crews met in the middle in April 2016. Expected to open Fall 2017, the highway has been a priority of the federal and territorial governments since it was first proposed in the 1960's.

### Why build the highway?

Due to climate change, things are warming up in the Northwest Territories (3 to 4 times faster than the global average) (Government of Northwest Territories, 2015). Resources and transportation routes are becoming accessible in the Arctic Ocean and there is a desire to connect isolated communities in the far north. Economic and social advantages along with an expression of arctic sovereignty can be achieved through the highway's construction. Benefits for the local residents include long-term employment, reduced costs of living, increased tourism, access to enriched health care, education and economic opportunities (Department of Transportation, Northwest Territories, 2016).

### Experimentation

The underlying permafrost provides opportunity for groundbreaking experimentation. The highway is considered a science project, with Transport Canada providing an additional \$670,000 implementing two experimental road-building applications. The first uses plastic culverts (rather than metal) to reduce heat transferred to the roadbed. The second is an experimental embankment, reinforced using layers of gravel and geotextiles and fitted with sensors to study settlement (Windeyer, 2015). The focus of these experimental applications highlights the paramount challenge faced in permafrost construction: keeping the permafrost intact. Permafrost is sensitive to changes in thermal conditions and only provides an excellent foundation if kept frozen.

### Embankment material

The embankment upon which the highway is built must provide enough strength to support the traffic above, and must be thick enough to insulate the permafrost in the ground below. Higher summer temperatures are shielded, preventing the ground underneath from thawing. Leaving the foundation of permafrost intact reduces settlement.

The embankment material was taken from local borrow sources. Construction took place during winter and embankment soils were compacted frozen on-site. Frozen soil is generally not recommended for

embankment construction because it is difficult to compact at high ice-contents. Local borrow sources did not contain the ideal soil type that was desired. The builders had to make do with what they could find locally as it is expensive to ship soil long distances. Due to the circumstances of this difficult project, compaction testing was not completed on the embankment material during construction.

Understanding the conditions that determine the stability of the compacted frozen soil and its responsiveness to changes in temperature are necessary in predicting the probability and severity of embankment settlement. This knowledge can be applied to reduce settlement and is instrumental for future permafrost construction; therefore testing on the embankment material was desired.

### Compaction and thaw-strain testing

Many factors affect the stability of the embankment: geometry, particle size distribution, ice-content, compaction effort, thermal regime, drainage and snow removal. Many of these factors can be studied by compaction testing. Because this testing was not undertaken on-site, samples from three of the project's borrow sources were delivered to the University of Calgary laboratory, with which we performed particle size distribution tests, hydrometer analyses, and compaction tests.

The Proctor compaction method subjects soil at varying water-contents to compaction forces using a hammer. The resulting dry density at various water-contents is determined. Compaction curves are formed in order to determine "maximum dry densities" and corresponding "optimum water-contents." Similarly, frozen soil at various moisture contents can be compacted, providing similar results. The compaction and thaw-strain data will be used to quantify the effects of ice-content within compacted soil and estimate conditions that could cause excessive settlement on the highway.

### Observations and results

The effectiveness of compaction on frozen material is dependent on the soil's moisture content. Figure 1 compares a sample's wet and frozen compactions at varying moisture contents. Frozen soil was found to have lower dry densities when compacted at given water-contents than unfrozen soil. Compacting had little effect when the samples contained ice-contents greater than approximately 10-12% (Figure 2). Many

site samples had moisture contents higher than the highest compactable ice content determined experimentally. Thaw-strain tests (yet to be performed) are expected to show increasing settlement with increasing ice-content. Results will be used to build a model to predict settlement.

### References

Department of Transportation, Northwest Territories, 2016. Inuvik-Tuktoyaktuk Mackenzie Valley Highway, <http://ith.dot.gov.nt.ca/>.  
 Government of Northwest Territories, 2015. *Northwest Territories – Environment and Natural Resources: Climate Change*, <http://www.enr.gov.nt.ca/node/3697>.  
 Windeyer, C. 2015. On the Road to Tuk: An Update, *EDGE North*, <https://edgenorth.ca/article/1021-on-the-road-to-tuk-an-update>.

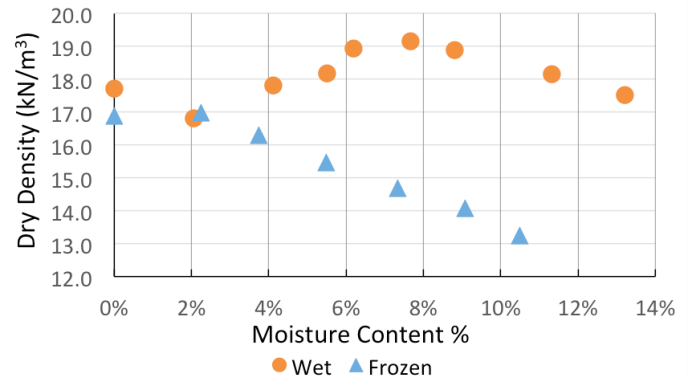


**Figure 1: “Wet” and “Frozen” compactions compared for Sample B.**



**Figure 2: Compaction cannot be achieved at high ice contents (12% moisture content after 50 compactions).**

## Debris flow effects on steelhead trout habitat in Shovelhead Creek



H. Van Hove  
BGC Engineering Inc., Vancouver  
[hvanhove@bgcengineering.ca](mailto:hvanhove@bgcengineering.ca)

### Introduction

Shovelnose Creek is tributary of the Squamish River located approximately 40 km north of the town of Squamish, British Columbia. It flows along the eastern extent of the Squamish River floodplain for approximately 2 km before discharging into the main stem of the river. The slow flowing meanders and deep pools of Shovelnose Creek have been designated by the Steelhead Society of British Columbia (SSBC) as the premier steelhead trout habitat within the Squamish River Valley. A site overview is shown in Figure 1.

Turbid Creek is located approximately 4 km upstream of the Shovelnose Creek outlet, and has a history of frequent, massive debris flow events (Cruden 1992). In the past, the large influx of water and sediment during one of these events has caused the Squamish River to overflow into Shovelnose Creek and destroy steelhead habitat.



Figure 1. Site overview showing Turbid Creek, Shovelnose Creek, and the Squamish River.

### Site History

Three major prehistoric debris flows occurred within Turbid Creek's watershed, initiated by the collapse of the western flank of Mount Cayley. All three events temporarily dammed the Squamish River (Evans 1991). The eventual debris-dam breached caused mass flooding and channel migration in the lower reaches of the Squamish River (Brooks 1991).

Recent debris flow events, albeit smaller in magnitude, continue to affect channel migration of the

Squamish River. A record of recent debris flow events is shown in Table 1.

**Table 1.** Documented debris flow events at Turbid Creek (Friele 2013)

Year	Date	Trigger	Volume (m <sup>3</sup> )
1963	July	..	5,000,000
1984	28-Jun	Rain	3,200,000
1993	29-Jul	Rain	300,000
2005	08-Jul	Rain	10,000
2010	06-Aug	Heat	100,000

### Objective

The objective of this project is to conceptualized strategies for the protection of Shovelnose Creek's steelhead habitat. The preliminary management strategies include taking no action, completing patch repairs after damaging events, or construction of a diversion berm. The SSBC will use the conceptual strategies for fund allocation in the coming year.

### Analysis and Future Work

A geomorphic assessment, including 2D flow modeling and air photo analysis, is currently in progress. The elements of the assessment are at varying stages of completion and ultimately will be used to determine the avulsion potential (frequency and magnitude) which dictates the feasibility and merit of the proposed management strategies.

Air photos from 1947 to 2003 have been compared in order to track changes in channel planform. A significant erosion and avulsion event coinciding with the 1984 debris flow event was observed to breach the left bank of the Squamish River and flood Shovelnose Creek. Figure 2 shows the avulsion channel.

The project team conducted unmanned aerial vehicle (UAV) reconnaissance of the Squamish River valley, which included the gathering aerial photographs. The photos were processed using PhotoScan to create a photogrammetry model which will be used to model both clear-water and debris flow events. The model will determine the magnitude and frequency of events with the potential to cause avulsion of the Squamish River into Shovelnose Creek.

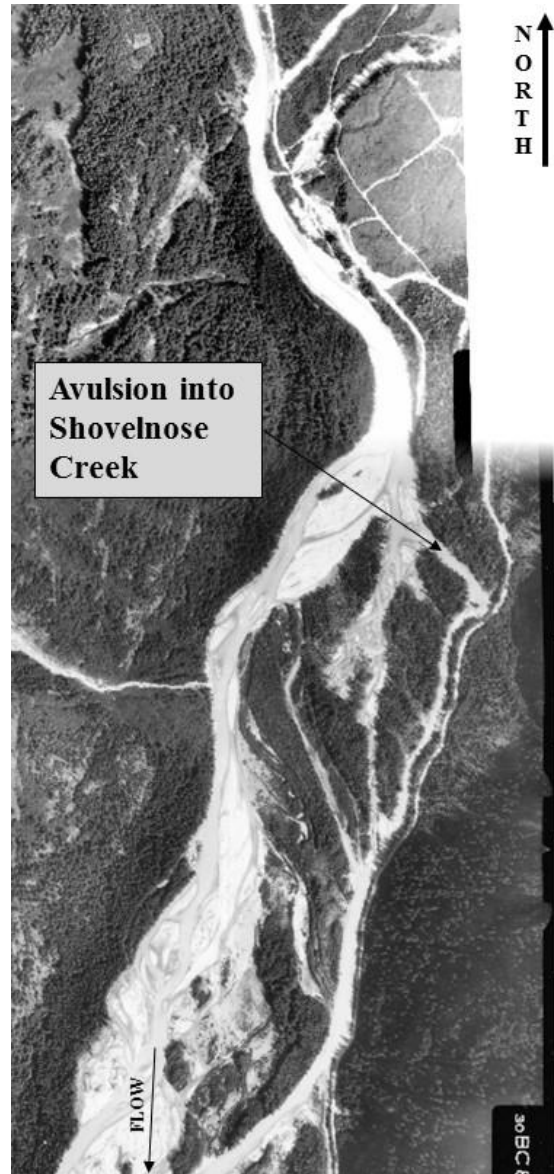


**Figure 2.** Airphoto from 1986 showing the avulsion channel created during the 1984 debris flow event.

### References

- Brooks, G.R. & Hickin, E.J. 1991. Debris avalanche impoundments of Squamish River, Mount Cayley area, southwestern British Columbia. *Canadian Journal of Earth Sciences* 28: 1375-1385.
- Cruden, D.M. & Lu, Z.Y. 1992. The rockslide and debris flow from Mount Cayley, B.C., in June 1984. *Canadian Journal of Earth Sciences* 29: 614-626.
- Evans, S.G. & Brooks, G.R. 1991. Prehistoric debris avalanches from Mount Cayley volcano, British Columbia. *Canadian Journal of Earth Sciences* 28: 1365-1374.
- Friele, P. 2013. Weather thresholds and operational safety planning, Turbid Creek, Mount Cayley, Squamish River Valley, BC.

# Evaluating rockfall hazard on the north wall of Stawamus Chief



C. Sampaleanu  
Simon Fraser University, Burnaby, BC  
[csampale@sfu.ca](mailto:csampale@sfu.ca)

D. Stead, B. Nghana  
Simon Fraser University, Burnaby, BC

P. Schlotfeldt  
Golder Associates, Squamish, BC

## Introduction

Stawamus Chief (often referred to as simply ‘The Chief’) is a granitic monolith located near Squamish, BC. The Chief comprises mostly massive granite with fresh to slightly weathered discontinuity surfaces (Tuckey 2012).

Discontinuities are predominantly surface parallel unloading joints, associated with glacial melting, a majority of which have greater than 20 m persistence. Orthogonal fractures form lateral release surfaces for exfoliation slab failures, which range in thickness from 10 cm to 5 m.

Rockfall on the Chief is a relatively rare occurrence, although several large magnitude events have been observed. The two most recent rockfall events occurred on April 19, 2015, and January 19,

1999. Both of these rockfalls initiated on the north wall of the Chief, an area which is referred to as either Zodiac Wall or Angel’s Crest.

Spatial susceptibility and temporal probability of rockfall on the Chief are poorly understood. In this study, we apply long range remote sensing techniques and evaluation of historical rockfall to provide a more systematic characterization of rockfall hazard on the north wall of the Chief.

## *Historical Rockfall on the Chief*

The most recent major rockfall occurred on April 19, 2015, and was estimated at 2000 m<sup>3</sup> to 3000 m<sup>3</sup>. The trigger for the event is believed to be root pressure behind the failed block causing a progressive topple, which in turn crushed the outer edge of the underlying block, resulting in failure (Golder Associates 2015).

Several blocks remain in the area of the rockfall, some of which were impacted by the original event, and may have been damaged (Golder Associates 2015). The largest of these blocks were assessed as stable, with a lower than 1:50 year return period of rockfall related to them.

## Methodology

Two remote sensing techniques were used in the evaluation of rockfall hazard on the Chief – terrestrial photogrammetry and terrestrial LiDAR. These techniques were used to create digital terrain models which served as the basis for the rockfall hazard analysis.

Parameters for each of the techniques are listed in Table 1.

## Hazard Evaluation

Three techniques were applied in assessing rockfall hazard – rockfall scar mapping to assess the mechanism of historical rockfall, structural and kinematic analysis of existing discontinuities, and mapping of vegetation in relation to zones of potential rockfall initiation.

**Table 1: Summary of remote sensing instrumentation**

<i>Photogrammetry</i>		
Approximate range (m)	750	1100
Camera station separation (m)	115	210
Camera	Canon 5DS	
Focal lengths used (mm)	200, 400	
Aperture	f/8	
<i>Terrestrial LiDAR</i>		
LiDAR System	Riegl VZ-4000	
Approximate range (m)	1100	
Approximate point spacing (m)	0.035	

### *Rockfall Scar Mapping*

Rockfall scars were identified by relatively fresh appearance in contrast to the surrounding rock, the presence of brittle fracture textures such as hackles and arrest marks, the presence of side-release surfaces, and a higher reflectivity in LiDAR. Fourteen major rockfall scars were identified, most of which appeared to have been wedge failures or associated with progressive tensile failure of exfoliation slabs.

### *Structural Analysis*

Structural mapping was carried out to determine discontinuity orientation, persistence and spacing along with the in-situ block size distribution. Mapping was done on both the photogrammetry and LiDAR models.

Structures were categorized by persistence, based on a modified ISRM (1978) classification, then by orientation favorability. Structures greater than 4 m equivalent persistence were mapped at the scale of the entire slope. Structure persistence and orientation classes were plotted on a matrix to determine relative contribution to rockfall hazard.

Thirteen potentially unstable blocks were identified based on slope scale mapped structures. Of these, six are tabular blocks, formed by a large back-release plane and perpendicular step-path fractures, which are kinematically favorable for block toppling or tensile failure of exfoliation slabs. The remaining blocks are wedges formed by steeply dipping intersecting discontinuities. The largest of these blocks is estimated at 2500 m<sup>3</sup>.

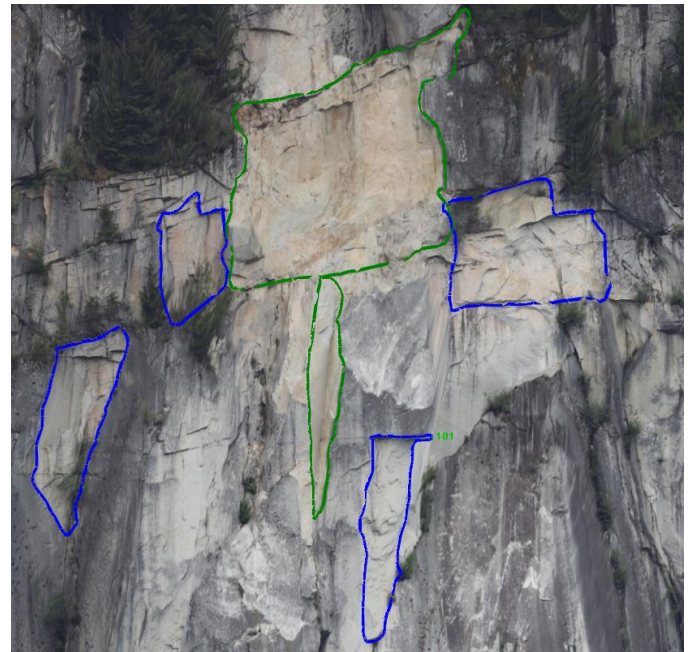


**Figure 1: Photogrammetric model with outlines of rockfall scars from April 19, 2015 (green) and historical rockfalls (blue)**

### *Vegetation Induced Rockfall*

Due to the relatively wet and temperate climate of the West Coast, vegetation growth on the Chief is rapid and has the potential to accelerate crack growth and block displacement. Areas where vegetation growth into cracks could lead to rockfall were identified. These areas are characterized by dense trees or bushes growing on top of or around previously identified blocks. Kinematic analyses were carried out in these areas and cracks likely to be affected by vegetation were identified.

### **Conclusion**

Rockfall hazard on Stawamus Chief is not well understood, given its popularity as a recreational area and proximity to population. Understanding the potential magnitude and failure mechanisms of rockfalls is the first step in evaluating and managing rockfall hazard.

### **References**

- Golder Associates. 2015. Report on Angel's Crest Rockfall Scaling Program
- ISRM. 1978. Suggested methods for the quantitative description of discontinuities in rock masses. *Int. J. Rock Mech. Min. Sci. Geomech. Abstr.* 15: 319-368
- Tuckey, Z. 2012 An Integrated Field Mapping-Numerical Modelling Approach to Characterising Discontinuity Persistence and Intact rock Bridges in Large Open Pit Slopes, *M.Sc. Thesis, Simon Fraser University*

# BC Hydro Transmission Engineering – Annual Geohazard Review Program & case studies



A. S. Woods, EIT  
BC Hydro, Burnaby, BC, Canada  
[Adam.woods@bchydro.com](mailto:Adam.woods@bchydro.com)

## Introduction

BC Hydro (BCH) owns, operates, and maintains thousands of high voltage (69kV and above) transmission assets spanning over 18,000 linear kilometers in the province of British Columbia in areas that include steep mountainous terrain, wet liquefiable soils and major river crossings. In order to continue to provide reliable electricity to their customers, an annual Geohazard Review Program is implemented by the BCH Transmission Engineering Geotechnical Design Team to identify and assess geotechnical risk to these assets.

## Geohazard Review Overview

### *Review Methodology*

In general, the primary methodology for carrying-out the geohazard reviews is by visual inspection of the transmission structures and surrounding area via

helicopter. This is due to the remote nature of many of the structure sites.

However, in more urban areas with good road access and restrictions on low-level helicopter flight, such as Vancouver, and in areas paralleling major rivers, ground and boat based reviews are carried-out respectively.

### *Regions*

In order to fully cover the extent of the transmission system, the province is divided into nine geographical regions.

### *Review Frequency*

A quantitative approach is taken to determine the review period (P) of a transmission circuit, based on four factors/categories: Development level (D), importance (I), voltage (V), and area type (A) and entered into the equation below:

$$P = 1 + \frac{(D \times I \times A)}{V}$$

### **Equation 1: Derivation of Review Period, P (in years)**

Exceptions to this equation include circuits that are completely within urban areas, circuits which parallel a circuit that is scheduled to be reviewed, per recommendations of BCH field operations staff, or after a maximum return period of twelve years.

## Geohazard Identification

### *Typical Hazard Types*

BCH transmission structures are exposed to a wide range of geotechnical hazards but most commonly include: Riverbank erosion, debris flow, slope failure, and avalanche.

### *Secondary Hazards*

Non-geotechnical secondary hazards also pose a risk to assets and are recorded during reviews. This includes risks due to land development, motor vehicle accidents, vegetation, and fire.

## Reporting

### *Geospatial Photo Archiving*

GPS enabled cameras are used for site photos to record observations during the reviews. These are then entered along with detailed description of the photos into a GIS database viewable in Google Earth.

### *STARR*

The System for Transmission Recording & Reporting (STARR) is an internal BCH asset management system where the results of each regional geohazard review are entered and recorded.

### *Region Summary Reports*

An annual summary report for each transmission region is submitted to BCH Asset and Investment Management (AIM) and BCH regional operation field staff. Each report contains detailed site photography, observations, measurements, and recommendations based on the identified hazards. In addition, a geohazard risk rating, see Table 1, is assigned to each structure deemed to be at risk.

**Table 1: Geohazard Risk Rating**

Rating		Description
A	Low	Asset is as good as new
B	Low	Asset shows evidence of weathering, moderate erosion, rip rap launching etc. No concern until next inspection
C	Moderate	Asset showing evidence of increased geotech risk, should be monitored next year prior to next scheduled inspection
D	High	Asset shows extensive geotech risks and potential impacts, protection structures in poor condition, possible structure damage or failure. Mitigation work should be scheduled at the earliest opportunity
E	Extreme	Assets shows extreme geotech risk, protection structures in very poor condition, failed, or no protection structure present and structure is at imminent risk of failure. Site should be remediated at the earliest opportunity on an emergency basis.

## Civil Protective Program (CPP)

The CPP is an annual plan developed to protect the transmission structures as recommended by the geohazard review program. Typical geohazard remediation techniques include riprap revetments,

debris flow barriers/berms, foundation reinforcement, soil nailing & shotcrete, and structure relocation.

## Case Studies

### *2L101 Skeena River*

2L101 is a 287kV circuit that runs from Terrace to Prince Rupert, BC along the Skeena River that has historically had multiple structures at high risk due to flooding and riverbank erosion.

### *5L063 210/1 Telkwa Landslide*

A 500kV guyed steel lattice tower that is situated on a large active landslide east of Terrace, BC with slope movements of up to 440mm/year.

### *2L001 Debris Flow*

On September 20<sup>th</sup>, 2015 a large debris flow near Pemberton, BC occurred destroying a 230kV transmission tower, washing out a CN rail line, a provincial highway. An emergency geotechnical review was carried out to allow crews to access the area to replace the structure and return power.



**Figure 1: Sept 2015 2L001 Debris Flow**

## References

- Gilpin-Jackson, A. 2013. BC Hydro, Transmission Maintenance Standard 82.40-01-00: Requirements for Civil & Geotechnical Hazard Inspections
- Scott, T. 2013. BCH Transmission Engineering Standard 41B Section 3: Geotechnical Hazard Review of Transmission Line Structures and Right of Ways
- Jurbin, T. 2003. Keeping Our Line and Towers in Good Service. In *Plugged In 9. Geotechnical Hazard Review Help to Ensure Electrical Reliability*: 16-18.